

**APPLICATION OF BOREHOLE-IMAGING LOGS TO
GEOLOGIC ANALYSIS, COTTON VALLEY GROUP
AND TRAVIS PEAK FORMATION, GRI STAGED
FIELD EXPERIMENT WELLS, EAST TEXAS**

TOPICAL REPORT

(January 1987 - February 1990)

**Bureau of Economic Geology,
The University of Texas at Austin**

Contract No. 5082-211-0708



TIGHT GAS SANDS

Gas Research Institute

8600 West Bryn Mawr Avenue
Chicago, Illinois 60631

**APPLICATION OF BOREHOLE-IMAGING LOGS TO GEOLOGIC ANALYSIS,
COTTON VALLEY GROUP AND TRAVIS PEAK FORMATION,
GRI STAGED FIELD EXPERIMENT WELLS, EAST TEXAS**

TOPICAL REPORT

(January 1987 - February 1990)

Prepared by

**Stephen E. Laubach, H. Scott Hamlin, Robert Buehring,
Robert W. Baumgardner, Jr., and Eric R. Monson**

**Bureau of Economic Geology
W. L. Fisher, Director
The University of Texas at Austin
Austin, Texas 78713-7508**

for

**GAS RESEARCH INSTITUTE
Contract No. 5082-211-0708
Mark Johnson, GRI Project Manager**

October 1990

DISCLAIMER

LEGAL NOTICE This report was prepared by the Bureau of Economic Geology as an account of work sponsored by the Gas Research Institute (GRI). Neither GRI, members of GRI, nor any person acting on behalf of either:

- a. Makes any warranty or representation, expressed or implied, with respect to the accuracy, completeness, or usefulness of the information contained in this report, or that the use of any apparatus, method, or process disclosed in this report may not infringe privately owned rights; or
- b. Assumes any liability with respect to the use of, or for damages resulting from the use of, any information, apparatus, method, or process disclosed in this report.

| | | | |
|--|-------------------------------------|---|-------------------------------------|
| REPORT DOCUMENTATION PAGE | 1. REPORT NO. GRI-90/0222 | 2. | 3. Recipient's Accession No. |
| 4. Title and Subtitle Application of borehole-imaging logs to geologic analysis, Cotton Valley Group and Travis Peak Formation, GRI Staged Field Experiment wells, East Texas | | 5. Report Date October 1990 | |
| 7. Author(s) Stephen E. Laubach, H. Scott Hamlin, Robert Buehring, Robert W. Baumgardner, Jr., and Eric R. Monson | | 8. Performing Organization Rept. No. | |
| 9. Performing Organization Name and Address Bureau of Economic Geology The University of Texas at Austin University Station, Box X Austin, TX 78713 | | 10. Project/Task/Work Unit No. | |
| | | 11. Contract(C) or Grant(G) No. (C) 5082-211-0708 (G) (Gas Research Institute) | |
| 12. Sponsoring Organization Name and Address Gas Research Institute 8600 West Bryn Mawr Avenue Chicago, IL 60631 | | 13. Type of Report & Period Covered Topical - January 1987- February 1990 | |
| | | 14. | |
| 15. Supplementary Notes | | | |
| 16. Abstract (Limit: 200 words) This report summarizes studies of two geophysical logging tools, the borehole televiewer and the Formation Microscanner, that were used in GRI's three Staged Field Experiment wells and in a cooperative well in East Texas. These tools can detect natural fractures and induced fractures that reflect in situ stress conditions, as well as lithologic features that can be important for geologic interpretation. Improvement in borehole televiewer and Formation Microscanner technology has been rapid in the past several years, but calibration of the logs with core is needed to ensure accurate interpretations of the logs. Our study compares borehole televiewer and Formation Microscanner logs with core from wells in low-permeability gas reservoir sandstone. Vertical fractures in Travis Peak and Cotton Valley sandstone usually are visible on borehole televiewer and Formation Microscanner logs, but some fractures were missed or are indistinct. Aspects of fracture shape can be determined and fractures can generally be separated from borehole breakouts, but natural fractures are difficult to distinguish from some types of drilling-induced fractures on either log. Fracture orientation is readily obtained for inclined fractures from either borehole televiewer or Formation Microscanner logs, but the orientation of vertical fractures, the common fracture type in East Texas reservoirs, can be ambiguous locally on both logs. Formation Microscanner images can be used to help document and interpret depositional environment, and they provide images of sedimentary structures and thin beds. | | | |
| 17. Document Analysis a. Descriptors East Texas, borehole televiewer, Formation Microscanner, geophysical log analysis, borehole breakouts, Travis Peak Formation, Cotton Valley Group, natural fractures, stress, tight gas sandstones b. Identifiers/Open-Ended Terms detection and characterization of fractures, determination of stress directions, analysis of sedimentary rocks c. COSATI Field/Group | | | |
| 18. Availability Statement Release unlimited | | 19. Security Class (This Report) Unclassified | 21. No. of Pages 129 |
| | | 20. Security Class (This Page) Unclassified | 22. Price |

RESEARCH SUMMARY

| | |
|------------------------|--|
| Title | Application of borehole-imaging logs to analysis of Cotton Valley Group and Travis Peak Formation, GRI Staged Field Experiment wells, East Texas |
| Contractor | Bureau of Economic Geology, The University of Texas at Austin, GRI Contract No. 5082-211-0708, entitled "Geologic Analysis of Primary and Secondary Tight Gas Sand Objectives." |
| Principal Investigator | S. P. Dutton |
| Report Period | January 1987 - February 1990 Topical Report |
| Objectives | To summarize the results of the application of borehole-televiewer and Formation Microscanner logs to evaluation of Cotton Valley Group and Travis Peak Formation in East Texas, including stratigraphic characterization, fracture analysis, and determination of stress direction from borehole breakouts. |
| Technical Perspective | <p>The Gas Research Institute (GRI) has sponsored investigations designed to develop knowledge necessary to efficiently produce low-permeability, gas-bearing sandstones through integration of geology, formation evaluation, and reservoir engineering. These studies are part of a broad research program designed to increase the understanding and ultimate utilization of gas resources in low-permeability formations. One facet of that program, a comprehensive study has been conducted on the geology of low-permeability sandstones in the Lower Cretaceous Travis Peak (Hosston) Formation and Cotton Valley Group in East Texas. One important aspect of this study involved drilling, coring, logging, and testing several research wells in East Texas between 1986 and 1988, the GRI Staged Field Experiment (SFE) wells. In addition, experiments were carried out in a number of wells with the cooperation of various companies and operators. During the Staged Field Experiment program, cores and a suite of borehole-televiewer and Formation Microscanner logs were acquired by GRI or contributed by industry research groups, providing an opportunity to evaluate various logging methods for detecting and characterizing natural fractures and sedimentary structures in low-permeability sandstone reservoirs.</p> <p>Fracture analysis and stratigraphic studies are necessary for reservoir evaluation in low-permeability-sandstone gas reservoirs, but standard</p> |

geophysical logs provide only limited information on essential fracture characteristics and sedimentary features. Two geophysical logging tools used for fracture detection and stratigraphic analysis are the borehole televiewer, an acoustic device that maps the smoothness of the borehole wall, and the Formation Microscanner, an electrical tool that produces a conductivity map of two or four 2.8-inch-wide (7.1-cm-wide) strips of the borehole wall. These tools can detect natural fractures and induced fractures that reflect in situ stress conditions, as well as subtle lithologic variations that can facilitate geologic interpretation and engineering operations. Borehole-imaging logs can be useful supplements to core analysis. Improvement in borehole-televiewer and Formation Microscanner technology has been rapid in the past several years, but more geological calibration of the logs is needed.

Results

The goals of these studies were to (1) determine whether fractures could be detected using the logs, (2) assess which fracture characteristics could be interpreted reliably from logs, and (3) calibrate Formation Microscanner images of sedimentary structures and depositional features with core.

Vertical extension fractures in Travis Peak and Cotton Valley sandstone usually are visible on borehole-televiewer and Formation Microscanner logs, but some fractures were missed or are indistinct. However, aspects of fracture shape can be determined, and fractures can generally be separated from borehole breakouts. Natural fractures are difficult to distinguish from some types of drilling-induced fractures on either log, and present commercial borehole-televiewer and Formation Microscanner techniques do not give a quantitative measure of fracture aperture. Fracture orientation is readily obtained for inclined fractures from either borehole-televiewer or Formation Microscanner logs, but the orientation of vertical fractures, the common fracture type in East Texas reservoirs, can locally be ambiguous on both logs. Formation Microscanner images can be used to help document and interpret depositional environment, and locally they provide high-resolution images of sedimentary structures and thin beds (0.2 inches [0.5 cm] in this study). These results show that borehole-televiewer and Formation Microscanner logs are useful adjuncts to core-based fracture and stratigraphic studies for evaluating some low-permeability reservoirs in East Texas.

Technical Approach

Fractures in the Travis Peak Formation were sampled using core and fracture-imaging logs from four wells in the East Texas Basin that are representative of this reservoir. We recovered 199 ft (61 m) of core from Prairie Mast No. 1-A, 470 ft (143 m) from Holditch Howell No. 5 (SFE No. 1), 359 ft (109 m) from Holditch SFE No. 2, and 372 ft (113 m) from Mobil Cargill No. 15 (SFE No. 3). Borehole televiewers belonging to AMOCO and Mobil and Schlumberger's Formation Microscanner were run in Holditch

Howell No. 5, a prototype Formation Microscanner (the MEST tool) was run in Prairie Producing Mast No. 1-A, and Mobil and Schlumberger research groups ran two borehole viewers in Holditch SFE No. 2. One of the borehole viewers used in this well was the Schlumberger-Doll Research digital borehole viewer. Borehole viewers belonging to Mobil and Schlumberger and the Formation Microscanner were run in Mobil Cargill No. 15.

Core was oriented by standard multishot photographic techniques and/or paleomagnetic methods with a level of accuracy of ± 10 degrees. Core/log depth matching was done by comparing logs with a core gamma scan and by comparing logs directly with core. In Holditch Howell No. 5 and Mobil Cargill No. 15, precise depth match to within a few inches (centimeters) was possible locally where crossbeds, bioturbated zones, or lithologic boundaries on the Formation Microscanner log provided accurate core-to-log correlations.

CONTENTS

| | |
|--|-----------|
| ABSTRACT | 1 |
| TECHNICAL PERSPECTIVE..... | 2 |
| Geologic Setting..... | 4 |
| SUMMARY OF BHTV AND FMS PRINCIPLES..... | 7 |
| PART ONE: APPLICATION OF FMS LOGS TO THE ANALYSIS OF SEDIMENTARY ROCKS IN THE COTTON VALLEY GROUP AND TRAVIS PEAK FORMATION, EAST TEXAS | 18 |
| OBJECTIVES..... | 18 |
| Methodology..... | 20 |
| Depositional Setting | 20 |
| GENERAL OBSERVATIONS..... | 22 |
| CORE/LOG COMPARISON EXAMPLES | 25 |
| SUMMARY..... | 46 |
| PART TWO: APPLICATION OF BHTV AND FMS LOGS TO FRACTURE DETECTION AND BOREHOLE-BREAKOUT ANALYSIS | 48 |
| FRACTURE STUDIES USING CORES AND GEOPHYSICAL LOGS | 48 |
| Fracture Analysis Methods | 51 |
| Fracture Characteristics Observed in Core..... | 52 |
| OBSERVATIONS OF FRACTURES USING BOREHOLE-IMAGING LOGS..... | 57 |
| Comparison of BHTV Images to Core..... | 59 |
| Natural Fractures..... | 59 |
| Drilling-Induced Petal and Petal-Centerline Fractures | 70 |
| Borehole-Breakout Detection and Evaluation Using BHTV and Caliper Logs | 74 |
| Features Visible on FMS Logs..... | 86 |
| Comparison of FMS Images with Cores..... | 94 |
| Fracture Orientation from Core Data and Logs..... | 96 |

| | |
|--|-----|
| FRACTURE INTERPRETATION USING BOREHOLE-IMAGING LOGS..... | 102 |
| SUMMARY..... | 106 |
| ACKNOWLEDGMENTS..... | 107 |
| REFERENCES..... | 109 |

Figures

| | |
|--|----|
| 1. Location of study area and wells that have core and fracture-imaging logs | 5 |
| 2. Stratigraphic nomenclature, East Texas Basin..... | 6 |
| 3. Diagram illustrating elements of the borehole televiewer..... | 8 |
| 4. Acoustic signal and amplitude and travel time of the reflected wave from which BHTV images are obtained..... | 9 |
| 5. Diagram illustrating the geometric relation of borehole images and the borehole wall..... | 10 |
| 6. Example of fractures and breakouts on BHTV log, Holditch SFE No. 2..... | 11 |
| 7. Simplified diagram of the Formation Microscanner tool..... | 13 |
| 8. Fractures in reservoir rocks imaged using FMS and BHTV logs | 14 |
| 9. FMS logs from the Mobil Cargill No. 15 (SFE No. 3) well..... | 15 |
| 10. Chart showing well depths cored and well depths surveyed by the BHTV and FMS in the four wells of this study..... | 17 |
| 11. Gamma-ray and resistivity logs, Mobil Cargill No. 15 (SFE No. 3) well..... | 19 |
| 12. Symbols used in core and log descriptions..... | 26 |
| 13. FMS log and core description from Mobil Cargill No. 15 (SFE No. 3) well (Example 1).... | 27 |
| 14. FMS log and core description from Mobil Cargill No. 15 (SFE No. 3) well (Example 2).... | 29 |
| 15. FMS log and core description from Mobil Cargill No. 15 (SFE No. 3) well (Example 3).... | 31 |
| 16. FMS log and core description from Mobil Cargill No. 15 (SFE No. 3) well (Example 4).... | 33 |
| 17. FMS log and core description from Mobil Cargill No. 15 (SFE No. 3) well (Example 5).... | 35 |
| 18. FMS log and core description from Mobil Cargill No. 15 (SFE No. 3) well (Example 6).... | 36 |
| 19. FMS log and core description from Mobil Cargill No. 15 (SFE No. 3) well (Example 7).... | 38 |

| | | |
|-----|---|----|
| 20. | FMS log and core description from Mobil Cargill No. 15 (SFE No. 3) well (Example 8).... | 39 |
| 21. | FMS log and core description from Mobil Cargill No. 15 (SFE No. 3) well (Example 9).... | 41 |
| 22. | FMS log and core description from Mobil Cargill No. 15 (SFE No. 3) well (Example 10)..... | 42 |
| 23. | FMS log and core description from Mobil Cargill No. 15 (SFE No. 3) well (Example 11)..... | 44 |
| 24. | FMS log and core description from Mobil Cargill No. 15 (SFE No. 3) well (Example 12)..... | 45 |
| 25. | FMS log and core description from Mobil Cargill No. 15 (SFE No. 3) well (Example 13)..... | 47 |
| 26. | Informal nomenclature of lower and upper Travis Peak producing sandstones, Holditch Howell No. 5 (SFE No. 1) well..... | 49 |
| 27. | Gamma-ray and resistivity logs and informal nomenclature for the Travis Peak Formation in Holditch SFE No. 2 well..... | 50 |
| 28. | Core gamma-ray log, core profile, fracture distribution, and environmental interpretation for core 1-3, Holditch SFE No. 2 well..... | 53 |
| 29. | Core gamma-ray log, core profile, fracture distribution, and environmental interpretation for core 9-15, Holditch SFE No. 2 well..... | 54 |
| 30. | Strikes of natural fractures in Travis Peak sandstones..... | 55 |
| 31. | Scanning electron photomicrograph showing quartz lining open-fracture-pore space, Holditch SFE No. 2, depth of 9,873 ft (3,009 m)..... | 56 |
| 32. | Typical patterns of natural fracture traces in core, Travis Peak Formation..... | 58 |
| 33. | Example of fractures on BHTV log, Holditch SFE No. 2 well..... | 60 |
| 34. | Example of fractures and breakouts on BHTV log, Holditch SFE No. 2 well..... | 62 |
| 35. | Fractures in core and tracing of BHTV image, Holditch SFE No. 2 well..... | 63 |
| 36. | Diagram illustrating fractures that intersect the borehole but not the core..... | 65 |
| 37. | Some sources of error in fracture-width measurements in core..... | 68 |
| 38. | Sketch of aligned petal and petal-centerline fractures, Holditch SFE No. 2 well, and BHTV log..... | 71 |
| 39. | Tracing from BHTV log and sketch of hydraulic fracture induced by open-hole stress test 2, Holditch SFE No. 2 well..... | 73 |
| 40. | Plan views and sections of ellipticity logs for in-gauge borehole, borehole breakout, and washout..... | 75 |

| | | |
|-----|--|-----|
| 41. | Plot of wells showing intervals in Travis Peak Formation covered by ellipticity logs in this study | 78 |
| 42. | Rose diagram of Bernshtein accuracy criterion for two significant peaks of wellbore ellipticity..... | 79 |
| 43. | Plots of ellipticity ratio versus stratigraphic depth in the Travis Peak Formation | 80 |
| 44. | Plot of shale lithology versus stratigraphic depth in the Travis Peak Formation..... | 82 |
| 45. | Plots of length of elliptical zones and BHTV breakouts versus depth | 84 |
| 46. | Plot of the azimuth of borehole breakouts versus depth..... | 85 |
| 47. | Linear vertical features seen on FMS logs, classified into three types..... | 87 |
| 48. | Natural fracture in sandstone core and imaged by FMS..... | 88 |
| 49. | Vertical FMS feature that does not correspond to any structure visible in core..... | 89 |
| 50. | Prominent natural fracture in core that was missed by FMS pads..... | 90 |
| 51. | Coring-induced fractures imaged by FMS..... | 91 |
| 52. | FMS image of fractures and bedding, illustrating fracture terminations | 92 |
| 53. | FMS image of fractures and bedding, illustrating multistranded fracture traces..... | 93 |
| 54. | Features on FMS and BHTV logs, Holditch Howell No. 5 well | 98 |
| 55. | Diagram illustrating inherent uncertainties in matching vertical fracture traces on borehole-imaging logs..... | 99 |
| 56. | Chart showing the orientation of core by paleomagnetic methods and the BHTV | 100 |

Tables

| | | |
|----|--|----|
| 1. | Borehole conditions during FMS logging, Mobil Cargill No. 15 (SFE No. 3) well | 21 |
| 2. | Depositional facies identified in core from the Mobil Cargill No. 15 (SFE No. 3) well..... | 23 |

ABSTRACT

Fracture analysis and stratigraphic studies are useful for reservoir evaluation in low-permeability sandstone gas reservoirs in East Texas, but standard geophysical logs provide only limited information on crucial fracture characteristics and sedimentary features. Two geophysical logging tools used for fracture detection and stratigraphic analysis are the borehole televiewer, an acoustic device that maps the smoothness of the borehole wall, and the Formation Microscanner,* an electrical tool that produces a conductivity map of two or four 2.8-inch-wide (7.1-cm) strips of the borehole wall. These tools can detect natural fractures as well as induced fractures that reflect in situ stress conditions and subtle lithologic features that can facilitate geologic interpretation. Fractures, in situ stress, and rock type may affect reservoir quality and the outcome of engineering operations in the reservoir. For example, natural fractures and in situ stress need to be evaluated for hydraulic fracture treatment design in low-permeability sandstone gas reservoirs because they can affect leakoff and the direction of fracture propagation. Consequently, borehole-imaging logs can be important supplements to core analysis. Improvement in borehole-televiewer and Formation Microscanner technology has been rapid in the past several years, but calibration of the logs with core is needed to ensure accurate interpretations of the logs. Our study compares borehole-televiewer and Formation Microscanner logs with core from four wells in low-permeability gas reservoir sandstone in East Texas. Vertical extension fractures in Travis Peak and Cotton Valley sandstone usually are visible on borehole-televiewer and Formation Microscanner logs, but in our study some fractures were missed or are indistinct. Aspects of fracture shape can be determined, and generally fractures can be separated from borehole breakouts; however, natural fractures are difficult to distinguish from some types of drilling-induced fractures on

*Trademark of Schlumberger, Inc.

either log. Present commercial borehole-televviewer and Formation Microscanner techniques do not give a quantitative measure of fracture aperture. Cemented fractures can be detected in some circumstances. Fracture orientation is readily obtained for inclined fractures from either borehole-televviewer or Formation Microscanner logs, but the orientation of vertical fractures, the common fracture type in East Texas reservoirs, can be ambiguous locally on both logs. Formation Microscanner images can be used to help document and interpret depositional environment, and locally they provide high-resolution images of sedimentary structures and thin beds (0.2 inches [0.5 cm] in this study). These results show that borehole-televviewer and Formation Microscanner logs are useful adjuncts to core-based fracture and stratigraphic studies for evaluating some low-permeability reservoirs in East Texas.

TECHNICAL PERSPECTIVE

The borehole televviewer (BHTV) and Formation Microscanner (FMS) are sophisticated geophysical logging tools that can provide images of rocks and fractures exposed in borehole walls. The BHTV creates an image of the borehole based on acoustic measurements, whereas the FMS is an electrical tool that creates an image based on measurements of current intensity, or conductance, and presents results as microresistivity (Bourke and others, 1989). These logs can help clarify the significance of measurements made by other geophysical logging tools that do not have imaging capability, and the complementary acoustic and electrical observations of the BHTV and FMS are particularly useful in low-permeability-sandstone gas reservoirs because they simulate fractures and subtle lithologic features such as thin interbeds that can have profound effects on reservoir quality and hydraulic fracture treatment design (Dutton and others, 1990). They are therefore becoming important supplements to core analysis for fracture detection and evaluation and for detailed interpretation of sedimentary structures and stratigraphy, among other applications, in low-permeability reservoirs. Whereas the technology of both of these devices has improved rapidly in the past several years (Zemanek

and others, 1970; Paillet, 1981; Taylor, 1983; Plumb and others, 1985; Dennis and others, 1987; Bourke and others, 1989), geological calibration and interpretation of the logs has been hindered by the small number of published comparisons of these logs with core. This report presents the results of such a comparison.

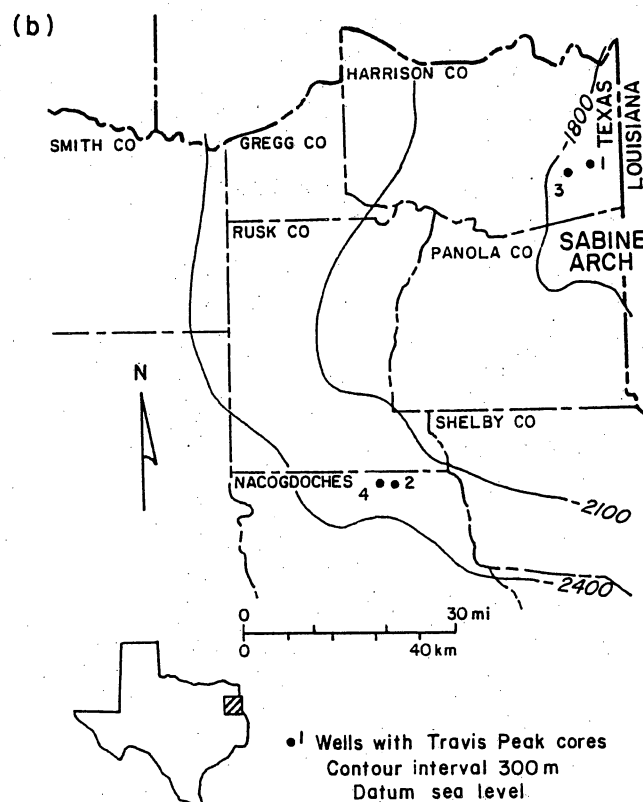
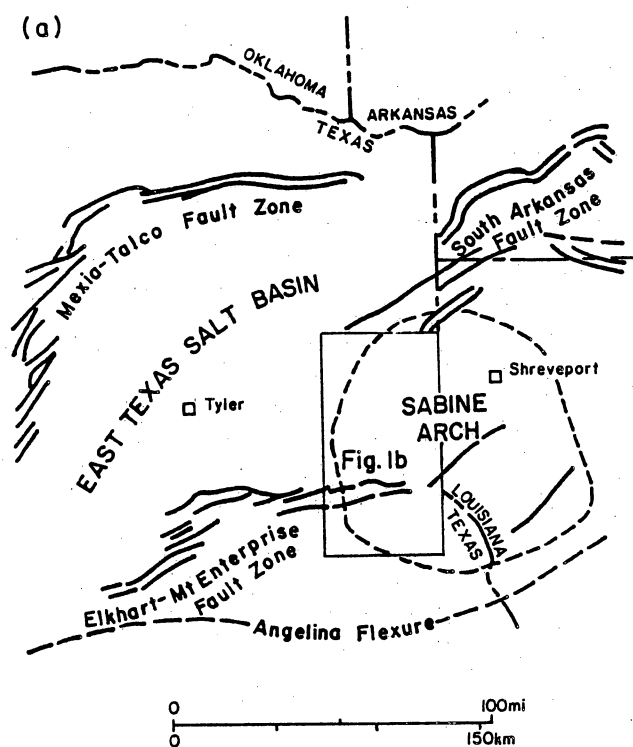
The Gas Research Institute (GRI) has sponsored investigations designed to develop knowledge necessary to produce gas efficiently from low-permeability sandstones through integration of geology, formation evaluation, and reservoir engineering. These studies are one component of a broad research program designed to increase the understanding and ultimate utilization of gas resources in low-permeability formations. As part of that program, a comprehensive study has been conducted on the geology of low-permeability sandstone in the Lower Cretaceous Travis Peak (Hosston) Formation and Cotton Valley Group in East Texas (Tye and others, 1989a and b; summary and references in Dutton and others, 1990). One aspect of this study involved drilling, coring, logging, and testing several research wells in East Texas between 1987 and 1989, the GRI Staged Field Experiment (SFE) wells (Holditch, 1989). In addition, experiments were carried out in a number of commercial wells with the cooperation of various companies and operators. During the SFE program, cores and a suite of BHTV and FMS logs were acquired by GRI or contributed by industry research groups, providing an opportunity to evaluate various logging methods for detecting and characterizing natural fractures and sedimentary structures in low-permeability-sandstone reservoirs.

This report summarizes the results of a comparison of BHTV and FMS logs with cores from four East Texas research wells (fig. 1) and provides the context for ongoing well log and petrophysical studies of these wells. The report is divided into two parts. Part One compares the sedimentary features visible in core from one well, the Mobil Cargill No. 15 (SFE No. 3), with those visible on the FMS log. Part Two describes fracture and borehole-breakout studies that utilized BHTV and/or FMS logs from three SFE wells, Holditch Howell No. 5 (SFE No. 1), Holditch SFE No. 2, Mobil Cargill No. 15 (SFE No. 3), and a cooperative well, the Prairie Producing Mast No. 1-A. The goals of the geologic studies were to (1) determine whether

fractures could be detected, (2) assess which fracture characteristics could be interpreted reliably from logs, and (3) calibrate FMS images of sedimentary structures with core and use logs to help interpret depositional environments.

Geologic Setting

The study area is in the East Texas Basin (fig. 1), which formed during Late Triassic and Jurassic rifting (Buffler and others, 1980). Subsequent cooling and subsidence caused a basin to form in which a thick sequence of Mesozoic and Cenozoic sediments accumulated. Carbonates dominated the early phases of deposition in the basin (Moore, 1983). The earliest progradation of terrigenous clastics in the basin is recorded by the Upper Jurassic-Lower Cretaceous Cotton Valley Group (fig. 2). In the study area, the Cotton Valley is composed of interbedded sandstone and shale (Dutton and others, in press). The Lower Cretaceous Travis Peak Formation represents a second period of fluvial-deltaic progradation, equivalent to the Hosston Formation of Louisiana, Arkansas, and Mississippi. It produces gas and some oil in the study area in East Texas (Saucier and Finley, 1984; Dutton and others, 1990) (fig. 1). There, the Travis Peak is approximately 2,000 ft (610 m) thick, and depth to the top of the formation ranges from 5,900 to 9,600 ft (1,800 to 2,930 m) (Saucier and others, 1985; Tye, 1989; Dutton and others, 1990). In updip portions of the basin, the Travis Peak unconformably overlies the Cotton Valley Group. Downdip, the Travis Peak is separated from the Cotton Valley Group by a thin, transgressive-marine deposit, the Knowles Limestone. The Travis Peak Formation is gradationally overlain by micritic and oolitic limestones of the Cretaceous Sligo Formation, which form a time-transgressive boundary (Bebout and others, 1981). The Travis Peak is composed primarily of interbedded fine-grained quartz-rich sandstone and subarkose, along with subsidiary mudstone. Abundant quartz cement reduces permeability in much of the formation to less than 0.1 md (Dutton, 1987).



QA13148

Figure 1. Location of study area and wells. (a) Structural setting of the Travis Peak Formation, East Texas. (b) Structure on the top of the Travis Peak and location of wells for which Travis Peak cores were available. Wells that have fracture-imaging logs are indicated by a number: (1) Holditch Howell No. 5 (SFE No. 1), (2) Holditch SFE No. 2, (3) Mobil Cargill No. 15 (SFE No. 3), and (4) Prairie Producing Mast No. 1-A.

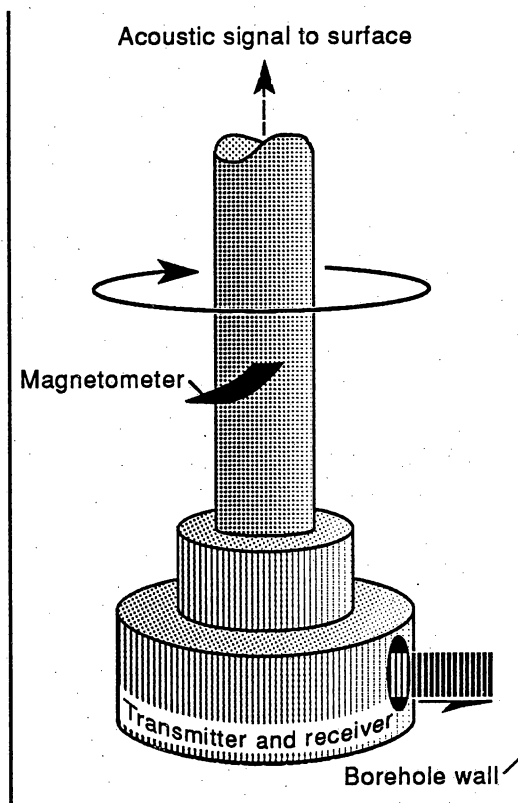
| SYSTEM | SERIES (AGE) | EAST TEXAS BASIN | |
|------------|--------------|---|--|
| QUAT | | | |
| TERTIARY | MIocene/PLIO | | |
| | OLIGOCENE | | |
| | EOCENE | YEGUA COOK MOUNTAIN SPARTA WECHES QUEEN CITY REKLAW CARRIZO | |
| | PALEO | WILCOX MIDWAY | |
| | | | |
| CRETACEOUS | GULFIAN | NACATOCHE → NAVARRO UPPER TAYLOR PECAN GAP WOLFE CITY LOWER TAYLOR AUSTIN SUB-CLARKSVILLE CORNER → EAGLE FORD HARRIS LEWISVILLE DEXTER WOOD-BINE | |
| | | | |
| | | | |
| | | | |
| | | | |
| | | | |
| | | | |
| | | | |
| | | | |
| | | | |
| | COMANCHEAN | BUDA GRAYSON GEORGETOWN FREDERICKSBURG PALUXY UPPER GLEN ROSE MOORINGSPOINT MASSIVE ANHYDRITE BACON LIME RODESSA JAMES LIME → PINE ISLAND | |
| | | | |
| | | | |
| | | | |
| | | | |
| | | | |
| | | | |
| | | | |
| | | | |
| | | | |
| JURASSIC | COAHUILAN | PETTET (SLIGO) PITTSBURG HOSSTON (TRAVIS PEAK) | |
| | | | |
| | | | |
| | | | |
| | | | |
| | UPPER | COTTON VALLEY SCHULER BOSSIER GILMER (COTTON VALLEY LIME) BUCKNER SMACKOVER NORPHLET | |
| | | | |
| | | | |
| | | | |
| | | | |
| PALEOZOIC | M | LOUANN SALT | |
| | L | WERNER | |
| | | EAGLE MILLS | |
| | | OUACHITA FACIES | |

Figure 2. Stratigraphic nomenclature, East Texas Basin. Modified from Galloway and others, 1984.

SUMMARY OF BHTV AND FMS PRINCIPLES

Principles of BHTV operation and use are described by Zemanek and others (1970), Taylor (1983), and Georgi (1985). The BHTV is an acoustic device that emits a high-frequency sonic pulse and measures amplitude and travel time of the reflected wave (figs. 3 and 4). Amplitude and travel-time values are assigned gray-scale levels and plotted as a function of azimuth and depth. These data are displayed as an "unwrapped" image of the borehole wall (fig. 5). South is at the center and north is at the left and right edges (fig. 6). The amplitude image is an acoustic impedance map (for a perfectly smooth hole) and surface roughness map, whereas the transit time indicates borehole shape and tool position (R. A. Plumb, written communication, 1988). Both measurements are affected by tool eccentricity and wellbore roughness (Zemanek and others, 1970; Georgi, 1985). Low-reflectivity features, or cavities such as fractures and borehole breakouts in the wellbore wall, appear as dark areas on the log. In our study, BHTV results were plotted at several different scales. For the Holditch Howell No. 5 well, a 1:30 vertical scale was used. Because the circumference of the wellbore varies and the width of the log is constant, horizontal scale is not constant. Width of the plot, representing circumference of the borehole, was 2.0 inches (5 cm). For the Holditch SFE No. 2, the entire log was presented at a vertical scale of 1:20 with a width of 4.5 inches (11.4 cm), and selected sections of the log were presented at larger scales and viewed on an interactive workstation through the courtesy of Dowell-Schlumberger.

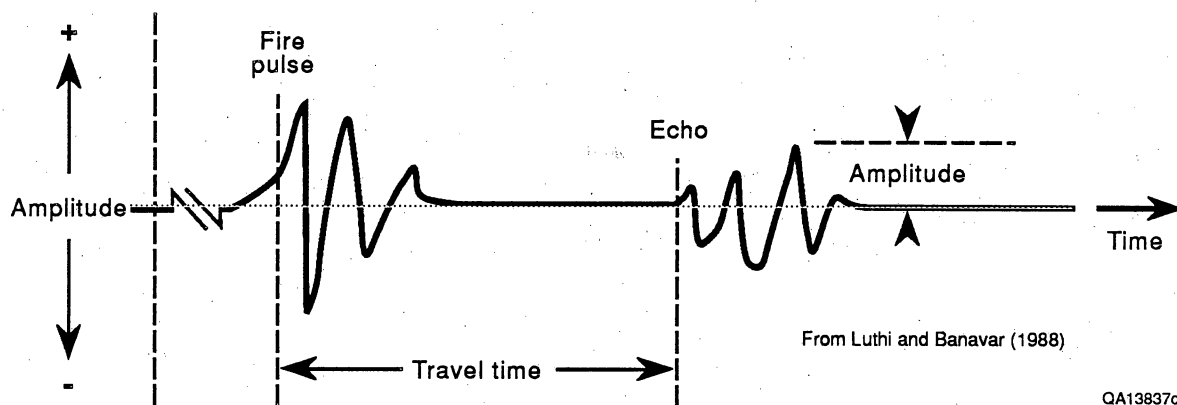
Principles of FMS operation and use are described by Ekstrom and others (1986), Pezard and Luthi (1988), and Bourke and others (1989). The FMS is an electrical tool that creates an image based on measurements of current intensity, or conductance, and presents results as microresistivity (Bourke and others, 1989). The tools used in our study employ two 2.8-inch-wide (7-cm) microelectrical scanning arrays of 27 0.2-inch-diameter (0.5-cm) electrodes placed on orthogonal dipmeter pads for sampling microconductance variations on the borehole wall



From Luthi and Banavar (1988)

QA13836c

Figure 3. Diagram illustrating elements of the borehole televiewer (BHTV) (from Luthi and Banavar, 1988). The acoustic BHTV utilizes a rotating transducer operating in pulse-echo mode to scan the entire circumference of the borehole wall. Variations in rock type, fractures, and borehole geometry change the measured travel times and amplitudes. These variations are used to create an image of the borehole wall.



QA13837c

Figure 4. Acoustic signal and amplitude and travel time of the reflected wave from which BHTV images are obtained. Modified from Luthi and Banavar, 1988.

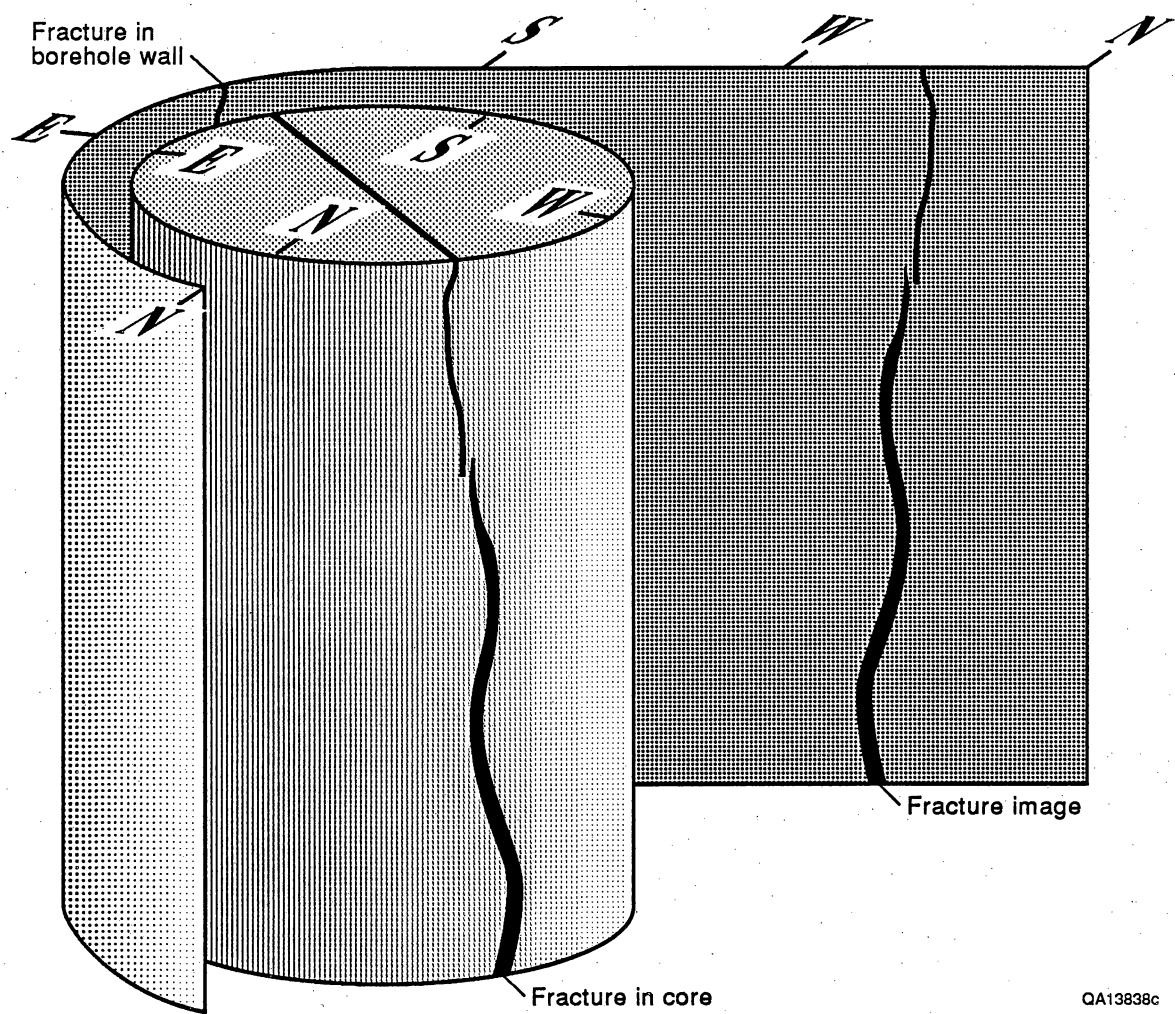


Figure 5. Diagram illustrating the geometric relation of borehole images and the borehole wall (the log presents an unwrapped image of the borehole wall).

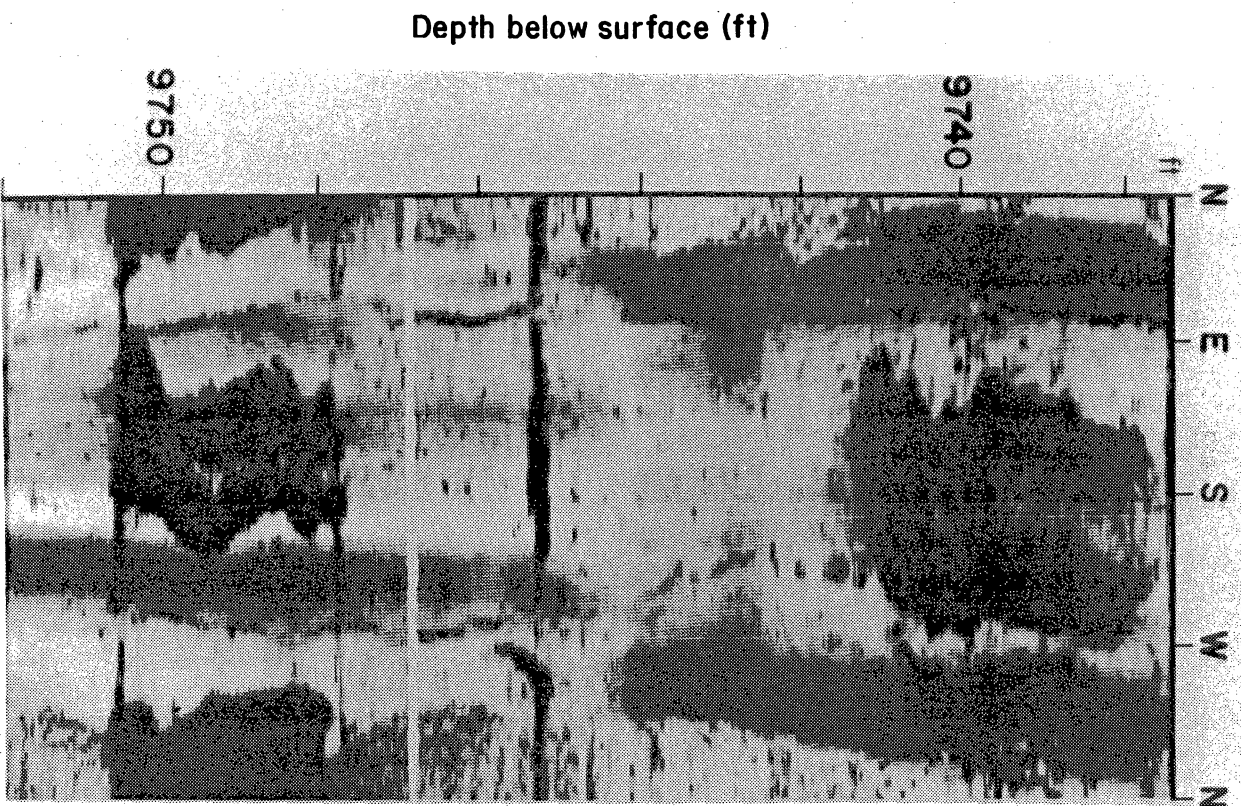
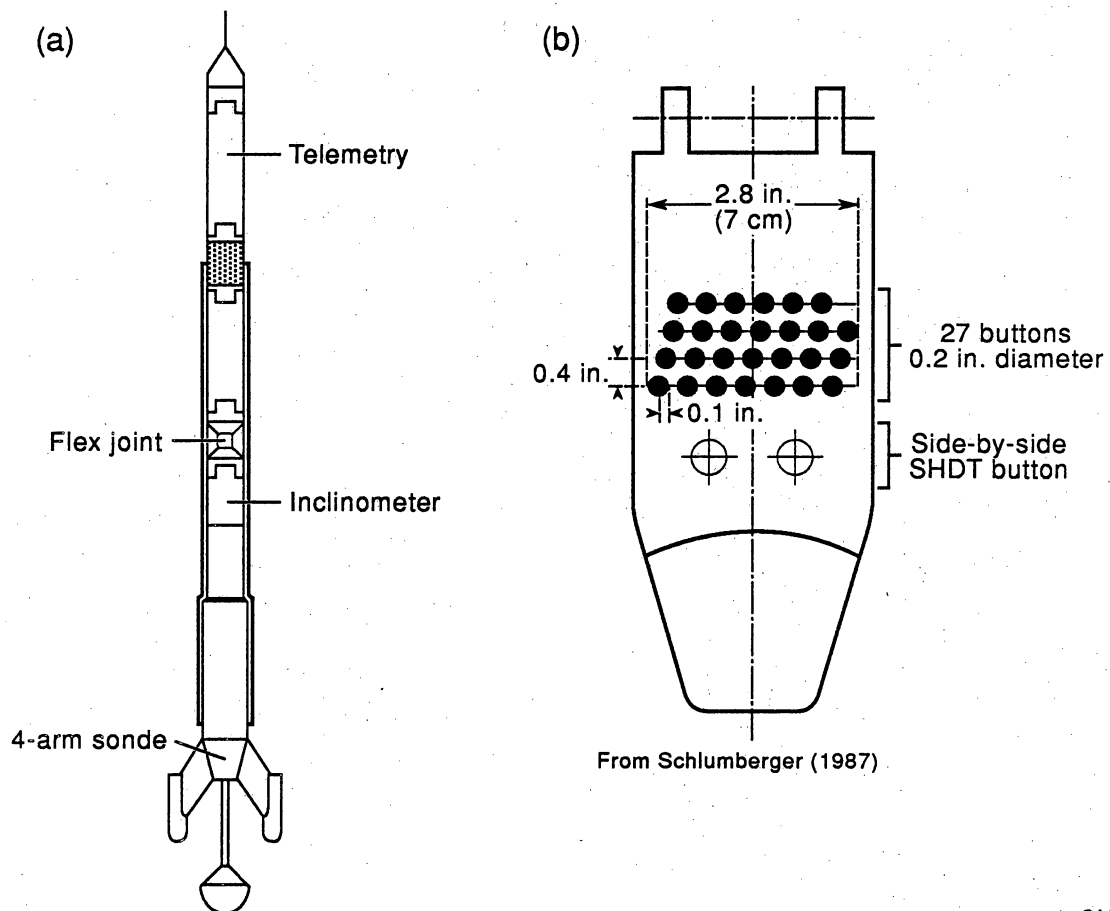


Figure 6. Example of fractures and breakouts on BHTV log, Holditch SFE No. 2 well.

(Schlumberger, Ltd., 1987) (fig. 7). This tool differs from some tools now used in industry that have four pads equipped with scanning arrays of 16 electrodes because such tools have inherently greater borehole coverage (Bourke and others, 1989). A single logging pass using a two-pad tool covers only about 20 percent of an 8.5-inch (21.6-cm) diameter borehole, but in this study, and in many industrial applications, multiple logging passes were used in an attempt to sample more of the borehole wall. In slightly elliptical boreholes, however, the tendency for the tool to track the same path on the borehole wall can prevent multiple passes from increasing coverage. The electrical resistance of the rock is sensed to a depth of a few centimeters beyond the borehole wall (Pezard and Lovell, 1990). The tool is designed for use in water-based drilling mud. The orientation of the tool is determined using three-axis accelerometers and flux-gate magnetometers.

Processing of FMS resistivity data (the continuous conductivity traces produced by each electrode in the closely spaced scanning array) produces a map on which high resistivity values correspond to light gray shades and low values correspond to dark gray shades (fig. 8). Open, conductive fractures filled with drilling mud and layers of conductive rock are dark on FMS images. Results of multiple logging passes were merged and presented in an "unwrapped borehole" format similar to that of the BHTV log (the BOREMAP format). Data were plotted at horizontal and vertical scales of 1:5.

The quality and information provided by BHTV and FMS images depend on image processing, scale of presentation, type of presentation (for example, color or grey scale), and other considerations. For instance, shading on FMS logs can vary depending on the scheme by which current intensity is translated into gray- (or color-) scale images (fig. 9). In one procedure, static normalization, tool response is normalized over a large depth interval. Given this normalization a certain shade of gray represents the same resistivity value through a large section of log. In other normalization schemes linear and nonlinear transformations are used over various intervals (Bourke and others, 1989, p. 19). The most useful presentation can be arrived at through interactive display of different formats on image-processing



QA13839c

Figure 7. Simplified diagram of the Formation Microscanner (FMS) tool. (a) Overall plan of tool. (b) Pad configuration. Modified from Schlumberger, Ltd., 1987.

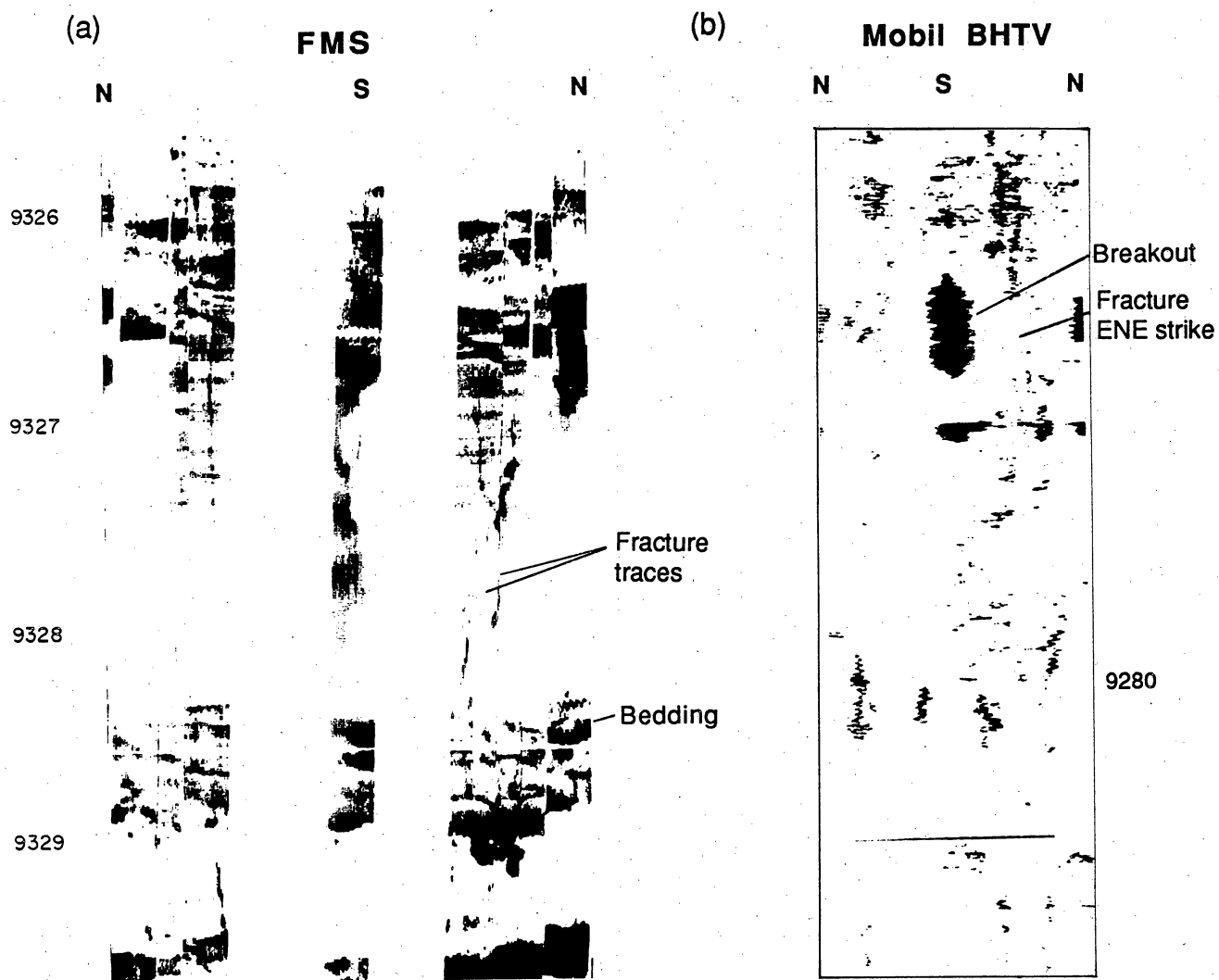


Figure 8. Fractures in reservoir rocks imaged using (a) FMS and (b) BHTV logs. Examples are from the Jurassic Cotton Valley Group, Mobil Cargill No. 15 (SFE No. 3) well, Waskom field, Harrison County. On FMS image, white areas are highly resistive, and black areas are conductive.

Depth
(ft)

(a) Static Normalized

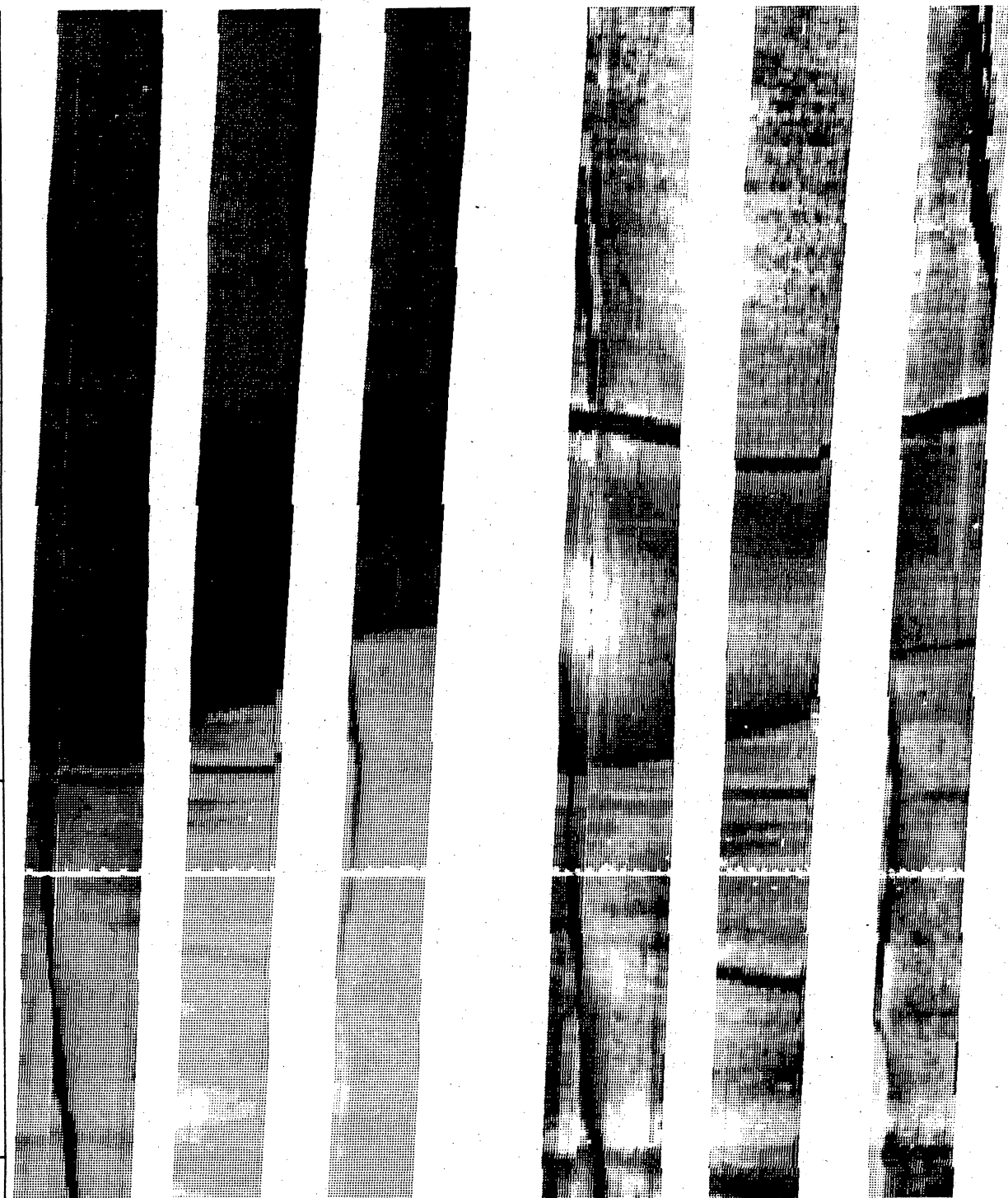
(b) Dynamic Normalized (HILITE)

9205

9206

9207

9208



QA 14459

Figure 9. FMS logs from the Mobil Cargill No. 15 (SFE No. 3) well showing (a) static normalized image and (b) dynamic normalized (HILITE) images.

workstations (Schlumberger, Ltd., 1987; ResTech, Inc., written communication, 1990). Because the application and assessment of these image-processing refinements are beyond the scope of our study, we used FMS logs that had been generated using static normalization for our comparisons with core, and our description and discussion focus on applications that do not depend on the fine-tuning of image quality (fig. 10).

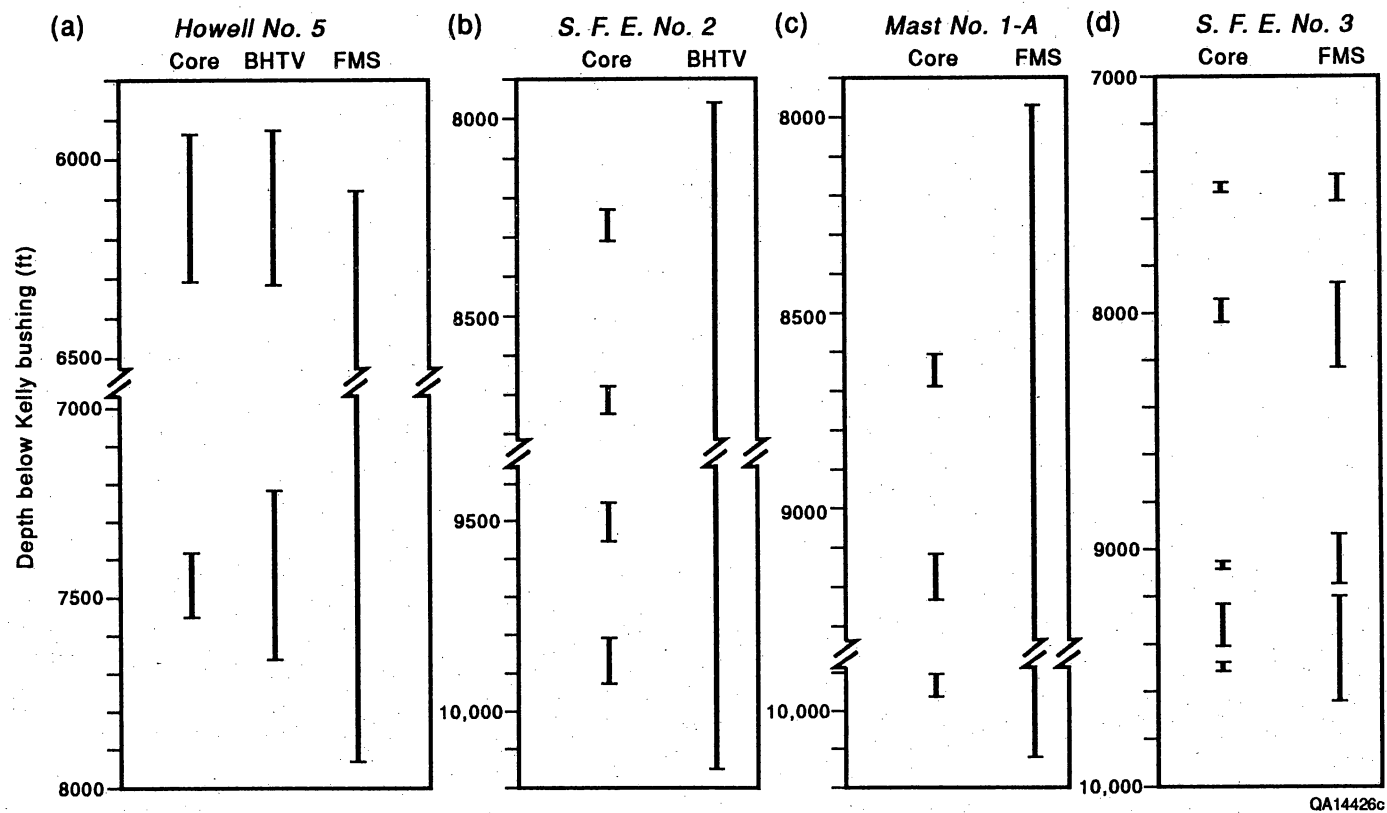


Figure 10. Chart showing well depths cored and well depths surveyed by the BHTV and FMS in the four wells of this study.

PART ONE: APPLICATION OF FMS LOGS TO THE ANALYSIS OF SEDIMENTARY ROCKS IN THE COTTON VALLEY GROUP AND TRAVIS PEAK FORMATION, EAST TEXAS

Robert L. Buehring and H. Scott Hamlin

OBJECTIVES

In this section we compare FMS log responses with sedimentary and diagenetic features observed in cores of nonmarine and marginal marine sandstone and shale sequences in the Cotton Valley Group and Travis Peak Formation of East Texas. The comparison is based on detailed study of lithologic, sedimentologic, and cementation patterns in core from one well in Waskom field, Harrison County—the Mobil Cargill No. 15 (SFE No. 3) (fig. 11)—and illustrated by 13 examples of core-to-log comparisons (figs. 12 through 25). Analysis of small-scale features that affect porosity and permeability distributions within a reservoir is essential to geologic reservoir characterization. Because of its centimeter- to millimeter-scale vertical resolution, the FMS is a useful tool for analyzing small-scale features. Interpretations of field- to regional-scale depositional setting and depositional facies can be refined by the identification of small-scale sedimentologic features and sequences in core or on the FMS log. Our objectives are to provide calibration of the FMS log that can be used to interpret logs from uncored wells in this area and to provide information useful for interpreting FMS images in clastic sequences in other areas. Other recent investigations of FMS performance in clastic sequences include Plumb and Luthi (1986); Harker and others (1990); and Luthi (1990).

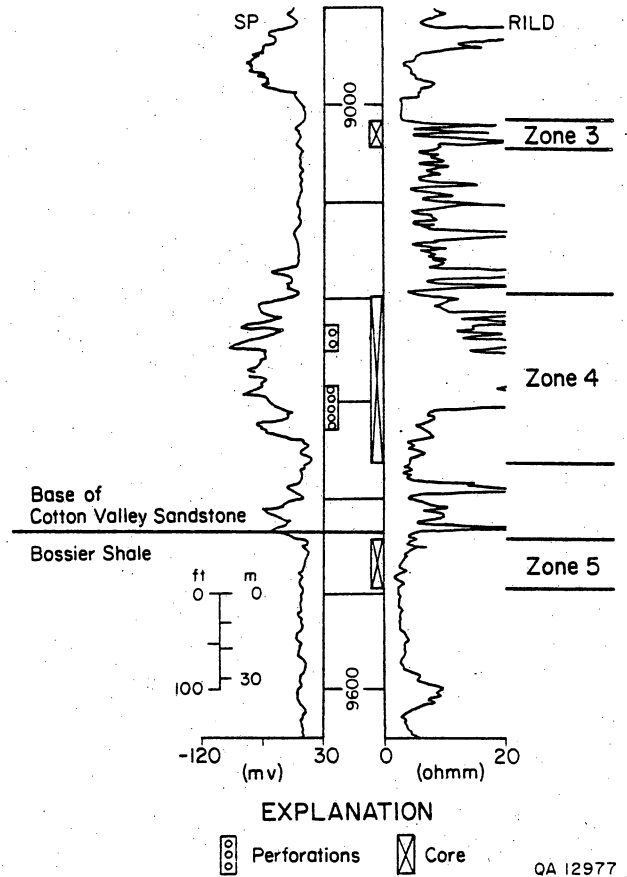
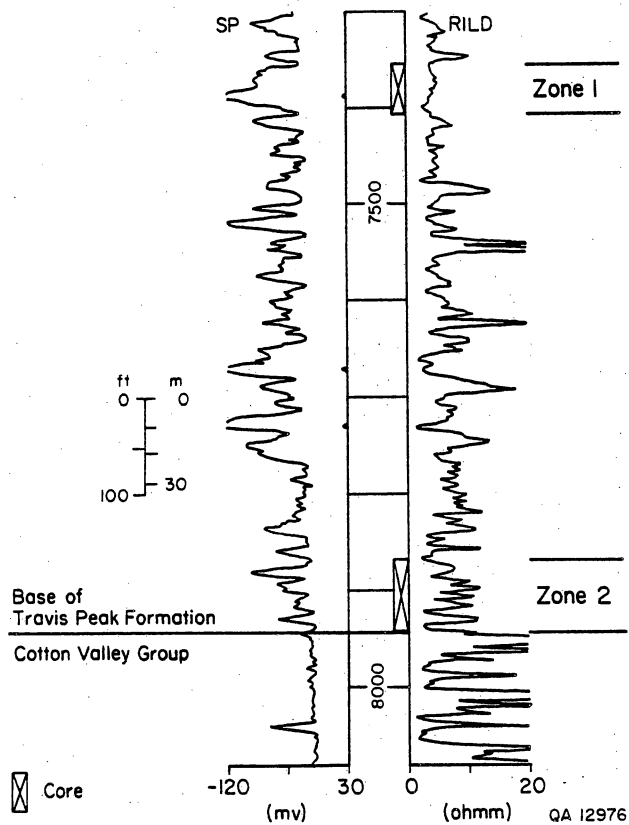


Figure 11. Gamma-ray and resistivity logs of lower Travis Peak Formation, lower Cotton Valley Sandstone, and Bossier Shale, Mobil Cargill No. 15 (SFE No. 3) well, showing cored and perforated intervals. From Dutton and others, 1990.

Methodology

Our study involved visual comparison of 129 ft (39 m) of Travis Peak core and 192 ft (59 m) of Cotton Valley core (fig. 11) with the FMS log displayed in gray-scale format using static normalization over 1,000 ft (300 m) intervals. An additional 51 ft (15 m) of Bossier Shale core and FMS log were not studied in detail, and we did not use color output or manipulate FMS images on a work station.

Cores were described in detail for lithology, sedimentary structures, and calcite cementation. Sand and mud percents were estimated under a binocular microscope; calcite content was determined by degree of reaction with 10 percent hydrochloric acid. Accurately assessing quartz overgrowth cementation and clay mineral content at the necessary vertical resolution of a few inches (centimeters) or less would have required a prohibitive amount of petrographic analysis and was therefore not included in this study. Core observations and photographs printed at a scale the same as that of the FMS log (1:5) were used to select intervals for study and to correct core-measured depths to log depths. Sixty-two core intervals 3 to 4 ft (1 m) in length were compared with corresponding FMS patterns.

Because only one well was studied, we will not address variations in FMS performance as a function of drilling-related variables such as borehole-fluid properties and hole diameter. Table 1 shows borehole conditions of Mobil Cargill No. 15 during logging using the FMS tool.

Depositional Setting

In East Texas, the Jurassic and Cretaceous Cotton Valley Group and Travis Peak Formation are composed of interbedded sandstone and shale facies, which record the first major period of progradation into the Gulf of Mexico Basin. In updip parts of the basin, such as the Waskom field area, the Travis Peak unconformably overlies the Cotton Valley Group,

Table 1. Borehole conditions during FMS logging,
Mobil Cargill No. 15 (SFE No. 3) well.

| | |
|---|--------------------------------------|
| Bit size | 8 ³ / ₄ inches |
| Type fluid in hole | K-LIG |
| Bottom Hole Temperature (BHT) | 245° F |
| Mud weight | 10.70 lb/gal |
| Mud resistivity | 1.490 ohmm at 102° F |
| Mud resistivity at BHT | 0.664 ohmm at 245° F Mudcake |
| Resistivity (calculated) | 2.250 ohmm at 80° F |
| Circulation ended 2 days before logging | |

whereas downdip, the Travis Peak is separated from the Cotton Valley Group by a thin, transgressive-marine deposit, the Knowles Limestone (Tye, 1989). In the SFE No. 3 well, core from the lower Cotton Valley Group (9,199 to 9,368 ft [2,803 to 2,855 m]) contains rock types and sedimentary structures characteristic of a marine-shoreline setting (table 2). Core from the Travis Peak Formation contains rock types and sedimentary structures characteristic of a coastal-plain fluvial setting (7,351 to 7,943 ft [2,240 to 2,420 m]) (table 2). The Cotton Valley Group is 1,494 ft (455 m) thick in SFE No. 2, the top at a depth of 7,942 ft (2,420 m). The Travis Peak is 2,034 ft (620 m) thick in the SFE No. 3 well, and the top of the Travis Peak lies at a depth of 5,908 ft (1,800 m). The Travis Peak Formation is gradationally overlain by micritic and oolitic limestones of the Cretaceous Sligo Formation forming a time-transgressive boundary (Bebout and others, 1981).

GENERAL OBSERVATIONS

This section summarizes the results of our core-log comparison. In the next section, 13 detailed examples are presented that illustrate our general conclusions. In most of the examples used in this study, variations in rock composition are clearly recorded on FMS images. Carbonate, quartz, (including chert), and coal are highly resistive and generally appear bright (light gray to white) on the FMS log. Clay-rich (shaly) rocks have low resistivities and correspondingly darker FMS images. Potential effects of pore-fluid composition were not considered in this study.

Variations in FMS-recorded resistivity in sandstone/shale sequences reflect primarily clay content but may also be responding to grain-size changes. Sandstone shaliness can be qualitatively ascertained in most cases where carbonate cement is a minor component of the rock. Quantitative shaliness determinations require calibration with core because FMS gray-scale intensity varies with processing (Bourke and others, 1989). In the examples used in this

Table 2. Depositional facies identified in core from the Mobil Cargill No. 15 (SFE No. 3) well. From Tye (1989).

A. Marine-shoreline facies in the lower Cotton Valley Group

| Facies | Environment |
|---|--------------------|
| 1. Sandstone, well sorted, well laminated, commonly crossbedded, locally bioturbated, sparsely fossiliferous | Shoreface |
| 2. Pebbly sandstone, erosionally based, ripple laminated, locally bioturbated and fossiliferous | Tidal inlet |
| 3. Sandy silty mudstone, bioturbated and fossiliferous | Lagoon-marsh |

B. Coastal plain and fluvial facies in the Travis Peak Formation

| Facies | Environment |
|--|--------------------|
| 1. Conglomeratic sandstone, erosionally based, abundant clay clasts | Channel-floor |
| 2. Sandstone, ripple and planar laminated, crossbedded | Channel |
| 3. Sandstone and mudstone, planar laminated, bioturbated | Abandoned channel |
| 4. Muddy sandstone ripple laminated, bioturbated | Overbank |
| 5. Sandy mudstone thoroughly bioturbated | Lacustrine |

C. Low-energy marginal marine facies in the Travis Peak Formation

| Facies | Environment |
|---|--------------------|
| 1. Silty sandstone ripple laminated, bioturbated, fossiliferous | Storm |
| 2. Sandy mudstone bioturbated, fossiliferous | Protected bay |

study, sandstone grain size has a narrow range, between very fine grained and fine grained. These slight differences generally could not be distinguished on the FMS log.

High-resistivity carbonate beds and cemented zones appear bright on the FMS log, masking responses from the clastic component of the rock and obscuring primary sedimentary structures. In our examples, carbonate rock generally has a bright, subtly mottled FMS pattern, whereas carbonate cemented sandstone generally has a bright, uniform to faintly laminated pattern. In some cases extensive carbonate cementation completely masks the log response to thin shale interbeds.

Sedimentary layering in sandstone and shale commonly can be interpreted directly from the FMS log. Laminae as thin as 2 mm are resolved where sufficient resistivity contrast exists (quartz/clay interlamination), where the tool is in good contact with the borehole wall, and where carbonate cement is absent. In clean (clay-free) sandstone, lamination (for example, horizontal and inclined bedding) is generally not recorded. However, a faint layered FMS pattern accurately reflects lamination in clean sandstone in a few of our examples. Grain-size variations and trace quantities of clay probably cause these slight resistivity differences.

Irregularly shaped objects, such as pebbles, mud clasts, burrows, and carbonate shells, are recorded on the FMS log by ambiguous mottled patterns. We found no universally reliable criteria for differentiating among these sedimentary features without core or specific knowledge of the geologic context. A mottled FMS pattern directly overlying a sharp erosional contact probably represents mud clasts or pebbles (or both). Mud clasts and mud-filled burrows (low resistivity) can locally be distinguished from quartz pebbles and carbonate shells (high resistivity). Burrows and shells can be identified in a few cases by distinctive shapes. Pebbles can be distinguished locally by their roundness, especially where they are enclosed in a fine-grained matrix.

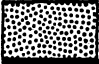


CORE/LOG COMPARISON EXAMPLES

Six examples of Cotton Valley core/log comparisons and seven Travis Peak examples illustrate the expression on FMS logs of the lithologic, sedimentologic, and diagenetic features discussed earlier. The description of each example interval includes a figure containing a core photograph, its correlative FMS log, and core description logs of sedimentary structures and rock type (fig. 12). FMS logs were displayed in the BOREMAP format, where the results of several passes of the tool are merged. In this format, the logs are unwrapped images of the borehole wall, and the horizontal axis of the plot is a scale from north to south to north. In the figures in this report, however, only part of the BOREMAP image has been presented, so the orientation of features cannot be read directly from the figures. The descriptions of sedimentary structures consist of sketches of the core that use symbols for some features. The lithology logs show percent sand, mud, and carbonate in 10-percent increments. The carbonate is in the form of cement unless otherwise noted as shells or limestone. Depths are log depths except where core depths are specified, and core photographs have been shifted to correspond to log depth. Accuracy of core-to-log matching of features is generally excellent in SFE No. 3. Fifty-eight of the core intervals studied could be confidently matched to the FMS to within 1 inch (3 cm) or less. Four intervals from a thick sequence of fossiliferous shale lacking distinctive bedding planes or sequences of bedding planes could be matched to the log only to within 2 to 4 inches (5 to 10 cm). Examples 1 through 6 are from the Cotton Valley Group and examples 7 through 13 are from the Travis Peak Formation. Metric equivalents will not be given in the examples.


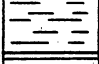

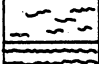
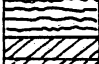

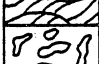
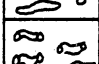
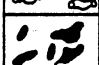
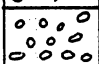
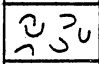
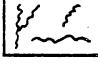

Example 1. This fairly uniform sequence of clean to slightly shaly sandstone contains faint to prominent horizontal and gently inclined laminations (fig. 13). The sandstone from 9,292.1 ft to 9,292.3 ft and below 9,292.6 ft has a clay content slightly higher than the

EXPLANATION

Lithology

| | |
|---|-----------|
|  | Sandstone |
|  | Shale |
|  | Carbonate |

Structures

| | |
|---|--------------------------------|
|  | Structureless |
|  | Faint laminae |
|  | Prominent laminae |
|  | Faint organic-rich laminae |
|  | Prominent organic-rich laminae |
|  | Tabular crossbeds |
|  | Trough crossbeds |
|  | Individual burrows |
|  | Intense bioturbation |
|  | Mud clasts |
|  | Chert pebbles |
|  | Mollusk shells |
|  | Fractures |

QA14020

Figure 12. Symbols used in core and log descriptions.

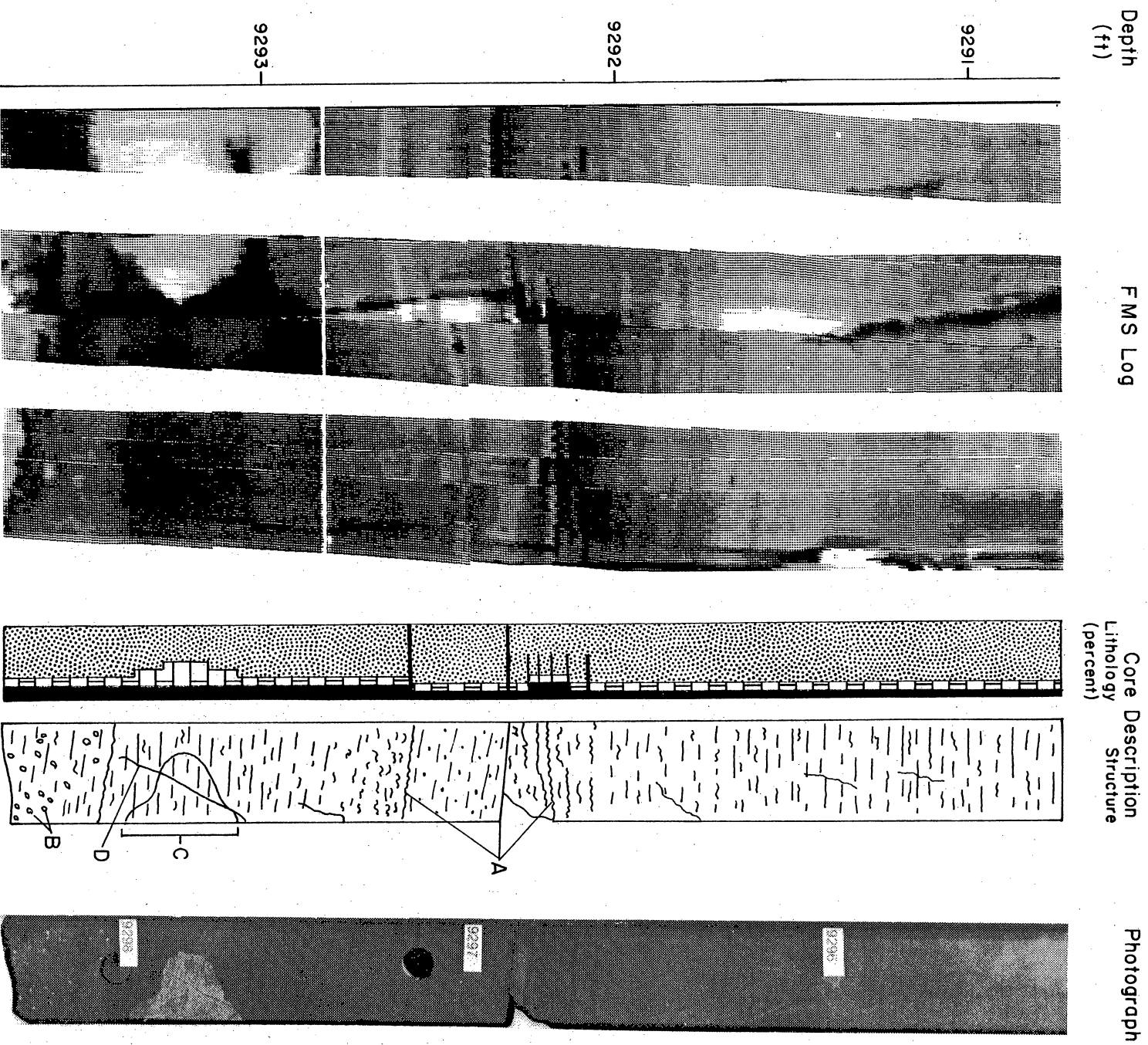


Figure 13. FMS log and core description from Mobil Cargill No. 15 (SFE No. 3) well (Example 1). This example illustrates log patterns of sandstone containing shale laminae (A), pebbles (B), patchy calcite cement (C), and coring-induced fractures (D and elsewhere) in the Cotton Valley Group. Features E and F on the log are a fold in the log paper and points where results of multiple logging runs have been spliced.

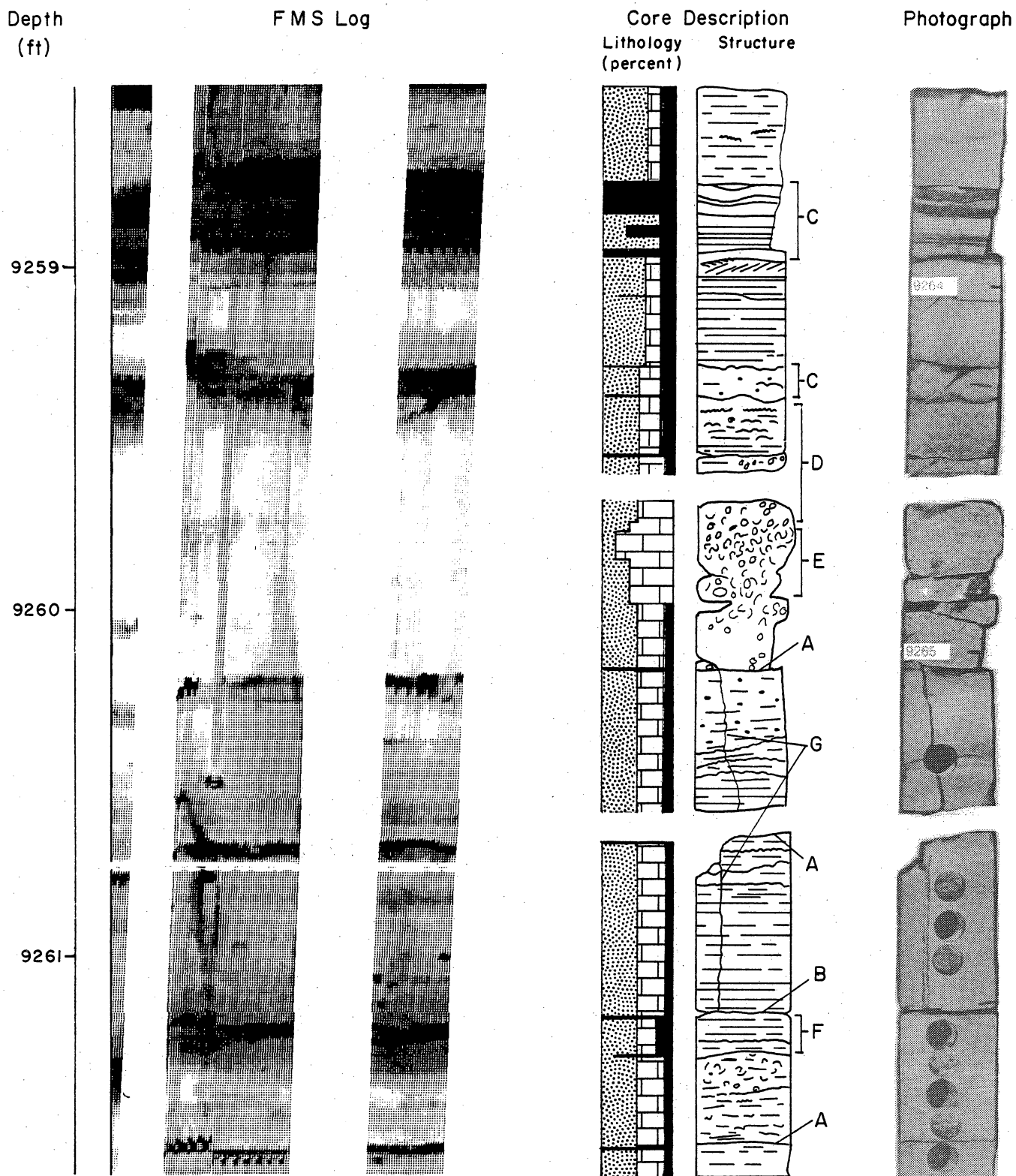
0A14007

surrounding sandstone and therefore appears darker on the log. Only the most prominent laminations in the core (A) can be distinguished on the log, where abundant clay particles provide a high-resistivity contrast with the surrounding sandstone. The mottled pattern below 9,293.5 ft represents scattered chert pebbles (B). These clasts range from 0.1 to 0.3 inches in diameter, and they produce a vague mottled pattern on the log that is difficult to distinguish from log patterns in parts of the borehole where clasts are absent, such as at 9,291 ft. Mud clasts and burrows cause mottled patterns similar or identical to those in B elsewhere on the Mobil Cargill No. 15 log, such as at A in example 7 (fig. 19) and from 7,875 ft to 7,876 ft in example 8 (fig. 20).

Minor calcite cement is uniformly distributed throughout this interval except from 9,293.0 ft to 9,293.4 ft, where a patchy zone of massive cementation (C) is well defined on the log by the light-colored area. This irregular pattern of massive cementation cuts across sedimentary features in the core, and it is bisected by a drilling-induced fracture (D). This core interval lacks natural fractures, and the conductive, linear, sharp-sided vertical features visible on the log may correspond to drilling-induced fractures in the borehole wall (see Part Two).

The sharp, horizontal white line (E) on the log is caused by a fold in the log paper. The sharp vertical lines (F) on the log occur where the results of merged logging passes overlap. Fold lines and overlaps occur in most of the following examples and should not be mistaken for FMS log features.

Example 2. Horizontally laminated sandstones and rare ripple-bedded sandstones are interbedded with thin shale layers and a shelly, pebbly limestone (fig. 14). Several types of FMS response to shale are shown here. One type is thin, distinct dark bands on the log that correspond to single, isolated shale lamina (A). A second type is a thin but indistinct dark band corresponding to a single shale lamina (B). A third type is the wide distinct dark bands that



QA14008

Figure 14. FMS log and core description from Mobil Cargill No. 15 (SFE No. 3) well (Example 2). This example illustrates log patterns of shales and shaly laminae (A, B, and C), calcite-cemented sandstone (D, F, and elsewhere), limestone (E), and natural fractures (G) in the Cotton Valley Group.

correspond to thinly interbedded sandstones and shales (C). Individual beds are not resolved on the log.

Calcite cement is abundant throughout the interval. The sandstone (D) overlying the limestone (E) is so completely cemented that it cannot be distinguished from the underlying limestone. The dark interval (F) is highly cemented; however, low resistivity here is caused by high clay content, which masks any increase in resistivity caused by cement.

The prominent natural fracture (G) is open and contains quartz and calcite and visible fracture porosity. Maximum open-fracture width is less than 0.02 inches in core. The faint linear vertical features on the log above 9,260.5 ft and below 9,259 ft are most likely image-processing artifacts or possibly a temporary malfunction of a button on the FMS pad. The vertical conductive anomaly above 9,261 ft may correspond to the natural fracture G.

Example 3. Horizontally laminated sandstone is overlain by pebbly sandstone grading upward into pebbly limestone containing sparse mud clasts (fig. 15). Within the sandstones are two prominent shaly laminae (A). The horizontal bedding in the sandstone is readily apparent on the FMS log; however, the thinness of the bedding is resolved only at the two shaly laminae. The pebbles are not visible at all. Faint dark spots on the log at 9,242.7 ft to 9,242.6 ft indicate that a few small mud clasts occur with the pebbles in the sandstone.

Although the entire interval contains at least minor calcite cement, two zones contain abundant cement (B and C). Cementation conforming to bedding at B is well displayed on the log. Cementation in C is similar to that in B but is sharply bounded below by a horizontal fracture (D) instead of a bedding plane.

The cemented zone (C) has a mottled FMS pattern, whereas zone B in this example and zones D and E in example 2 have a more uniform FMS pattern. The mottled pattern in zone C most likely reflects the presence of the mud clasts in this zone.

A calcite-filled vertical fracture in the core (E) appears on the log in the strip to the left as a thick, vertical dark area (Type 2 FMS feature; see Part Two). The apparent offset and

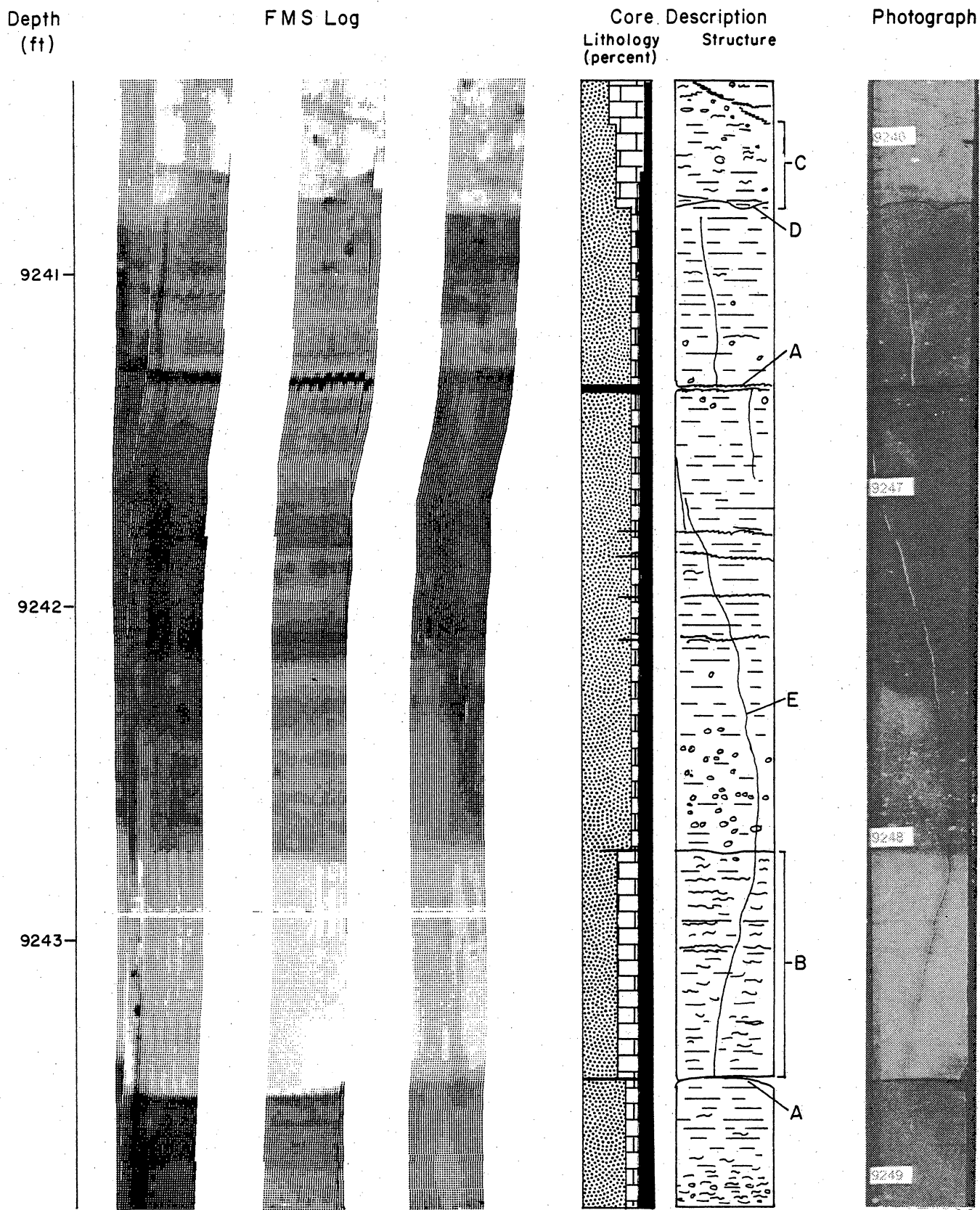


Figure 15. FMS log and core description from Mobil Cargill No. 15 (SFE No. 3) well (Example 3). This example illustrates log patterns of pebbly sandstone containing shaly laminae (A), calcite-cemented beds (B and C), and mineral-filled fractures (D and E) overlain gradually by sandy limestone (above C) in the Cotton Valley Group. Log images (G and F) correspond to the mineral-filled fractures visible in the core.

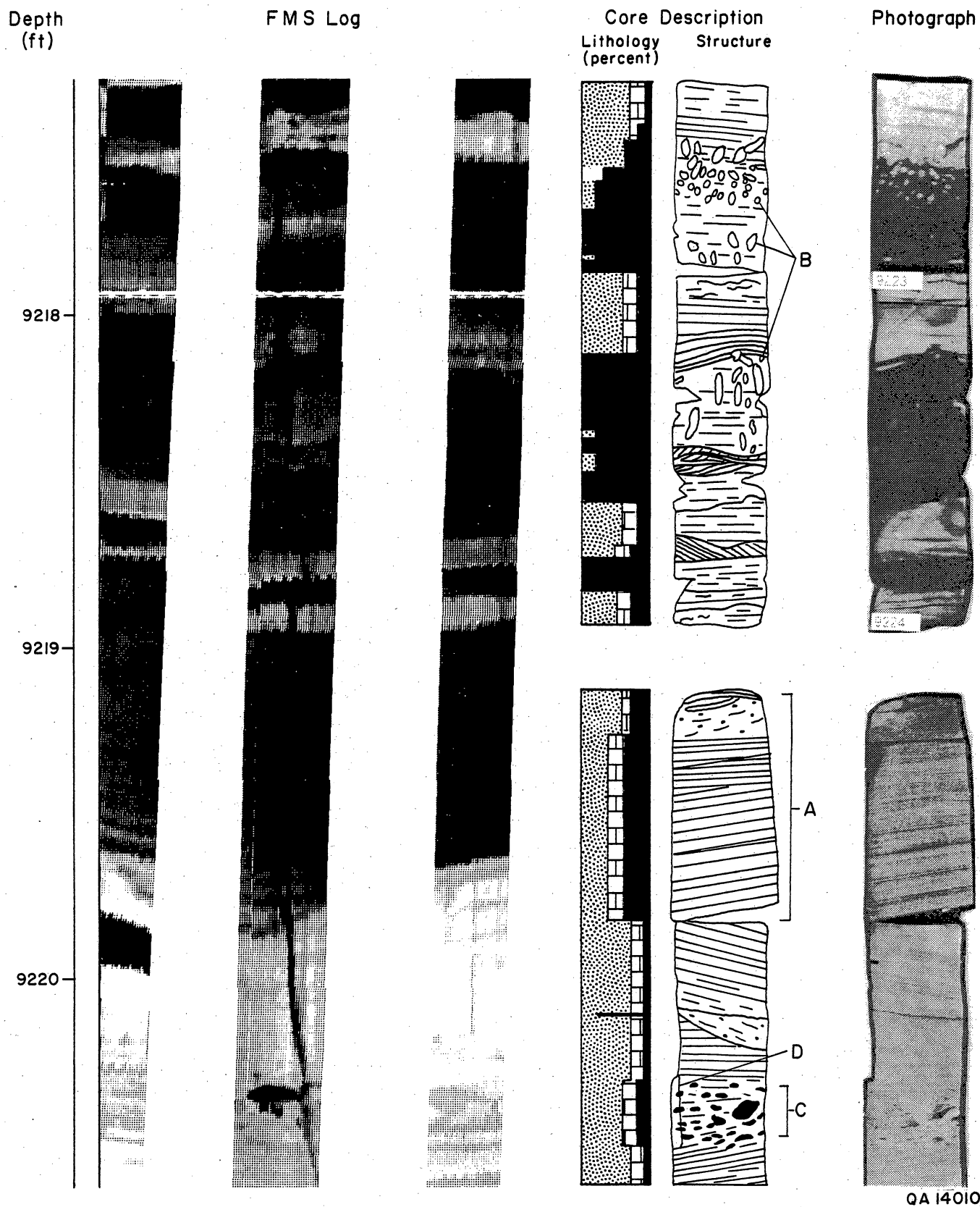
truncation of the fracture in the photograph at the shale lamina (A) at 9,241.3 ft is caused by slabbing of adjacent core pieces along different vertical planes and is not representative of the true shape of the fracture. The fracture probably does not produce a sharp-sided conductivity anomaly on the log because the fracture is largely filled with secondary minerals. The curve of the fracture is partly visible on the right-hand FMS track (F). Near the top of the left log strip (G) the tapering termination of the fracture within sandstone (corresponding to the fracture termination below D on the core photograph) is visible. The lower termination of the fracture at the shale lamina (A) at 9,243.4 ft is not visible on the log, apparently because this feature was not encountered by an FMS pad.

Example 4. Low-angle crossbedded sandstone is interbedded with burrowed shale. In this example the FMS log records a rock type that is difficult to interpret (fig. 16). Interval A is a clean sandstone but it appears black on the log. Low-angle cross-laminae in this sandstone are not visible on the log, whereas similar laminae in the underlying sandstone are. The sandstone is anomalously well cemented, and it possibly contains a conductive mineral such as clay.

Above interval A, the thicknesses and number of sandstone beds cannot be accurately determined from the FMS. Burrows (B) cause a faint mottled texture on the log. A similar mottled appearance is caused by mud clasts (C). The typical dark shades of gray of mud clasts on the log may help distinguish them from more resistive pebbles.

Below interval A, clean quartz-cemented sandstone corresponds to a high resistivity (white) FMS pattern, which is similar to patterns produced by limestone or by carbonate cement in examples 2 and 3.

A drilling-induced fracture (D) is present in the core between 9,220.5 ft and 9,219.8 ft. The fracture image at this depth in the middle log strip corresponds to this fracture. Comparing this fracture image with the drilling-induced fracture in example 1 (fig. 13) and natural



QA 14010

Figure 16. FMS log and core description from Mobil Cargill No. 15 (SFE No. 3) well (Example 4). This example illustrates log patterns of interbedded shale containing large burrows (B) and cross-bedded sandstone that has locally low resistivity (A), mud clasts (C), and a coring-induced fracture (D).

fracture image in example 3 (fig. 15), the drilling-induced fracture appears dark and sharply defined, whereas the natural fracture is less dark and is poorly defined.

Example 5. Muddy, shelly sandstone containing faint, gently inclined laminae overlies interbedded sand and shale with a fluid escape structure (A), pebbles (B), and sparse burrows (C) (fig. 17). As in example 4, sandstone layers appear black or thin where interbedded with shale (below contact D).

Mottling on the log between 9,213.4 ft and 9,213.0 ft is caused by a fluid escape structure. Without core this mottling could be misinterpreted as resulting from burrows or mud clasts.

Above D, the irregular light patches on the log are caused by patches of massive calcite cement in sandstone. This interval contains one large bivalve (E) and abundant small bivalves, the distribution of which appears to influence (localize) the pattern of calcite cementation. Areas of sandstone above D that contain only a trace of carbonate appear black on the log and could be misinterpreted as shale.

Patchy cementation here is similar to cementation in figure 13. The corresponding irregular pattern on FMS is clearly not a primary sedimentary feature and must therefore be a diagenetic feature. The sandstone above D on the right-hand FMS track does not have a uniform pattern on the log. This may partly be a result of the nonuniform cementation in this interval.

Drilling-induced fractures were logged in the core between 9,216.2 ft and 9,216.5 ft (core depth) (9,210.9 ft and 9,211.2 ft, log depth) and from 9,216.8 ft to 9,217.7 ft (core depth) (9,211.5 ft and 9,212.4 ft, log depth). Conductive features that may correspond to these fractures are visible on the left log strip between 9,212.7 ft and 9,211.3 ft.

Example 6. Pebbly, muddy sandstone that has horizontal and inclined laminae is overlain by shelly shale (fig. 18). Mud clasts, chert pebbles and small bivalves (A) correspond to small dark and light spots on the log. A shale lamina (B) is sharply defined on the middle and

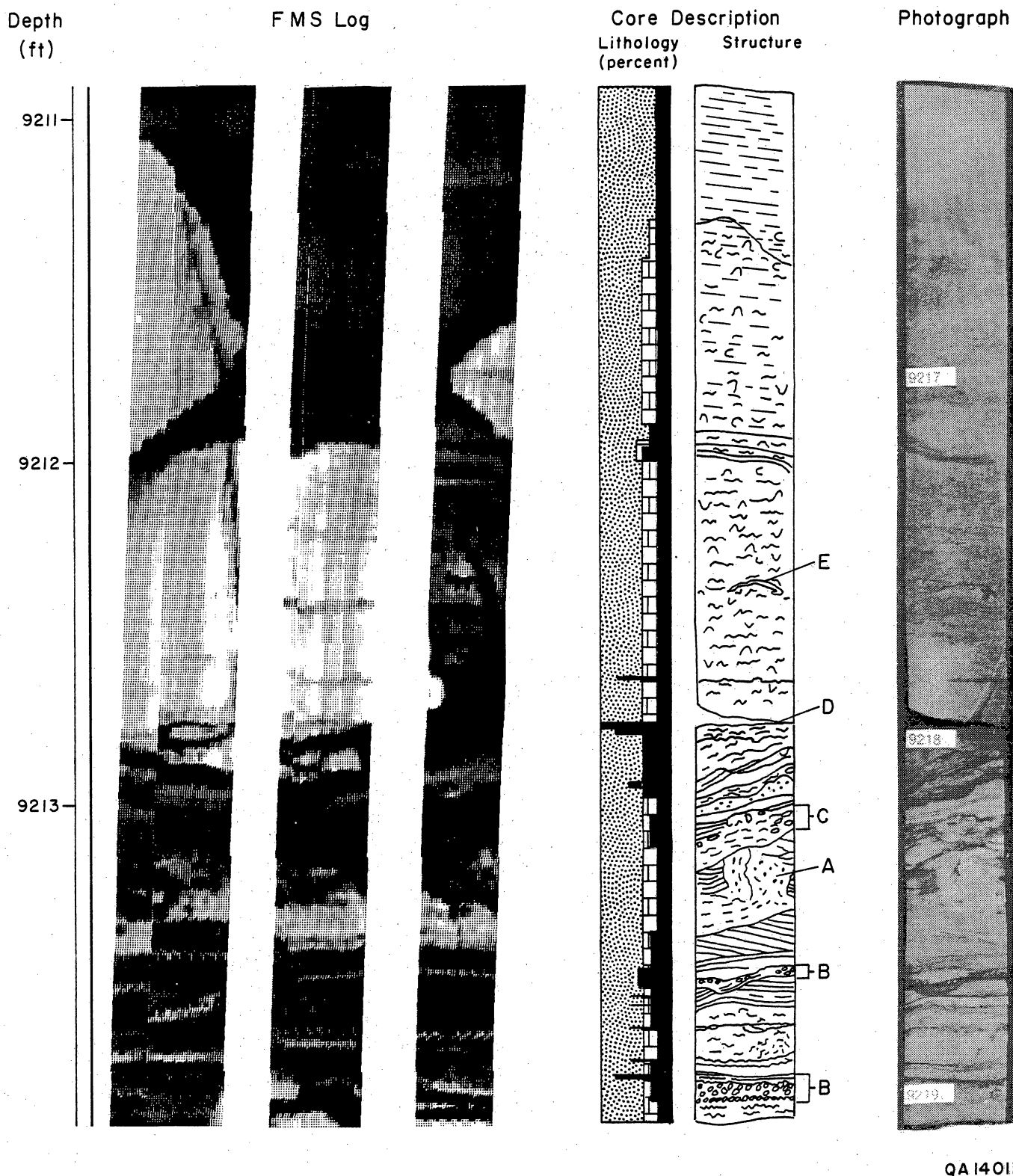


Figure 17. FMS log and core description from Mobil Cargill No. 15 (SFE No. 3) well (Example 5). This example illustrates log patterns of shaly sandstone having soft sediment deformation (A), pebbles (B), mud clasts (C), and thin shale (D), and abundant large and small bivalves (E) in the Cotton Valley Group.

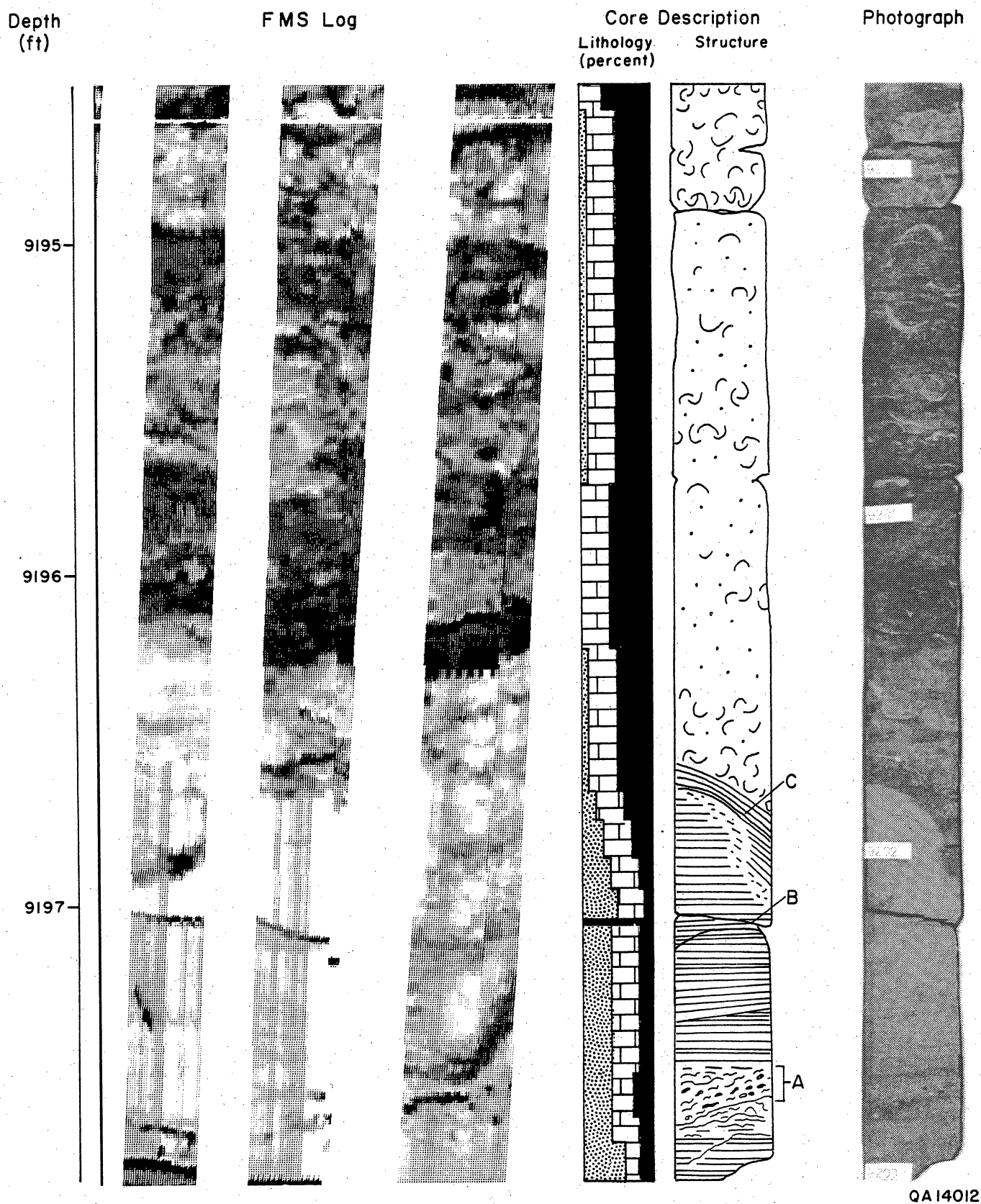


Figure 18. FMS log and core description from Mobil Cargill No. 15 (SFE No. 3) well (Example 6). This example illustrates log patterns of horizontal to low angle crossbedded sandstone exhibiting pebbles and mud clasts (A), a shale lamina (B), and soft sediment deformation (C) overlain by shale containing scattered large bivalves in the Cotton Valley Group.

left log strips. The sandstone-shale contact (C), which shows soft sediment deformation, appears on the middle and left log strips as a wavy boundary between a solid white pattern and an overlying mottled pattern.

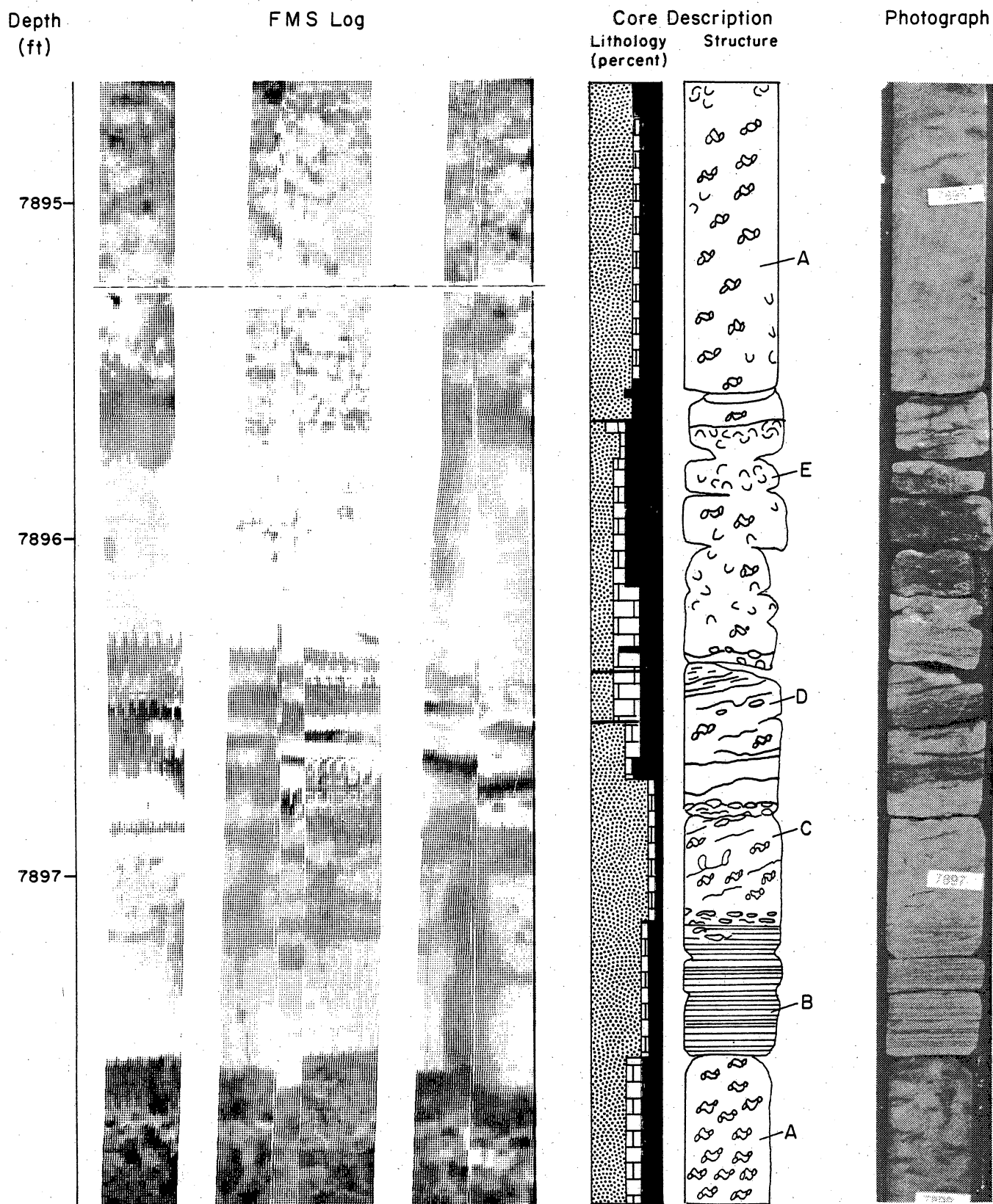
The entire interval contains abundant calcite cement. High resistivity of the cement in the sandstone overprints any resistivity contrast across laminae. The mottled pattern within the shale is caused by abundant large bivalves and gastropods and by uneven carbonate cementation. Though shells are large and easily defined in the core, individual shells cannot be distinguished on the log.

Example 7. Thoroughly bioturbated muddy sandstone at the bottom of this interval (A) is overlain by several interbedded lithologies: horizontally laminated shaly sandstone (B), bioturbated, slightly shaly sandstone (C), shaly sandy limestone (D), and sandy shelly shale (E) (fig. 19). Overlying these is a highly bioturbated, shaly sandstone similar to that at the bottom of this example (A).

The mottling in A is caused by intense bioturbation. The mottling caused by bioturbation and rare shells in this example is nearly identical to mottling caused by abundant shells and cementation in example 6 (fig. 18).

Intervals C and D have similar log patterns. Intervals B and E have identical log patterns. Here different combinations of primary mineralogy, cementation, and possibly pore-fluid type create the same log patterns.

Example 8. Clean sandstone having wavy horizontal laminae is overlain by a thin shale bed (A), bioturbated sandy shale, and bioturbated, shelly shaly sandstone (fig. 20). Though it appears in the core photograph to contain shaly laminae, the sandstone below shale bed A is virtually shale free and has negligible clay cement. This sandstone contains abundant quartz overgrowth cement (~15 %), which apparently causes its bright FMS record.



QA 14013

Figure 19. FMS log and core description from Mobil Cargill No. 15 (SFE No. 3) well (Example 7). This example illustrates log patterns of highly bioturbated shaly sandstone (A), horizontally laminated sandstone (B), bioturbated sandstone (C), shaly, sandy limestone (D), and sandy, shelly shale in the Travis Peak Formation.

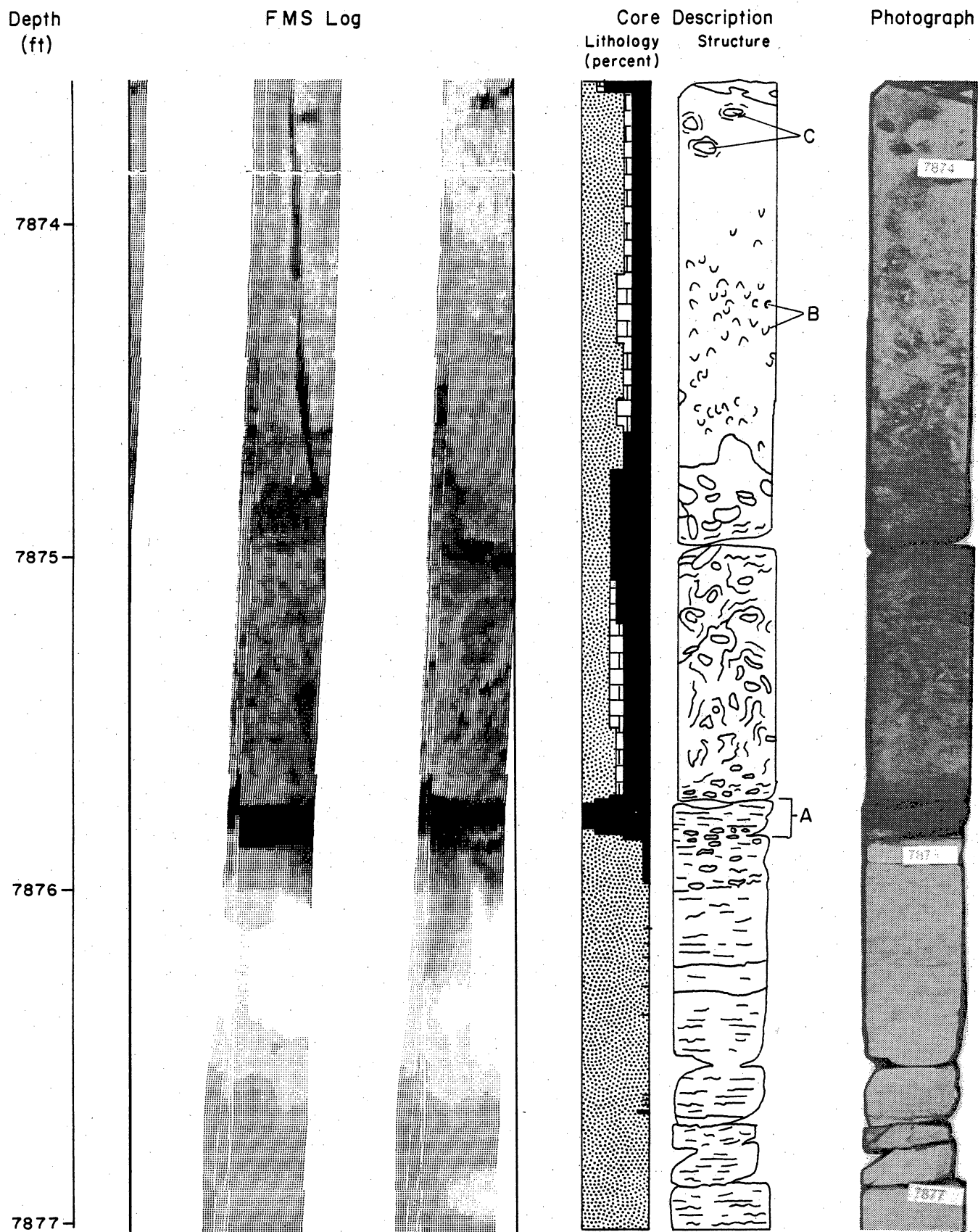


Figure 20. FMS log and core description from Mobil Cargill No. 15 (SFE No. 3) well (Example 8). This example illustrates log patterns of clean sandstone displaying wavy horizontal laminae overlain by shale (A) and bioturbated shaly sand to sandy shale containing abundant small shells (B) and large mud-filled burrows (C) in the Travis Peak Formation.

Above A, the sand/shale ratio generally increases upward, which is reflected on the log by its becoming lighter upward. Individual shells in this interval appear on the log as small white spots, whereas large, mud-filled burrows (C) are seen as large black spots.

A drilling-induced fracture was observed in the core between 7,874.2 ft and 7,872.9 ft. The fracture image on the log extends down nearly to 7,875 ft and has a curve that resembles that of some drilling-induced fractures seen in core (see Part Two).

Example 9. Clean, tabular crossbedded sandstone (A) and faintly horizontally bedded sandstone (B) enclose a single shale bed (C) (fig. 21). Laminae are not recorded on the log, probably because clay is not concentrated along laminae. Similar looking laminae in other examples contain clay concentrations and are recorded on log (around 9,292 ft in example 1 [fig. 13], between 9,241 ft and 9,242 ft in example 3 [fig. 15], and below 9,220 ft in example 4 [fig. 16]).

In this case, however, the boundaries between the black interval and the surrounding gray intervals at 7,395.1 ft and 7,394.7 ft on the log are also poorly resolved. This poor resolution at a sharp resistivity contrast may indicate tool standoff from the borehole wall (Bourke and others, 1989). Mudcake buildup, and therefore probably tool standoff, may be common in more permeable beds.

Shale bed C is located in a thick sequence (13 ft) of uniform sandstone that contains no other distinctive, correlatable features. This shale provides an excellent marker for precisely correcting the core-measured depth of a potential reservoir interval, which is 5.7 ft off from the log depth.

Example 10. Clean to slightly shaly, horizontal, ripple, and medium-scale crossbedded sandstone contains thin shale beds (A), shaly laminae (B), and rare burrows (C) (fig. 22). Thin shale beds and shaly laminae are recorded on the log between 7,385.2 ft and 7,385.6 ft, but other laminations are not recorded and sandstone-shale contacts appear diffused on the FMS. As in

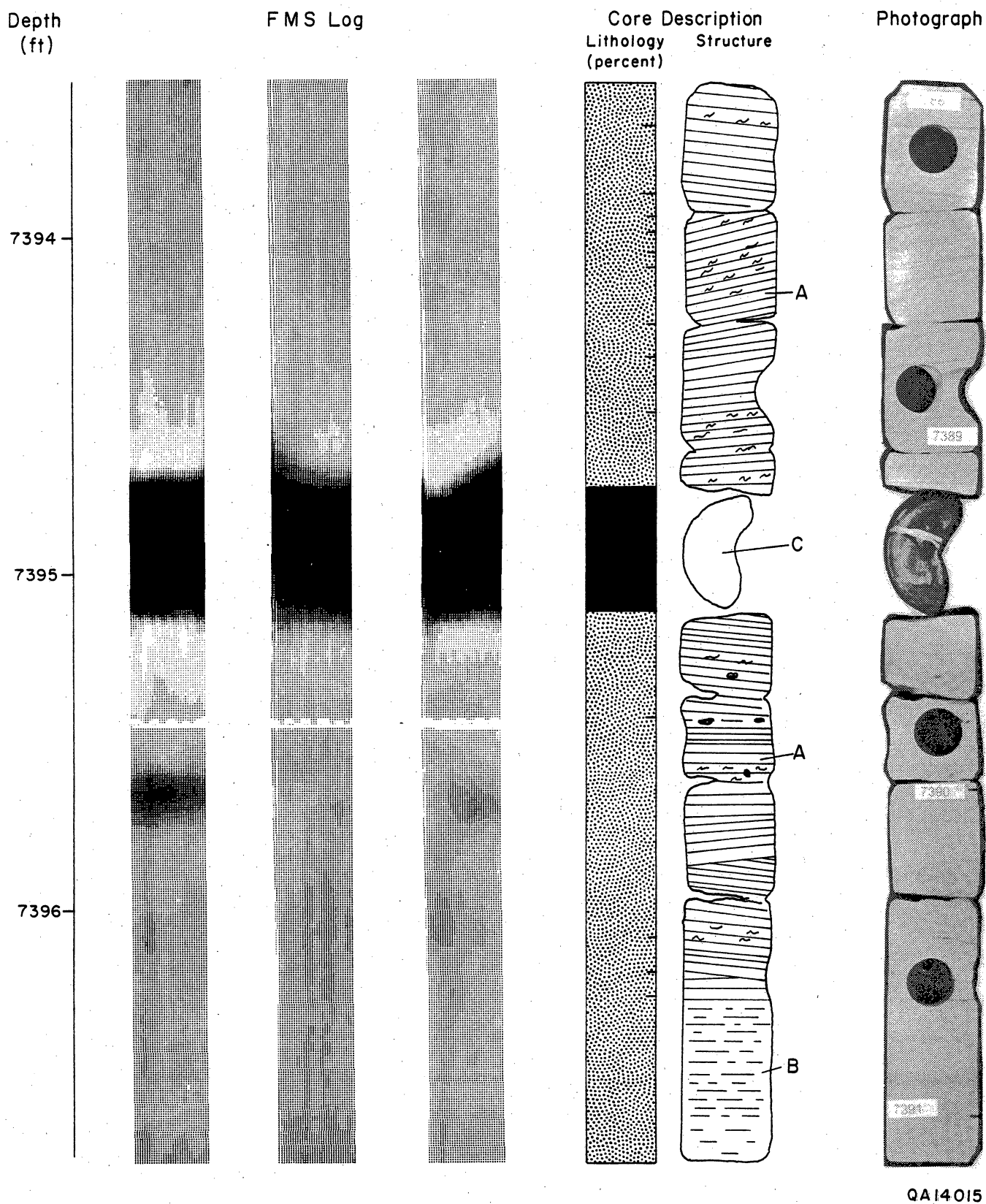


Figure 21. FMS log and core description from Mobil Cargill No. 15 (SFE No. 3) well (Example 9). This example illustrates log patterns of clean sandstone having prominent crossbeds (A), faint horizontal beds (B), and a clay shale (C) in the Travis Peak Formation.

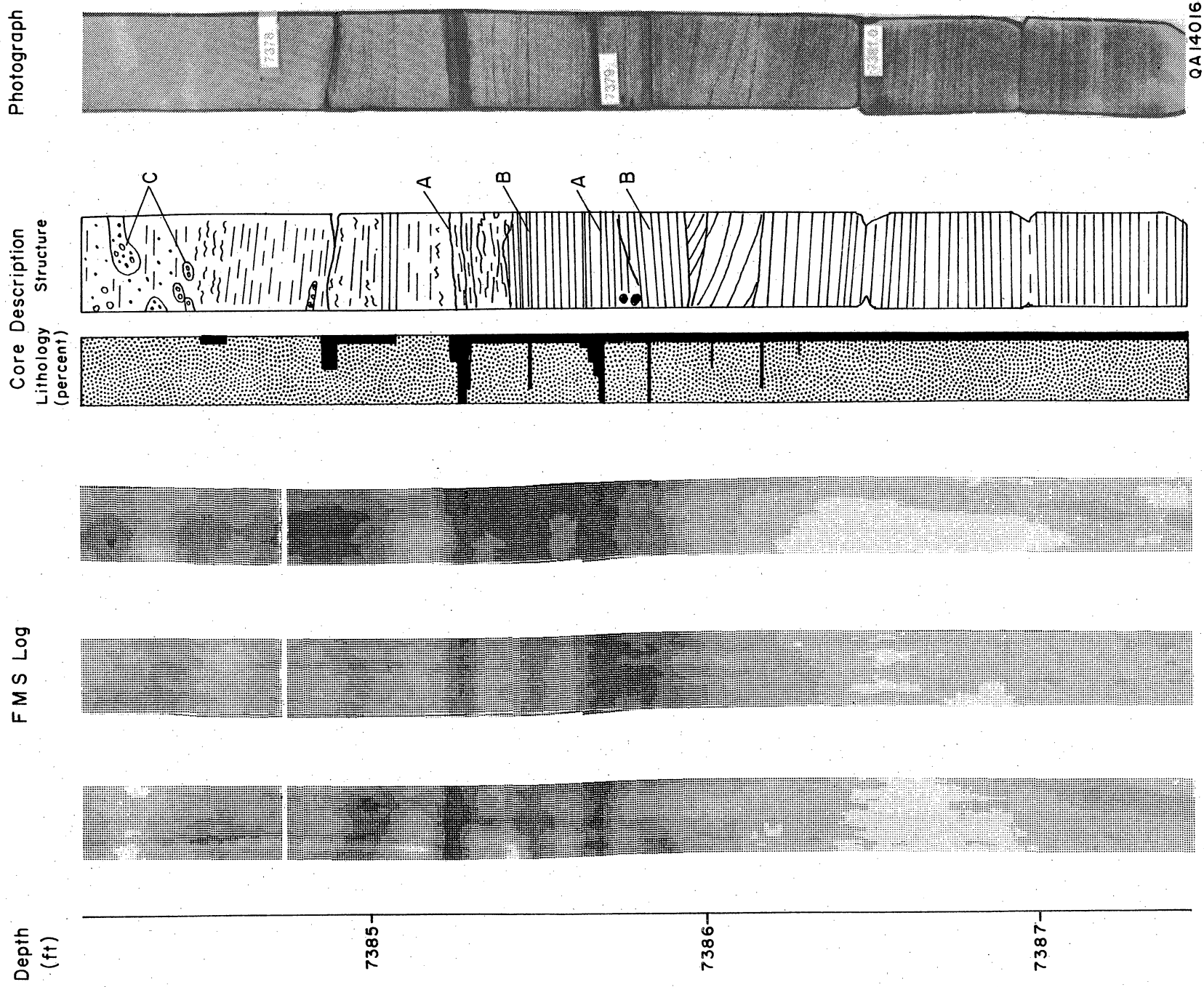


Figure 22. FMS log and core description from Mobil Cargill No. 15 (SFE No. 3) well (Example 10). This example illustrates log patterns of sandstone that have thin shales (A) and shaly laminae (B) and clusters of small burrows displaying reduction haloes (C) in the Travis Peak Formation.

example 9, this poor bed resolution may be due to the lack of clay along unrecorded laminae or to tool standoff.

At 7,384.2 ft clusters of small burrows are surrounded by gray reduction haloes (C). The corresponding FMS log interval displays both light and dark areas, which are about the same size as the haloes. It is unclear how these spots relate to the burrows. The cause of the spot on the left log strip at 7,384.9 ft was not evident in the core because of the distance between the core and the borehole wall.

Example 11. Horizontally laminated sandstone is overlain by bioturbated shaly sandstone to sandy shale containing locally abundant mud clasts and burrows and horizontal to low-angle crossbedded sandstone (fig. 23). Dark gray shades on the log correlate well with mud content except below 7,380.8 ft where clean sandstone is the same medium gray as the slightly shaly sandstone above. In interval A, the shale content is concentrated in mud clasts and burrows; the encasing sand is clean and therefore bright on the log. Faint mottling below interval A represents scattered organic-rich fragments and burrow fills (B), which are similar in composition to that of the surrounding matrix.

Horizontal lamination is not recorded on the log. The 0.2 ft black interval 0.2 ft above interval A represents a shale bed that was not recovered in the core.

Example 12. Clean to shaly, horizontally laminated to low-angle crossbedded sandstone contains thin shale layers and shaly laminations (fig. 24). Dark gray patterns on the log generally reflect shale content throughout this interval except at 7,376.5 ft, where no cause for the black spot on the log was observed in the core, but which was possibly due to the distance between the core and the borehole wall. The darkness of the sandstone in the core photo above 7,375.1 ft does not reflect high shale content. Above 7,375.1 ft the core is highly oxidized and dark red (A), whereas below this it is reduced and light gray (B). This change in oxidation state, however, appears to have little if any effect on log response.

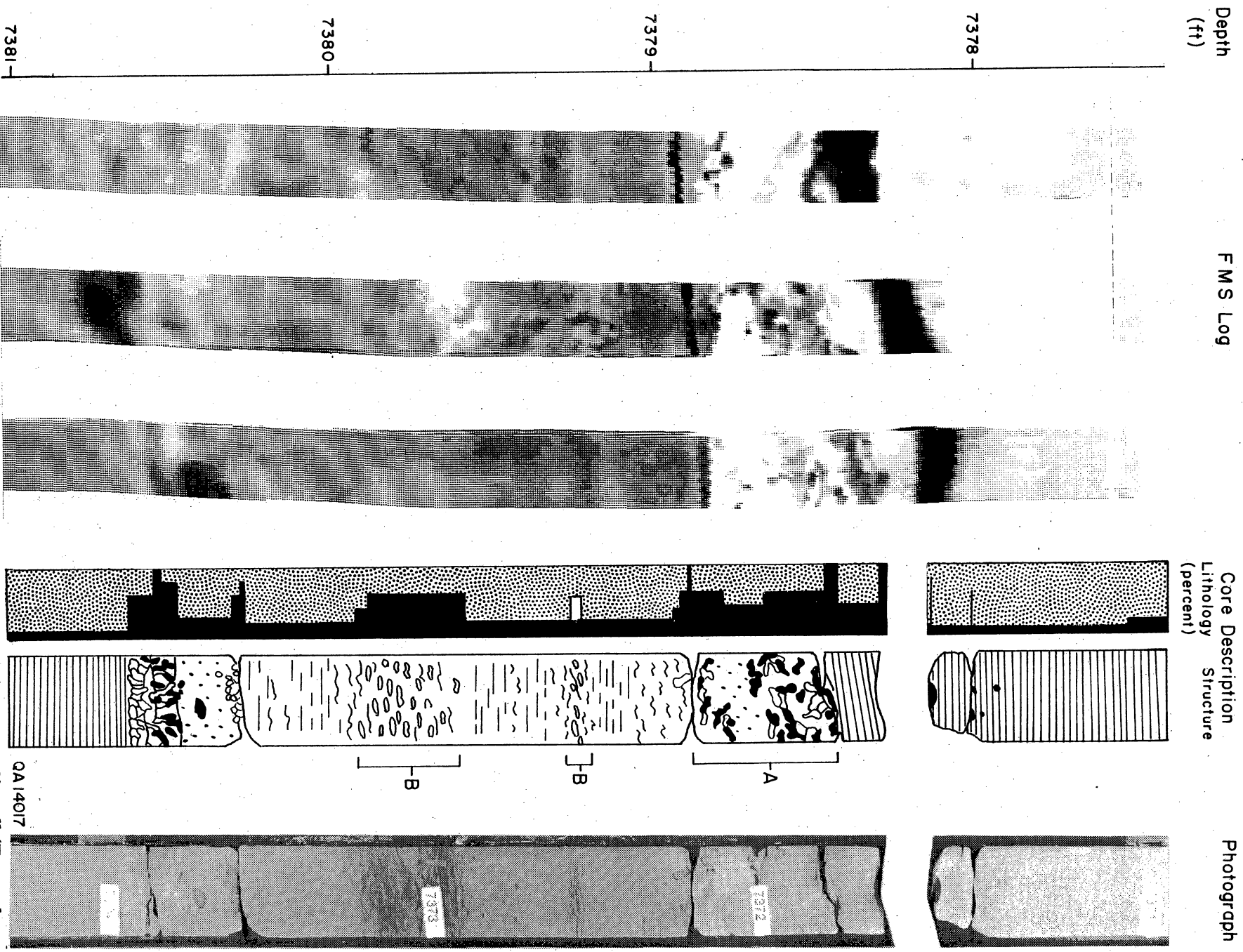


Figure 23. FMS log and core description from Mobil Cargill No. 15 (SFE No. 3) well (Example 11). This example illustrates log patterns of horizontally laminated sandstone, shaly sandstone to sandy shale revealing abundant mud clasts (A), burrows (B), and an unrecovered shale at 7378.1 ft to 7378.4 ft from the Travis Peak Formation.

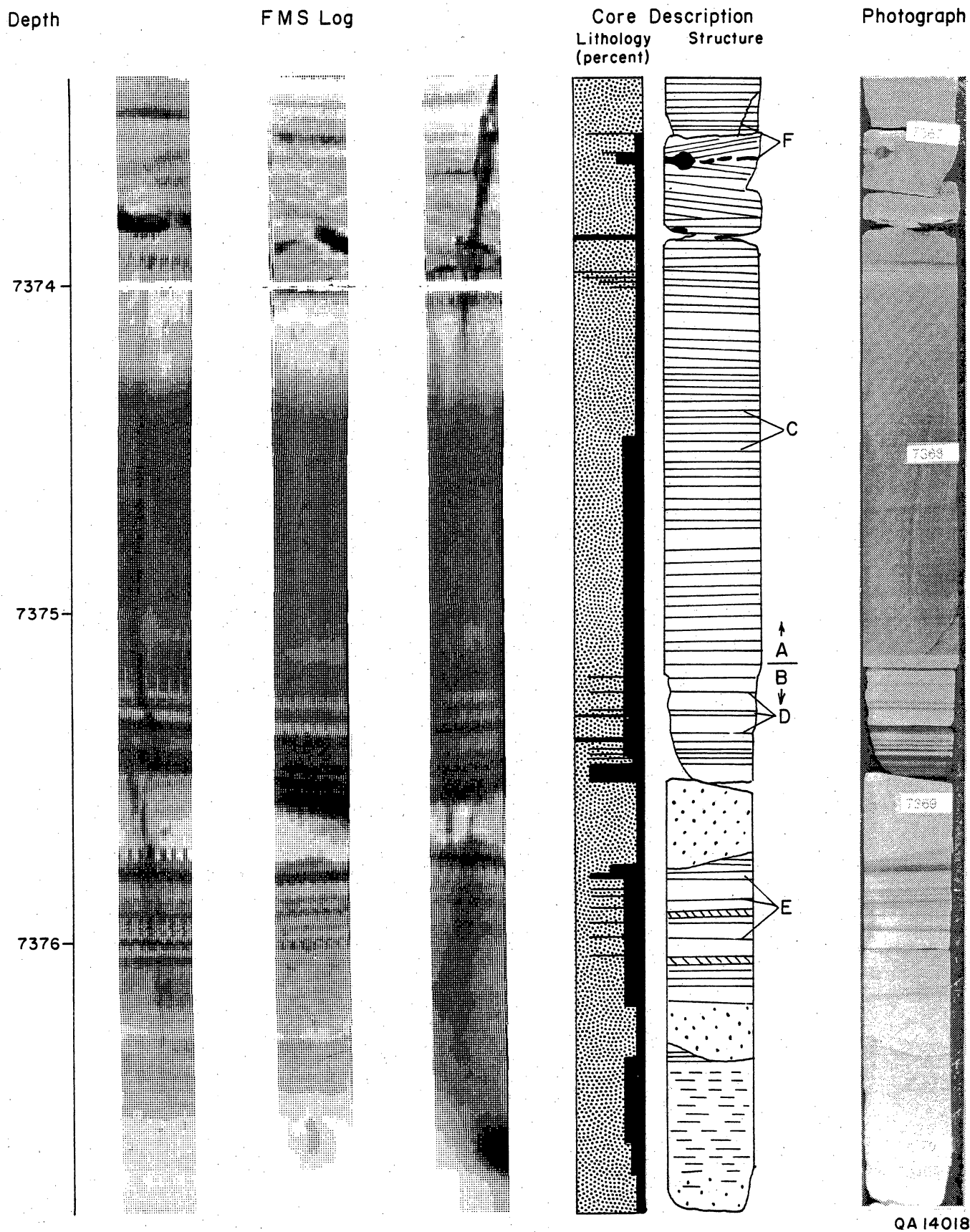


Figure 24. FMS log and core description from Mobil Cargill No. 15 (SFE No. 3) well (Example 12). This example illustrates log patterns of oxidized (A) and reduced (B) sandstone displaying nonshaly horizontal laminae (C), shaly laminae and thin shales (D and E), and coring-induced fractures (F) in Travis Peak sandstone.

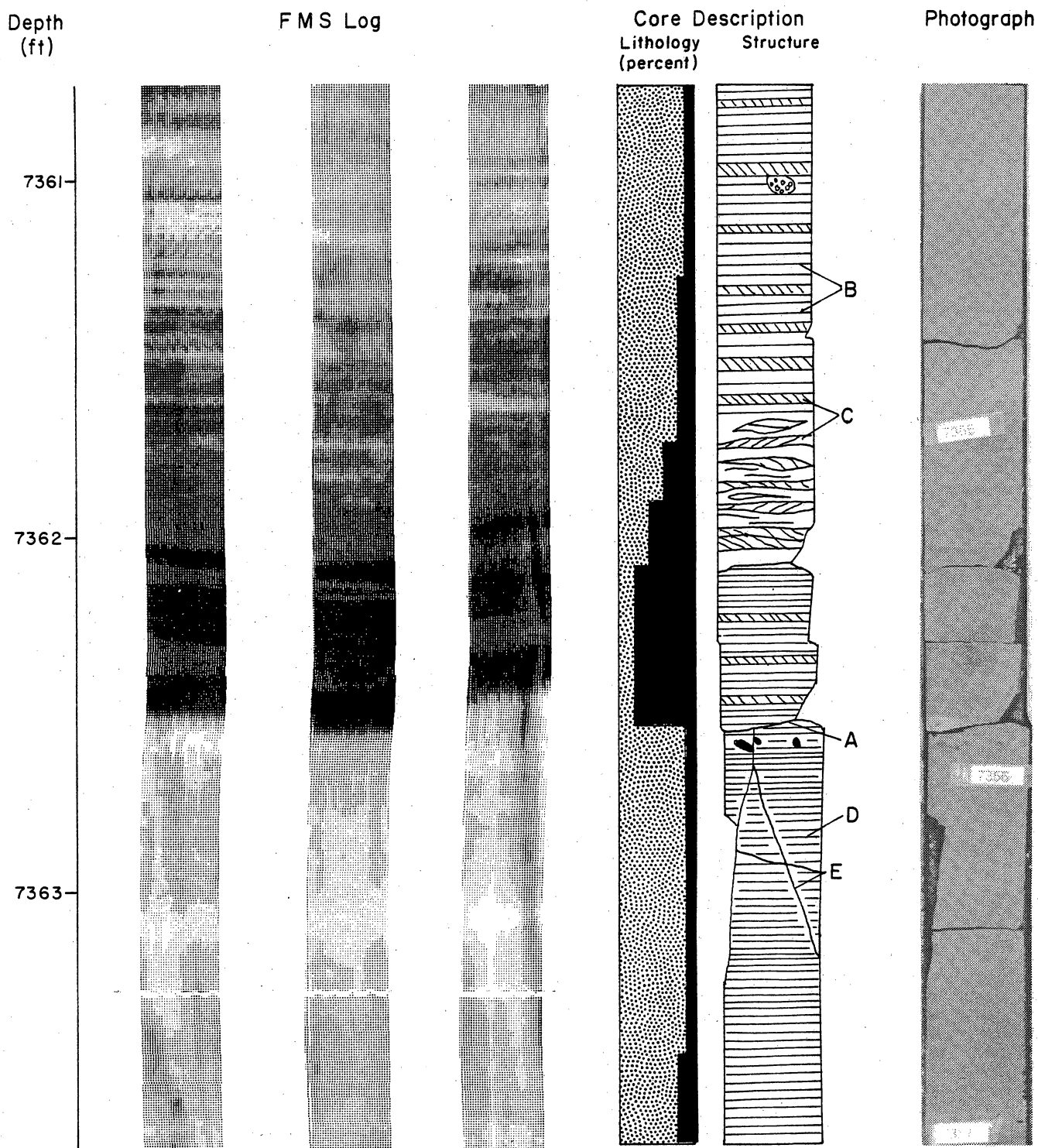
Faint nonshaly laminations, near 7,374.6 ft (C), for example, are not recorded, but thin shale layers and shaly laminations are well recorded. Around 7,375.9 ft individual shaly laminations as thin as 0.01 inch (E) are well defined. Short drilling-induced fractures are visible in the core (F), which may correspond to the conductive feature in the right log strip above 7,374 ft.

Example 13. Horizontally laminated sandstone is overlain by horizontal- and ripple-laminated sandy shale that grades upward into shaly sandstone and clean sandstone (fig. 25). The contact (A) between the sandstone and shale and the upward-cleaning sequence above this contact is clearly visible.

Also clearly visible above the sandstone-shale contact A are the horizontal (B) and ripple (C) laminations. Below 7,362.5 ft, low clay concentrations along laminae (D) cause them to be barely visible on this FMS log. The faint to distinct vertical conductivity anomaly corresponds to a mineralized fracture in the core (E).

SUMMARY

The FMS log in SFE No. 3 is an excellent tool for recognizing fine-scale sedimentary and diagenetic features. Features such as shale interbeds, laminae, and crossbeds can locally be interpreted without reference to core. Most features, however, such as bioturbation, clasts and shells, and massive and irregular cementation patterns require a comparison with core for accurate interpretation. The FMS log can be used for correcting core-measured depths to log depths. Where precise core-to-log correlations can be made, many of the lithologic, sedimentary, and diagenetic features that are visible in core can be seen on the FMS log.



QA14019

Figure 25. FMS log and core description from Mobil Cargill No. 15 (SFE No. 3) well (Example 13). This example illustrates log patterns of a sharp contact (A) between a cleaning upward sequence above displaying horizontal laminae (B) and ripple laminae (C) and sandstone below displaying horizontal laminae (D) and mineral-filled fractures (E) in the Travis Peak Formation.

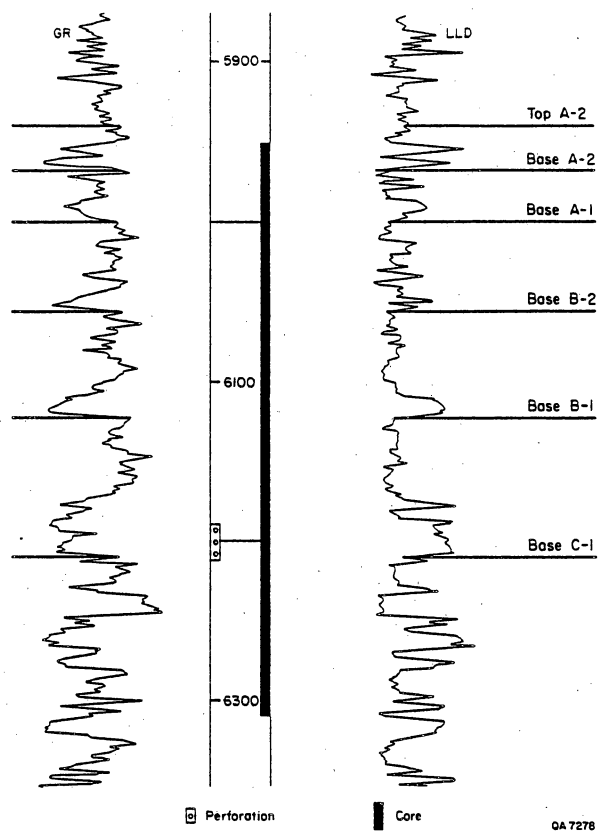
PART TWO: APPLICATION OF BHTV AND FMS LOGS TO FRACTURE DETECTION AND BOREHOLE-BREAKOUT ANALYSIS

S. E. Laubach, R. W. Baumgardner, Jr., and E. R. Monson

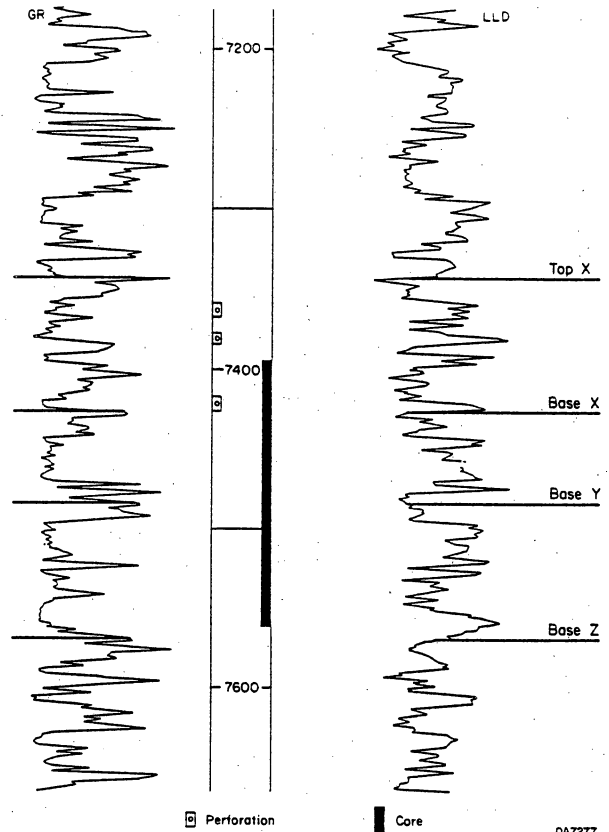
FRACTURE STUDIES USING CORES AND GEOPHYSICAL LOGS

Detection and characterization of fractures in low-permeability reservoirs are important goals of reservoir analysis. Natural fractures may increase permeability and porosity in low-permeability rock, but there are many limitations in exploiting reservoir fractures, and they stem directly from difficulties in characterizing fracture orientation, geometry, width, and type (Nelson, 1987). For example, natural fractures need to be distinguished from fractures induced by drilling that have no significance for reservoir fracture permeability. Hydraulic fracture treatments, which are required in many low-permeability reservoirs, can be detrimentally influenced by open (nonmineral filled) natural fractures unless accounted for in fracture-treatment design (Medlin and Fitch, 1988; Tye and others, 1989c; Holditch, in press). Whole core provides the most direct information on fractures and their relation to reservoir rock, but core recovery in fractured rock may be unsuccessful and core orientation methods may fail. Geophysical logs that produce images of the borehole can provide information on some critical aspects of reservoir fractures (Zemanek and others, 1969, 1970; Paillet, 1981; Taylor, 1983; Plumb and others, 1985; Lloyd and others, 1986; Dennis and others, 1987; Grace and Stephens, 1987; Hackbarth and Tepper, 1988).

Our analysis compares BHTV and FMS logs with 1,400 ft (426 m) of sandstone and shale core from four wells in the 2,000-ft-thick (610-m) Lower Cretaceous Travis Peak Formation (figs. 10, 11, 26, and 27). The Travis Peak provides a good test of fracture-imaging logs because natural fractures have complex geometry and variable mineral fill that challenge the



QA 7276



QA 7277

Figure 26. Informal nomenclature of lower and upper Travis Peak producing sandstones, Holditch Howell No. 5 (SFE No. 1) well. Cored and perforated intervals are shown. From Dutton and others (1990).

resolution of the tools and because there are borehole breakouts, drilling-induced fractures, and vertical sedimentary structures that must be distinguished from natural fractures for successful fracture analysis. Core was obtained from depths of between 5,900 and 9,900 ft (1,800 and 3,020 m) (fig. 10).

Fracture Analysis Methods

Fractures in the Travis Peak Formation were described from core and fracture-imaging logs from four wells in the East Texas Basin that are representative of this reservoir (Holditch and others, 1987; Dutton and others, 1990). We recovered 470 ft (143 m) of core from Holditch Howell No. 5, 199 ft (61 m) from Prairie Mast No. 1-A, 359 ft (109 m) from Holditch SFE No. 2, and 372 ft (113 m) from Mobil Cargill No. 15 (figs. 1 and 10). BHTV's belonging to AMOCO and Mobil and Schlumberger's FMS were run in Holditch Howell No. 5; a prototype FMS (the MEST tool) was run in Prairie Producing Mast No. 1-A; and two BHTV's were run in Holditch SFE No. 2 (fig. 10) by Mobil and Schlumberger research groups. One of the BHTV's used in this well was the Schlumberger-Doll Research digital BHTV. BHTV's belonging to Mobil and Schlumberger and the FMS were run in Mobil Cargill No. 15.

Core was oriented by standard multishot downhole techniques (Nelson and others, 1987) or by paleomagnetic methods, or both (Van Alstine, 1986), with a level of accuracy of approximately 10 degrees, as is discussed below. Core/log depth matching was done by comparing logs with a core gamma scan and by comparing logs directly with core. In Holditch Howell No. 5 and Mobil Cargill No. 15, precise depth match to within a few inches (centimeters) was possible locally where distinctive crossbeds, bioturbated zones, or lithologic boundaries on the FMS log could be identified in core for accurate core-to-log correlations.

Fracture Characteristics Observed in Core

Natural fractures in the Travis Peak include vertical extension fractures in sandstone that are partly filled with quartz and other secondary minerals and gently dipping striated shear fractures (small faults) in mudstone and siltstone (Laubach and others, 1987; Laubach, 1988b, 1989). Caliper logs and core analyses show that various vertical and inclined drilling-induced fractures also are present in the borehole and in core (Laubach and Monson, 1988; Dutton and others, 1990). Drilling-induced fractures include petal and petal-centerline extension fractures in core, inadvertent hydraulic fractures created during drilling, and variously oriented fractures in the borehole wall associated with the development of borehole breakouts (Plumb, 1989).

Natural fractures are widespread in the Travis Peak Formation. They were observed at a range of depths in core throughout the geographic area of study and in all stratigraphic subdivisions of the Travis Peak Formation, but they are particularly abundant in highly indurated, deeply buried parts of the formation in northern Nacogdoches County (fig. 1) (Laubach, 1988a). The variability and local high density of fracture development are illustrated by two cores from the Holditch SFE No. 2 well from North Appleby field in northern Nacogdoches County. Only a few short fractures are present in the core from the shallow interval (fig. 28), but numerous fractures can be found in the core from the deeper interval of this well (fig. 29). Significant fracture development is not restricted to deeper parts of the formation, however. Fractures as tall as 7 ft (2 m) from ~6,200 ft (~3,050 m) in the Arkla Scott No. 5 cooperative well in Waskom field are among the tallest recovered in this study (Laubach, 1989, p. 5). The fractures generally strike northeast (fig. 30).

A distinguishing characteristic of many Travis Peak extension fractures is that they are partly or completely open when observed in core. Petrographic evidence of delicate fracture-lining (fig. 31) and bridging minerals in fractures demonstrates that many were also open in

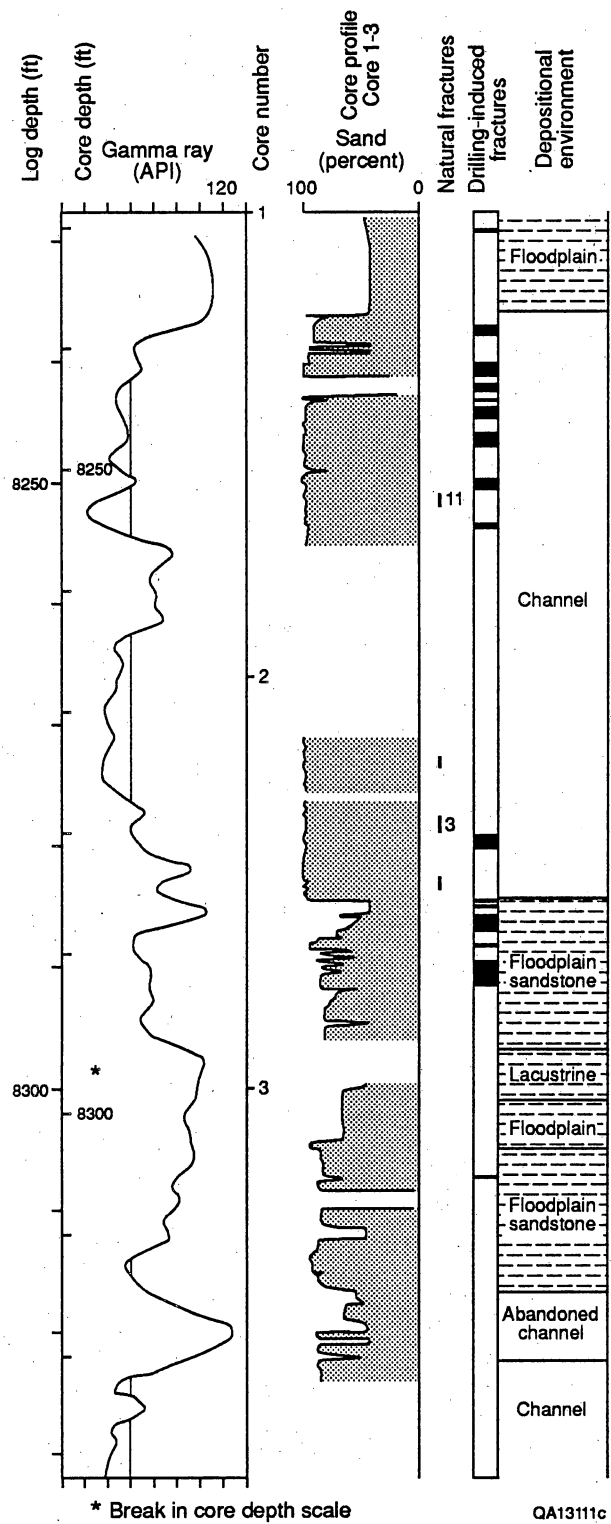


Figure 28. Core gamma-ray log, core profile, fracture distribution, and environmental interpretation for core 1-3, Holditch SFE No. 2 well.

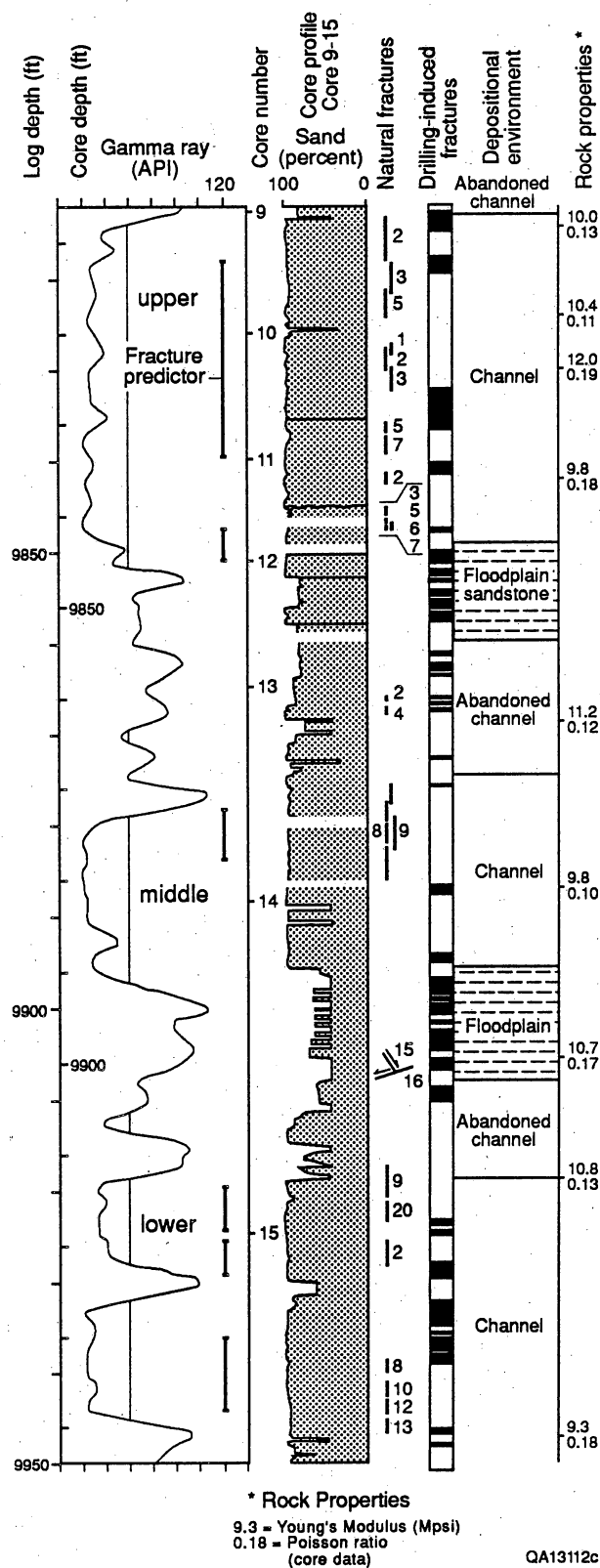


Figure 29. Core gamma-ray log, core profile, fracture distribution, and environmental interpretation for core 9-15, Holditch SFE No. 2 well. Rock-property measurements from core plugs in this interval are also shown.

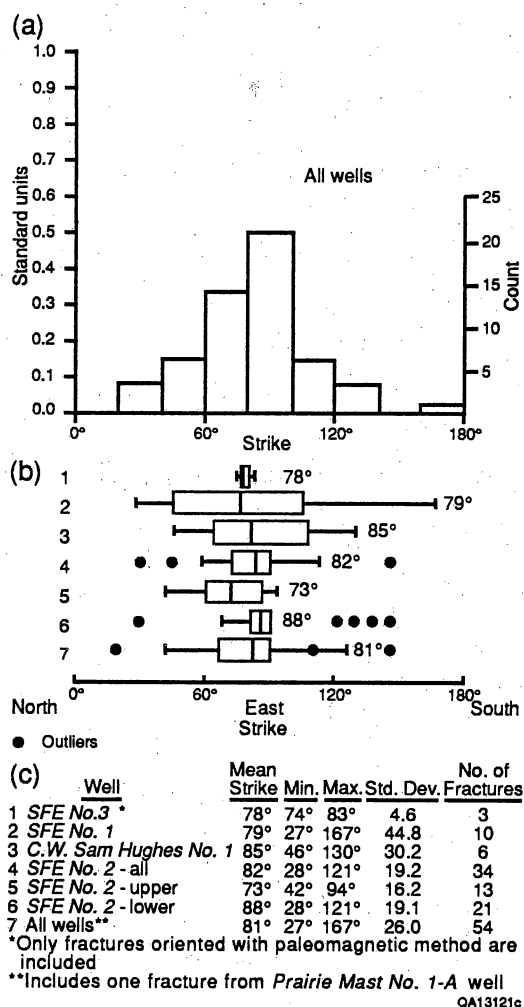


Figure 30. Strikes of natural fractures in Travis Peak sandstones. (a) Histogram showing data from all wells in the study that have oriented core. (b) Box plots of data from indicated wells and intervals within wells. The center half of the data (from the first to the third quartile) is represented by the rectangle (box) containing the median indicated by a bar. The horizontal lines right and left of the box extend to values that represent 1.5 times the spread from the median to the corresponding edge of the box. Points plotted separately are outliers.

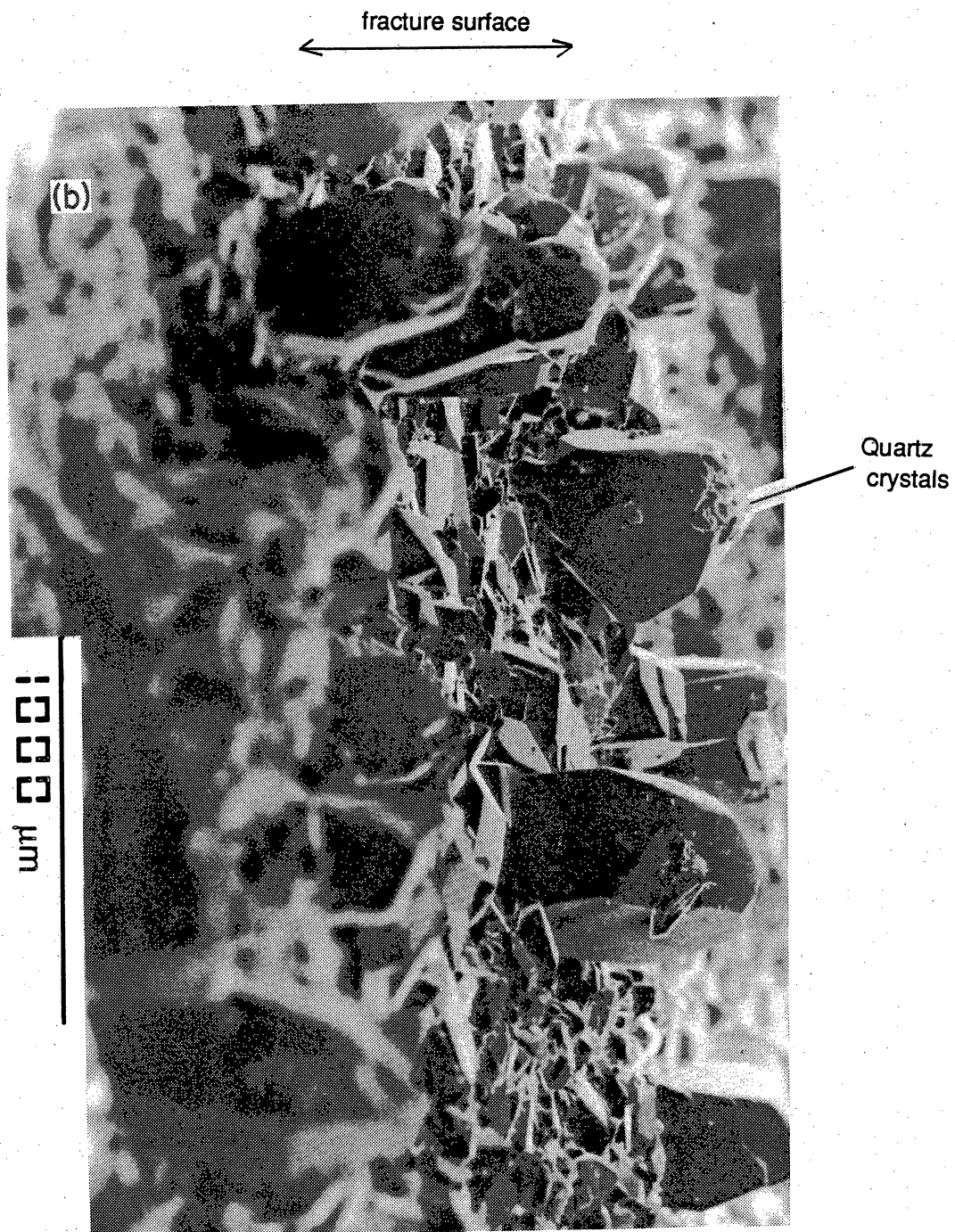


Figure 31. Scanning electron photomicrograph showing quartz lining open-fracture-pore space, Holditch SFE No. 2, depth of 9,873 ft (3,009 m). Evidence from microstructures such as these demonstrates that many fractures in the Travis Peak and Cotton Valley are open in the subsurface (Laubach, 1988b).

the subsurface, including fractures from as deep as 9,934 ft (3,028 m). Open fractures are lens shaped in cross section and have widths ranging from less than 0.05 to 5 mm. Because the mineral fill in fractures is irregularly distributed, open pore networks or channelways within fractures are curved, anastomosing, rough-walled, and may or may not be interconnected. Open fractures were sampled from both the upper and lower Travis Peak, but the widest fractures are from the lower Travis Peak in the Holditch SFE No. 2 well. These fractures are also the shortest and most highly segmented, and they are truncated locally by stylolites.

OBSERVATIONS OF FRACTURES USING BOREHOLE-IMAGING LOGS

Two main categories of BHTV features that have low sonic amplitudes and long travel times, and which are inclined to and distinct from bedding, are visible on Travis Peak logs. These features correspond to different types of fractures, such as natural fractures and several distinct types of drilling-induced fractures or to different appearances of a given type of fracture on the BHTV log. Type 1 features are narrow, dark, and curvilinear and have sharply defined edges; they are interpreted to be narrow natural fractures and narrow drilling-induced fractures. They appear as isolated, single, linear to curvilinear features, or, more commonly, as features arranged in relay and en echelon patterns (fig. 32). Some Type 1 linear features have splays or subparallel, subsidiary features along part of their length. Locally, more intricate arrangements of traces are found. Sinusoidal traces that can result from an inclined plane intersecting the borehole are rare; most sinusoidal traces on the log correspond to inclined bedding planes. Partial or discontinuous sinusoidal traces that match inclined fractures in core are evident locally. Type 1 features are generally elongate subparallel to the vertical borehole axis, but locally they have shallow (less than 5 degrees) inclinations from horizontal. Where visible, Type 1 feature terminations are typically sharply tapered (fig. 33). In the Travis Peak this feature type is commonly visible on the east and west sides of the borehole in symmetric pairs.

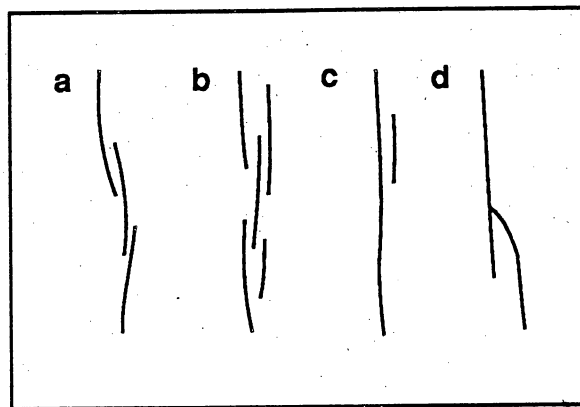


Figure 32. Typical patterns of natural fracture traces in core, Travis Peak Formation. (a) En echelon pattern. (b) Relay pattern. (c) Subsidiary fracture. (d) Splay fracture. Similar patterns are evident on borehole-imaging logs.

Locally Type 1 features pass along their traces into Type 2 features, which are wider and more irregularly shaped (figs. 33, 34, and 35). Type 2 features are interpreted to be borehole washouts and borehole breakouts and are 5 to 10 times wider than Type 1 features. They have either sharp or diffuse edges, and many have straight-sided inflections along their edges where they intersect subhorizontal traces of bedding planes (fig. 34). In some instances many short Type 1 features seem to coalesce to form areas of large borehole diameter (long travel times), but more commonly they are not associated with Type 1 features (fig. 33). Type 2 features are generally elongate parallel to the vertical borehole axis, as are Type 1 features, but Type 2 features are shorter and their terminations are blunt or rounded rather than sharply tapered. In the Travis Peak these features are concentrated along the north and south sides of the borehole. They may occur at the same depth as Type 1 features but at right-angles to them, so that they are on the opposite side of the borehole (except where they occur along continuations of Type 1 features). Type 2 features on the north or south side of the borehole are wider than the Type 2 features associated with Type 1 features.

Comparison of BHTV Images to Core

Natural Fractures

In BHTV images, fractures visible in Travis Peak sandstone core may be dark, narrow, curvilinear Type 1 features that have low sonic amplitudes and long travel times (fig. 35), or they may correspond to images that have more diffuse boundaries. Fractures are generally detected by BHTV because they are topographic depressions on the borehole wall. The difference in travel time from the topographic depression and adjacent smooth borehole wall to the BHTV produces a density contrast in the BHTV image. In the Travis Peak, fractures are detectable because they are partly open in the subsurface or have delicate mineral fill that may

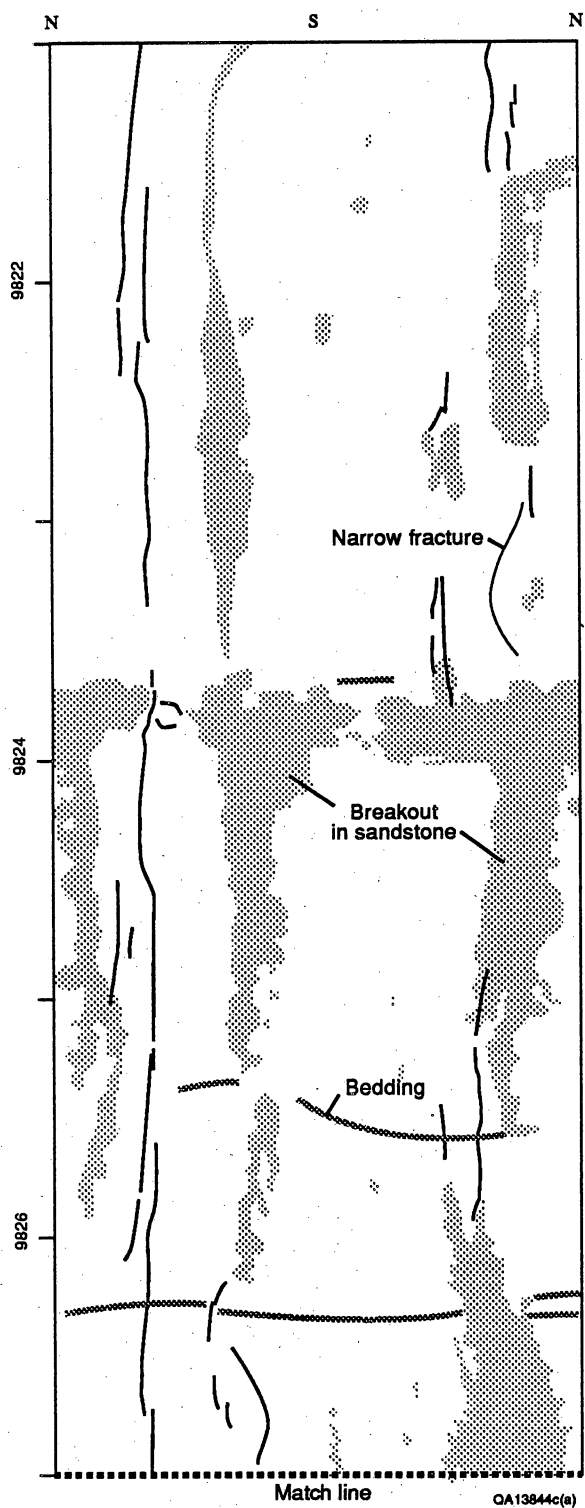
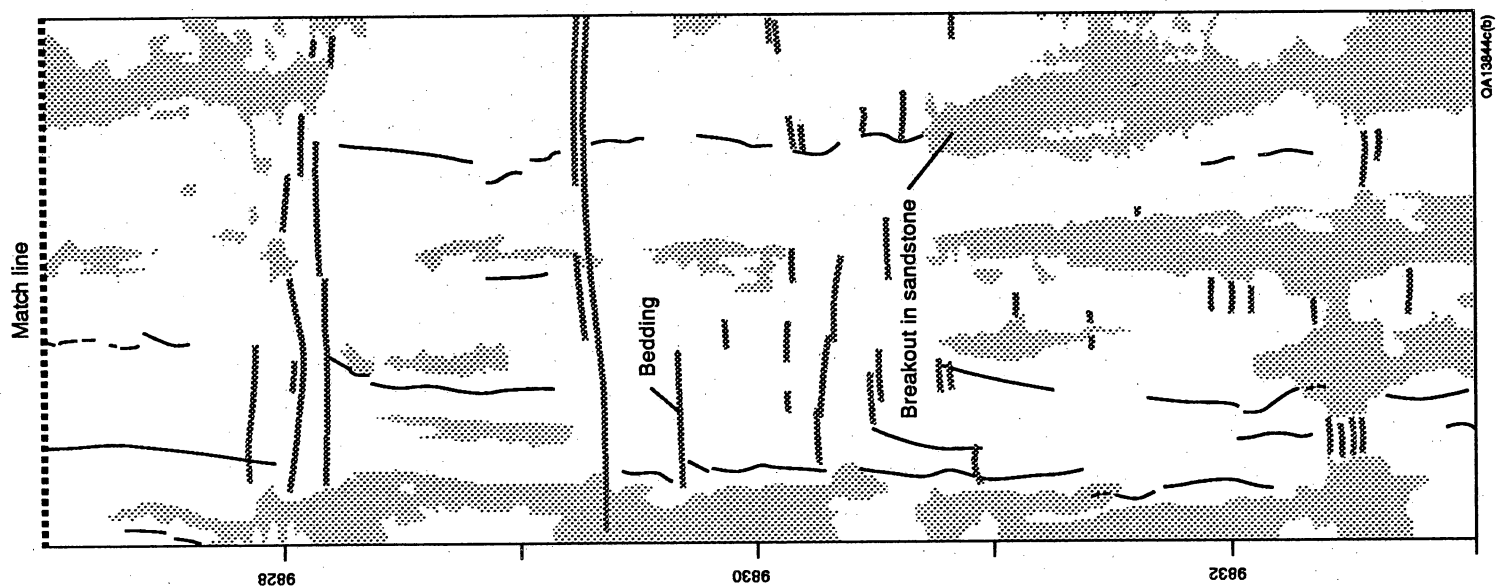


Figure 33. Example of fractures on BHTV log, Holditch SFE No. 2.



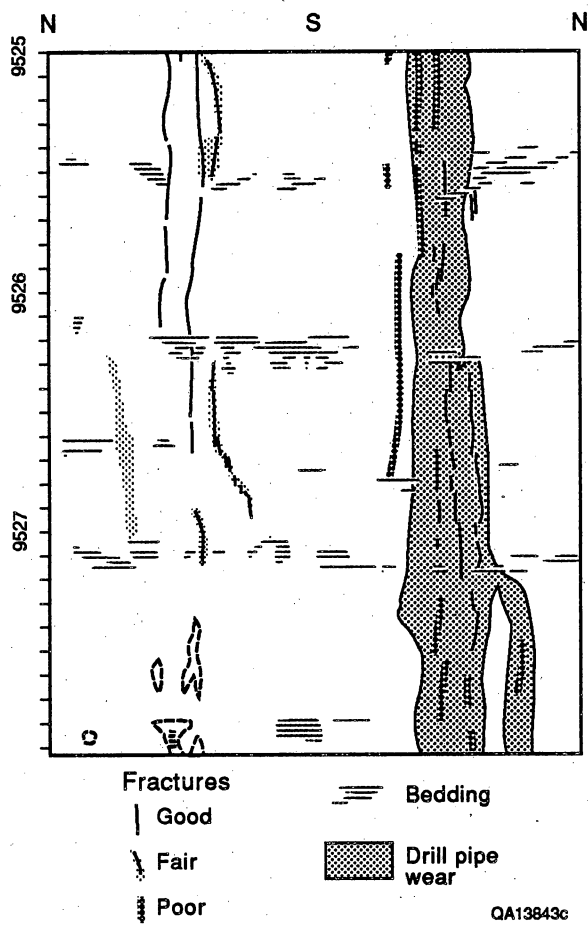


Figure 34. Example of fractures and breakouts on BHTV log, Holditch SFE No. 2.

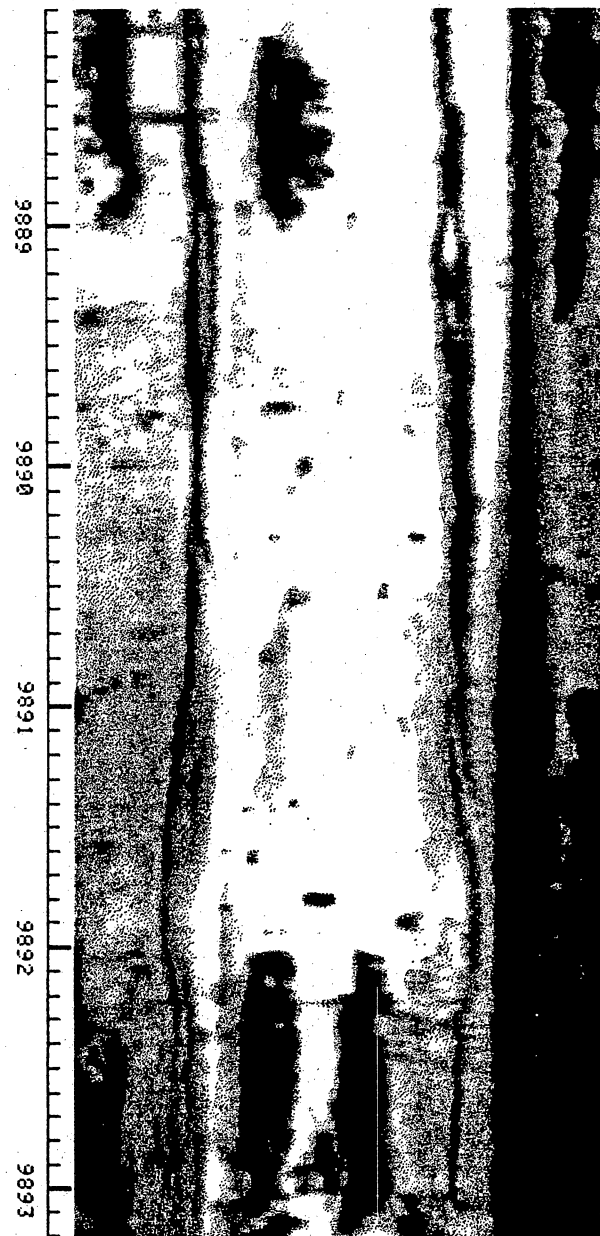
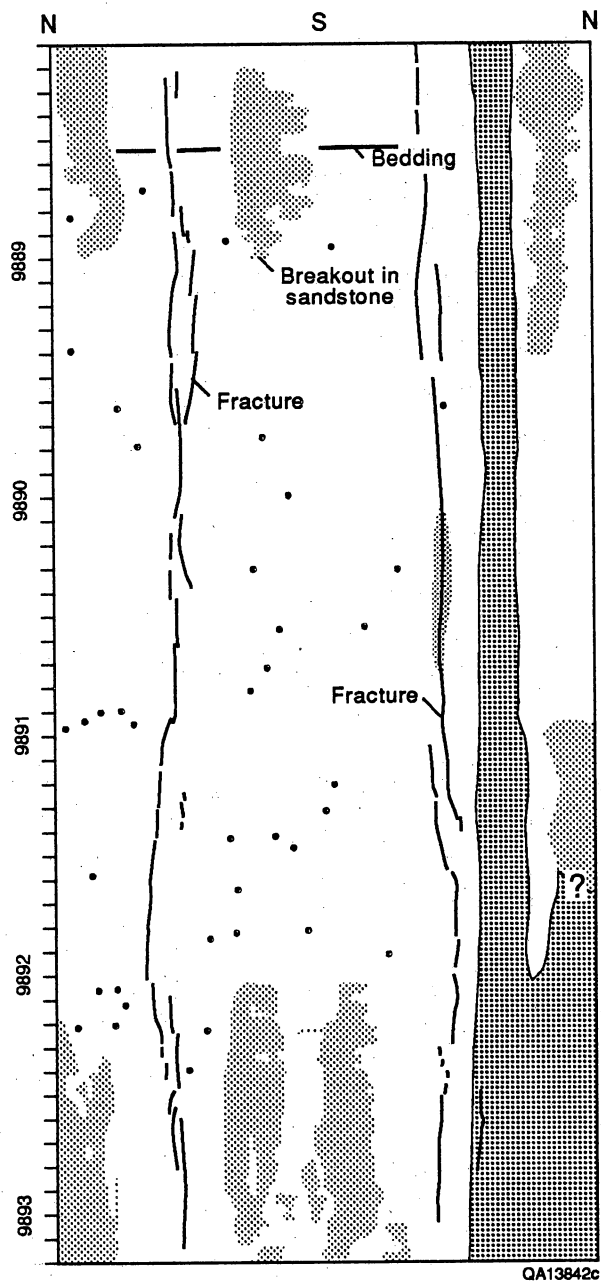


Figure 35. Fractures in core and tracing of BHTV image, Holditch SFE No. 2. See figure 34 for explanation.

be eroded by drilling fluid (fig. 31). We could not correlate differences in Type 1 BHTV features to differences in the type or mineralogy of fracture fill of corresponding fractures in core.

Many vertical and near-vertical extension fractures in sandstone are visible in BHTV and FMS logs in cored intervals of the Travis Peak Formation. Because of the spatial separation between core and borehole wall caused by the difference between 4-inch (10-cm) diameter core and the wall of the larger diameter borehole (fig. 36), core and log are not sampling the same rock, and fractures in core and on logs should not be expected to match exactly in abundance, length, or shape. In the Travis Peak, the borehole has a diameter of as much as 17 inches (43 cm) in some elliptical zones. Moreover, in the common situation where fractures do not exactly bisect the borehole and intersection with the borehole wall is oblique, the fracture image will not be a true cross section of the fracture and the fracture will appear distorted even if perfectly depicted. This geometric effect tends to exaggerate the apparent width of fractures.

Fractures in core and on logs were matched by comparing fracture lengths and patterns and by using prominent bedding planes visible on logs to help accurately match core and log depth. Correlation of BHTV image and core is hindered in the Travis Peak and Cotton Valley because beds commonly are not distinct on the logs we studied. Caliper logs were also used to match depths on BHTV to other geophysical logs and to the core gamma scan log. For Holditch Howell No. 5, approximately 40 percent of all fractures described in core were observed on BHTV log. Of natural extension fractures in sandstone, more than 70 percent were visible on the log. Approximately 30 percent of fractures visible on BHTV do not correspond to fractures in core; these could be fractures that are present only in the borehole wall. In some intervals, there are more fractures visible on logs than were observed in the core. Open natural fractures less than approximately 6 inches (15 cm) long were difficult to distinguish as distinct vertical features on BHTV logs because they resemble short image-density anomalies caused by irregularities in the borehole wall. Short fractures are locally abundant in the lower Travis Peak Formation (fig. 29).

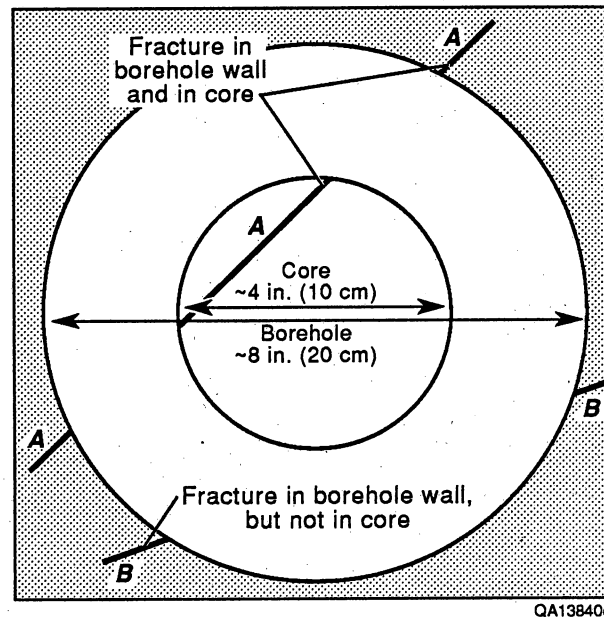


Figure 36. Diagram illustrating fractures that intersect the borehole but not the core.

If drilling-induced petal and petal-centerline and natural fractures in core are considered, BHTV logs accurately portray the abundance of fractures observed in core. Natural-fracture abundance is difficult to quantify using vertical core in the Travis Peak because fracture dip is subparallel to the core axis. Fracture spacing is generally greater than the 4-inch (10-cm) diameter of the core, implying a fracture spacing of greater than 4 inches (10 cm). Log information from the walls of the borehole, which has a larger diameter, is potentially useful for increasing the volume of rock used to define fracture abundance. In cores that we studied, natural extension fractures in sandstone are more abundant in the lower Travis Peak than in the upper (Laubach, 1989). The most highly fractured rocks encountered in this study having fracture spacing in core of as little as approximately 1 inch (2 to 3 cm), are found in North Appleby field, where the Holditch SFE No. 2 and Prairie Producing Mast No. 1-A are located. Overall patterns of natural fracture abundance could not be demonstrated using fracture-imaging logs alone because of the difficulty in distinguishing natural from other fracture types, as is discussed in the following section (Drilling-Induced Petal and Petal-Centerline Fractures).

Short, vertical and inclined, striated shear fractures in siltstone and mudstone were not apparent on the BHTV logs, partly because of the sampling rate and scale used and partly the scarcity of microtopographic expression of these structures on the borehole wall. In the Travis Peak, shear fractures are common in siltstone and mudstone but are closed in core, and they do not create recognizable BHTV or FMS features. Having dips that are commonly less than 5 degrees, these fractures are difficult to distinguish from bedding planes, and they may be obscured locally by washouts. Vertical elongate sedimentary features are uncommon in the cored intervals of the Travis Peak that we studied, and they are generally short (6 inches [15.2 cm] or less); we did not identify such features on the BHTV logs that we used.

The widths of fracture images on the BHTV that were produced using current commercial techniques apparently are not representative of true fracture widths. Apparent widths on the log are greater than those observed in core. Width determination is complicated by erosion of

fractures by drilling and spalling (fig. 37). As a result fracture widths at the borehole wall may not be representative of actual fracture widths in the formation. Core observations in the Travis Peak show that fracture widths may be doubled near the core surface by spalling. Changes in fracture image width along fracture traces and between fractures are visible on BHTV logs, however, and this type of information can be useful for interpreting fracture style and origin. We could not resolve internal structure of fractures, such as degree of openness or extent of mineral fill, on the BHTV or FMS log.

The attitudes of Type 1 features are readily determined from the BHTV image. The dip and strike of short inclined fractures were determined from partial sinusoidal traces. However, most natural and drilling-induced fractures in cores and on BHTV and FMS logs in these wells are subvertical, producing slightly curvilinear traces parallel to the vertical borehole axis, rather than a sinusoidal trace. For these fractures, strike must be determined by matching or correlating fracture traces on different parts of the borehole wall. Some ambiguities in fracture strike determination can arise if fracture traces cannot be confidently matched, such as where traces are of unequal length or are not mirror images, or if more than two fracture traces are visible. In these cases, the traces may correspond to different fractures.

For vertical fractures, height can be measured directly from the log if fracture terminations are visible. If the fractures are inclined, however, or the wellbore axis and the fracture planes are not aligned, then the fracture height measured in the borehole is indeterminate. This is important if the height of fractures created in hydraulic fracture treatments or stress tests is being investigated (Hunt, 1990). In Holditch Howell No. 5, average height of vertical fractures having clearly defined terminations on the BHTV log is 2.8 ft (0.85 m) compared with 1.9 ft (0.58 m) for vertical fractures in core. In Holditch SFE No. 2, fracture and fracture-zone lengths on the BHTV and in cores are dissimilar (fig. 25). The average trace length on the log is longer than that for the 4-inch (10-cm) core, probably reflecting more complete sampling of long fractures by the log (in an ~8-inch-diameter [~20-cm] borehole). These observations show that fracture heights on BHTV images are similar, in

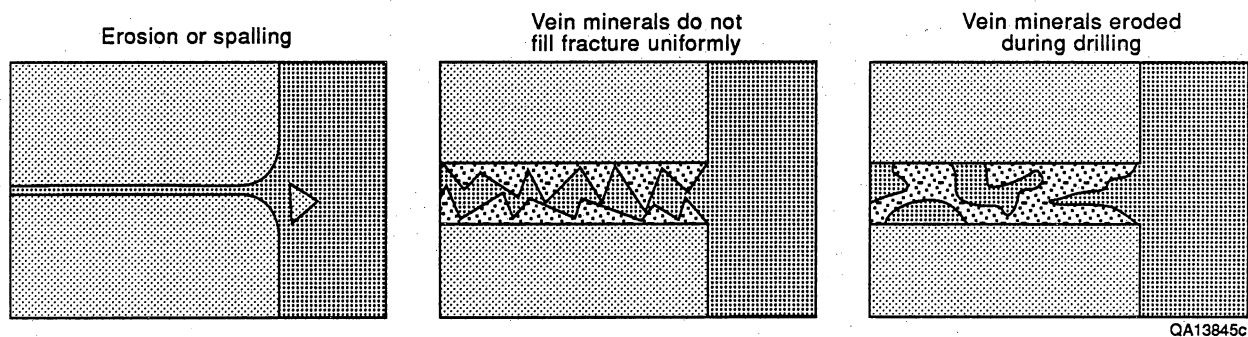


Figure 37. Some sources of error in fracture-width measurements in core. These processes may also cause fracture widths at and near the borehole wall to differ from widths in undisturbed rock.

general, to fracture heights in core, and that the BHTV provides information that supplements core data on the range of fracture heights in the Travis Peak.

Large-scale (1:20) BHTV images from Holditch SFE No. 2 show intricate fracture patterns and branching and intersecting fractures that resemble fracture patterns observed in core. Blunt and tapered fracture terminations (fig. 34) and terminations at bedding planes are visible locally. En echelon and relay patterns, splay fractures, curved and intersecting fractures, and short, relatively wide fractures that terminate at bedding planes are all visible. On small-scale presentations, fracture shape is distorted on BHTV and FMS logs because the compressed vertical scale gives fractures the appearance of having larger width/length ratios than they actually have, but this can be compensated for by expanding the vertical scale. Expanded-scale digital BHTV images, which can be displayed at scales of 1:1, accurately portray many aspects of fracture style, such as curvature, overlap of fracture segments, and shape of fracture terminations, that are visible in core (fig. 34).

Locally, image artifacts obscure fractures or produce dark linear features that resemble them. The BHTV image is dependent upon borehole shape and tool position in the borehole. If the borehole is elliptical, BHTV images may be obscured by as many as four dark vertical bands where signal returns from the borehole wall are deflected away from the BHTV tool. If the tool is off-center in a round borehole, two dark bands appear (Georgi, 1985). Occasionally these dark bands obscure so much of the image that vertical fractures cannot be detected. Generally these image artifacts are symmetrical and are several tens of feet (meters) long. These characteristics distinguish them from fractures. These bands affect approximately 20 percent of the BHTV logs in Holditch Howell No. 5 but are largely absent on the digital BHTV in Holditch SFE No. 2.

Drilling-Induced Petal and Petal-Centerline Fractures

Drilling-induced fractures need to be distinguished from natural fractures in order to have an accurate estimate of natural fracture abundance. Drilling-induced fractures in core were distinguished from natural fractures based on criteria described by Kulander and others (1979). The criteria for recognizing induced fractures include (1) fracture origins near or within core, (2) characteristic fracture shapes, and (3) absence of mineralization. Fracture surface structures (plume structure and arrest lines) were used to identify fracture origins (Kulander and others, 1979).

Drilling-induced petal and petal-centerline fractures have a distinctive geometry in core. They characteristically curve into the core in the downhole direction. Petal fractures are short, inclined fractures that are concave downward and that have dips measured at the edge of the core that range from 50 degrees to subvertical (fig. 38). Petal-centerline fractures are single fractures that are composed of a short, smoothly curving concave-downward petal segment that gradually merges in the down-core direction with a planar subvertical centerline fracture segment that may bisect the core. The upper terminations of petal and petal-centerline fractures occur outside of the core, but the lower terminations generally occur within core, either at interbeds or in homogeneous rock. Core is commonly not completely separated (split) along petal- centerline fractures because fracture planes are composed of multiple strands rather than single fracture planes. Petal and petal-centerline fractures propagate in front of the core bit, as indicated by scoring of the edges of petal-centerline fractures by the bit or by grooves created on the edges of fractures by scribe knives located inside the core barrel assembly.

Petal and petal-centerline fractures strike predominantly east-northeast throughout the study area in East Texas. The vector mean strike of 101 petal and petal-centerline fractures is 085 degrees, ranging from 029 to 143 degrees. Petal-centerline fractures have a mean strike of

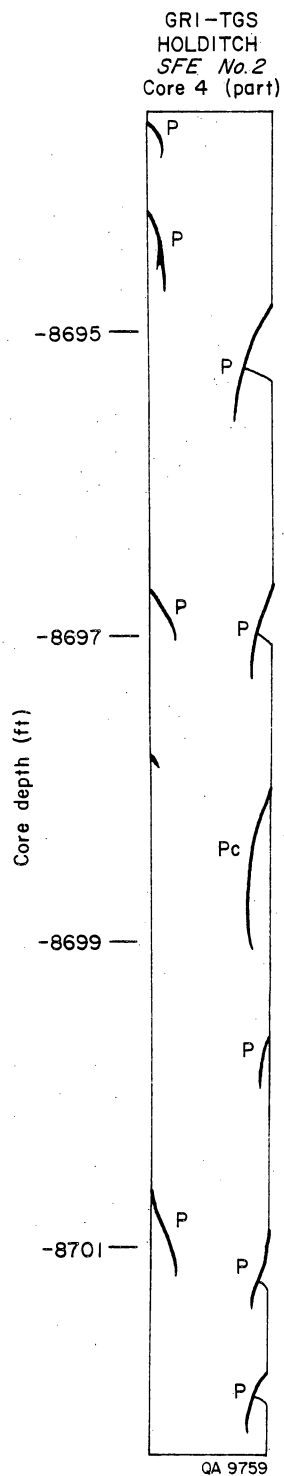


Figure 38. Sketch of aligned petal (P) and petal-centerline (P-C) fractures, Holditch SFE No. 2 well, 8,694 to 8,702 ft (2,649 to 2,652 m) (from Laubach, 1989a) and BHTV log of the same interval.

081 degrees and are strongly grouped between 070 and 090 degrees. Within intact core, petal and petal-centerline fractures are parallel and have a strong preferred orientation. For example, 10 petal and petal-centerline fractures in one 10-ft-long (3-m) unoriented core from Holditch SFE No. 2 are precisely parallel.

More than half (65 percent) of the fractures described in Holditch Howell No. 5 core are petal, petal-centerline, or other drilling-induced fracture types. Of the fractures in core that are visible on Holditch Howell No. 5 BHTV logs, 52 percent are interpreted to be drilling induced. We interpret drilling-induced petal and petal-centerline fractures to be visible on BHTV logs because we observe narrow Type 1 BHTV traces bisecting the borehole in cored intervals of the well wherein core natural fractures are absent but drilling-induced fractures are present. Drilling-induced fractures on the log are indistinguishable from natural fractures; both types may be represented by Type 1 features. In the absence of core, the distinctive curve of a drilling-induced petal-centerline fracture, where visible, might be useful for separating natural and drilling-induced fractures, but observations of natural and drilling-induced fractures in Travis Peak core show that inclined drilling-induced petal fractures commonly curve or hook into vertical natural fractures, creating composite fractures that have shapes similar to those of drilling-induced petal-centerline fractures.

The BHTV also detected fractures created in hydraulic stress tests in Holditch SFE No. 2 and Holditch Howell No. 5. These hydraulic fractures were designed to measure the magnitude of in situ stresses by means of controlled open-hole hydraulic fracture stress tests using arrangements of packers and pressurized drilling mud (Whitehead and Robinson, 1989). The fractures were recovered in core and imaged with logs. In figure 39 the fractures created in a stress test are visible on the BHTV log. The orientation of these fractures can be used to infer horizontal stress directions, and the style of fracturing provides insight into how the rock in the test zone behaves during fracture treatment. The strike of the fractures is east-northeast, parallel to the greatest horizontal stress in this area. The multiple fracture strands created during this test are visible, showing that in this interval branching hydraulic fractures need to

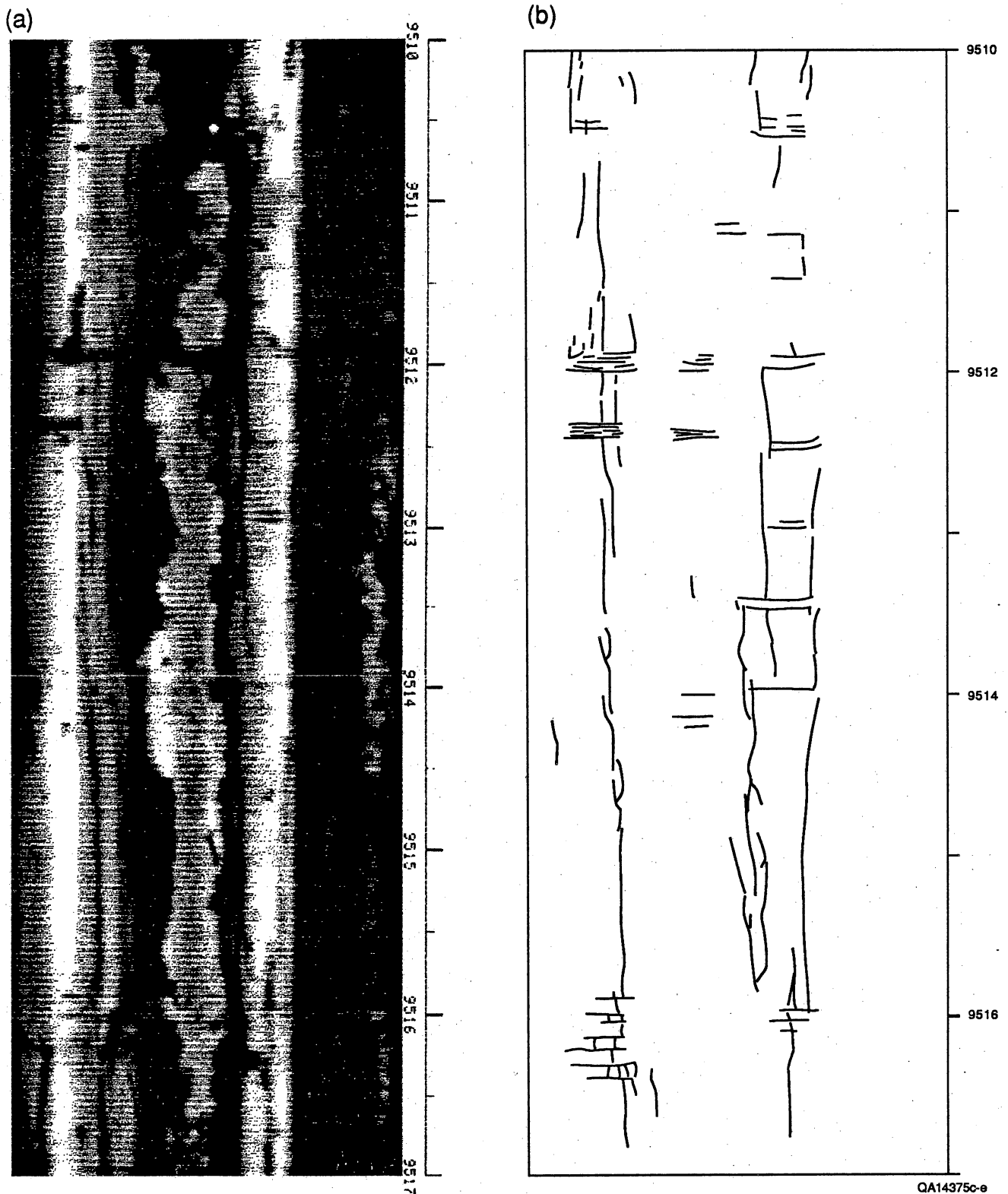


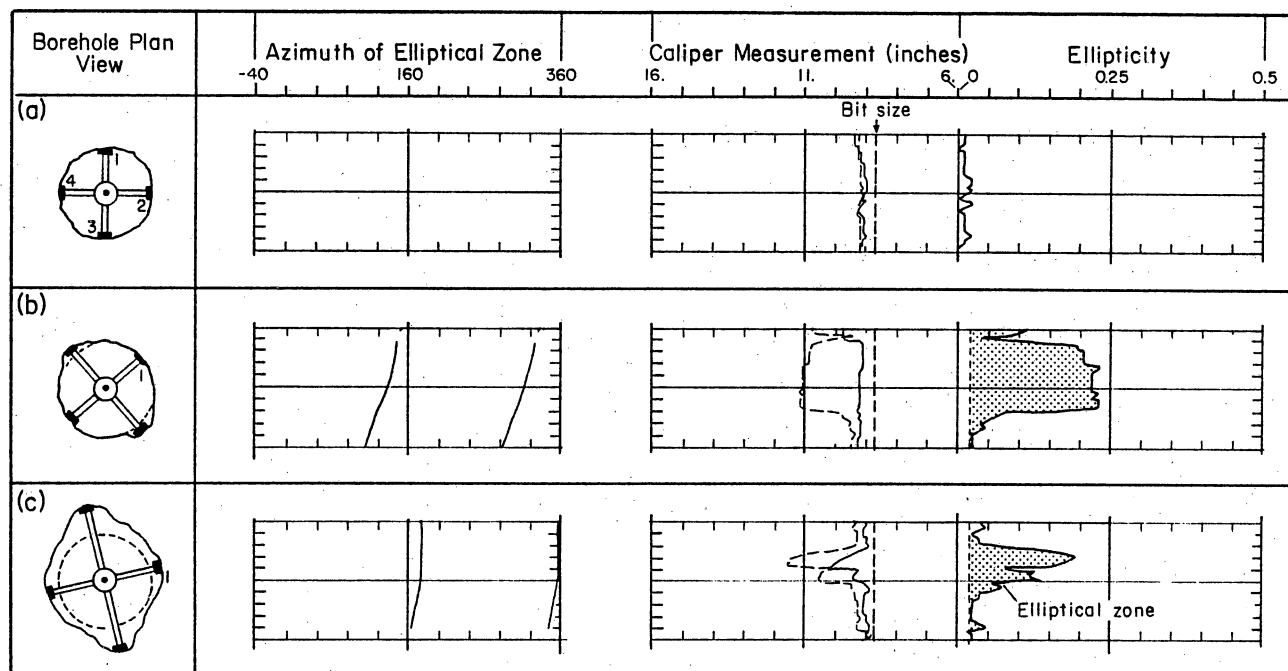
Figure 39. (a) Tracing from BHTV log and (b) sketch of hydraulic fracture induced by open-hole stress test 2, Holditch SFE No. 2 well. Overall sketch of the fractured interval shows multiple fracture strands. The fracture strands occur in very fine sandstone and locally in gradational to muddy sandstone, characterized by local thin beds of gray shale.

be considered during modeling of hydraulic fracture growth. The extent of the fracture on the BHTV image provides an indication of the thickness of rock being tested by the hydraulic fracture stress test.

Borehole-Breakout Detection and Evaluation Using BHTV and Caliper Logs

When regional tectonic stresses are amplified around a borehole and exceed the strength of the wallrock, and horizontal stresses are anisotropic, borehole-wall failure will occur by the development of extension and shear fractures, or both (Plumb and Hickman, 1985). The resulting spalls and open fractures in the borehole wall create an ellipse that is termed a borehole breakout. One goal of subsurface studies using borehole-imaging logs in low-permeability gas sandstones is to determine the azimuth of maximum horizontal stress. This information is important because the propagation direction of hydraulic fractures is largely controlled by stress anisotropy. Borehole breakouts are a reliable method for determining stress directions in many geologic settings, and breakouts can be detected using the BHTV and caliper logs. In this study we used both to determine breakout trends. The orientation of breakout failure in a near-vertical borehole is perpendicular to the direction of the largest horizontal principal compressional stress (Bell and Gough, 1979).

On BHTV logs, borehole breakouts are readily distinguished from fractures by their width and shape (fig. 40) (Plumb, 1989); they correspond to Type 2 features described earlier. Locally, narrow spalls and incipient breakouts may be difficult to distinguish from natural fractures or other types of induced fractures, such as inadvertent hydraulic fractures, but in general breakouts have a distinctive appearance in the Travis Peak on BHTV logs, and travel-time information can be used to make an accurate map of borehole shape. Fracture trace patterns are associated with incipient breakouts (Plumb, 1989). Well-developed or mature borehole breakouts and other fracture types mentioned above can be readily distinguished using the BHTV. On the logs we studied, breakouts are more apparent and more easily distinguished and



After Plumb and Hickman (1985, fig. 3)

— Cal 1-3
- - - Cal 2-4

QA8295

Figure 40. Plan views and sections of ellipticity logs for (a) an in-gauge borehole, (b) borehole breakout, and (c) washout. (a) Caliper readings for in-gauge hole are near bit size, hence no azimuth of elliptical hole is recorded. (b) Caliper 1-3 in breakout is near bit size. Caliper 2-4 marks the larger diameter (11 inches [28 cm]). Maximum ellipticity is 0.23. Azimuth of elliptical zone in upper 10 ft (3 m) of log section (b) is between 300 and 320 degrees. (c) Both calipers measure larger than bit size in washout. Caliper 2-4 marks the larger diameter (11.5 inches [29 cm]). Maximum ellipticity is 0.19. Azimuth of elliptical zone in upper 10 ft (3 m) of log section (c) is 355 degrees. Major vertical divisions on log represent 10 ft (3 m).

interpreted on the BHTV than on FMS or caliper logs. On FMS logs breakouts sometimes appear as diamond-shaped features (Bourke and others, 1989, p. 26), but they can be difficult to distinguish from areas of tool-pad standoff.

Wellbore ellipticity and borehole breakouts were studied to determine the directions of horizontal principal stresses and to predict the direction of hydraulic fracture propagation. Where core is unavailable, wellbore elongation and breakouts can be used as substitutes for core-based analysis, such as anelastic strain recovery, to determine stress directions. In this study, zones of wellbore elongation in eight wells were measured on ellipticity logs produced by ResTech, Inc. Ellipticity logs are derived from caliper readings and drill-bit size as follows (B. Ward, ResTech, Inc., personal communication, 1987) (fig. 40):

$$\text{ellipticity} = |C1 - C2| / \text{bit size}$$

where: C1 = reading from caliper 1-3 (inches)

C2 = reading from caliper 2-4 (inches)

bit size = diameter of drill bit as recorded on well log (inches)

In addition, BHTV logs from the Holditch SFE No. 2 well were examined to define the orientation of stress-related breakouts.

In deeper parts of the Travis Peak Formation in the study area (depth range = 7,300 to 9,900 ft [2,225 to 3,020 m]) ellipticity trends northwest, subparallel to minimum principal horizontal stress in the region, as determined by hydraulic fracture stress tests (Whitehead and Robinson, 1989). Breakouts on BHTV logs are subparallel to elliptical zones indicated by ellipticity logs; most breakouts were found on the deepest part of the BHTV log (9,600 to 9,900 ft [2,930 to 3,020 m]). The northwest-oriented elliptical boreholes and breakouts are a function of the regional stress regime. This conclusion is consistent with the predominant northeast orientation of natural and induced fractures observed in the Holditch SFE No. 2 well. Thus, two independent measures of wellbore shape—wellbore ellipticity and wellbore breakouts—gave consistent indications of least horizontal stress direction in the deeper part of the Travis Peak

Formation, which was confirmed by analysis of fractures in core. The same techniques of log analysis could be applied in any well where these logs are available.

Based on data from eight wells (fig. 41), two peaks of elliptical zones are significant, one at 74 degrees (composed of 10-degree-wide sectors between 60 and 100 degrees) and one at 344 degrees azimuth (composed of 10-degree-wide sectors between 340 and 350 degrees) (fig. 42). For ellipticity data plotted relative to the top of the Travis Peak Formation, a marked difference exists between the vertical distribution of the northeast- and northwest-trending peaks (fig. 43). For the northwest-trending data, ellipticity ratios significant at the 99-percent confidence level (and all but one data point larger than the mean) occur only lower than 1,500 ft (460 m) below the top of the Travis Peak Formation (fig. 43a). For the northeast-trending data, there are no zones significant at the 99-percent confidence level, but those larger than the mean are mostly within the upper 1,000 ft (300 m) of the formation (fig. 43b).

The difference in ellipticity orientation with respect to depth below the top of the formation is quite strong. The northeast orientation of natural and drilling-induced fractures (fig. 30) parallels the trend of borehole ellipticity in the upper Travis Peak; thus, it is possible that either preexisting natural fractures, or drilling-induced fractures are controlling ellipticity in this part of the formation. In deeper parts of the formation, northwest-trending ellipticity probably is caused by spalling of the borehole (breakouts) in response to the regional stress regime. This hypothesis is consistent with observations of fracture length in the Holditch Howell No. 5 well. Fractures in the upper 460 ft (140 m) of Travis Peak are significantly longer than those in the interval between 1,394 and 1,786 ft (425 and 544 m) below the top of the formation (Laubach, 1989).

Similar results have been reported by Stock and others (1984) from studies in Nevada. Natural fractures observed on BHTV logs had a preferred azimuth of 10 to 40 degrees. Moreover, at relatively shallow depths (1,725 to 2,225 ft [525 to 680 m]), near-vertical, drilling-induced fractures were observed having orientations of 25 to 30 degrees. These were interpreted to be perpendicular to the minimum horizontal principal stress. However, wellbore breakouts near

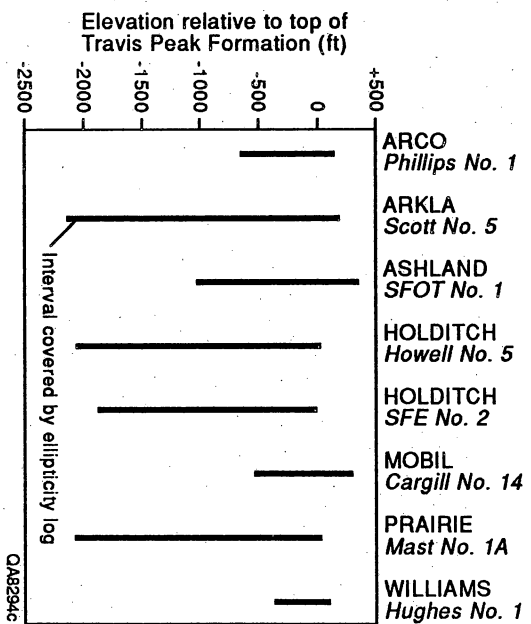


Figure 4.1. Plot of wells showing intervals in Travis Peak Formation covered by ellipticity logs in this study.

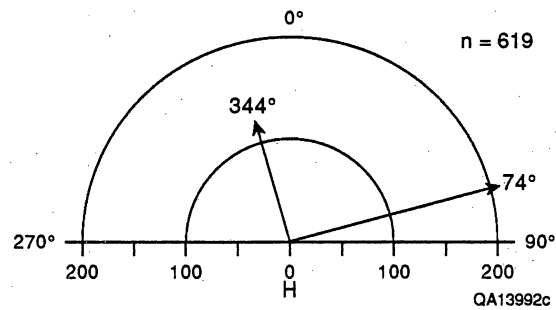


Figure 42. Rose diagram of Bernshtein accuracy criterion (H) for two significant peaks (at 99-percent confidence level) of wellbore ellipticity. These peaks comprise sums of adjacent 10-degree-wide sectors that are larger than the mean value. The northeast-trending peak is subparallel to the trends of natural and drilling-induced fractures. The northwest-trending peak is subparallel to the minimum principal horizontal stress in the region.

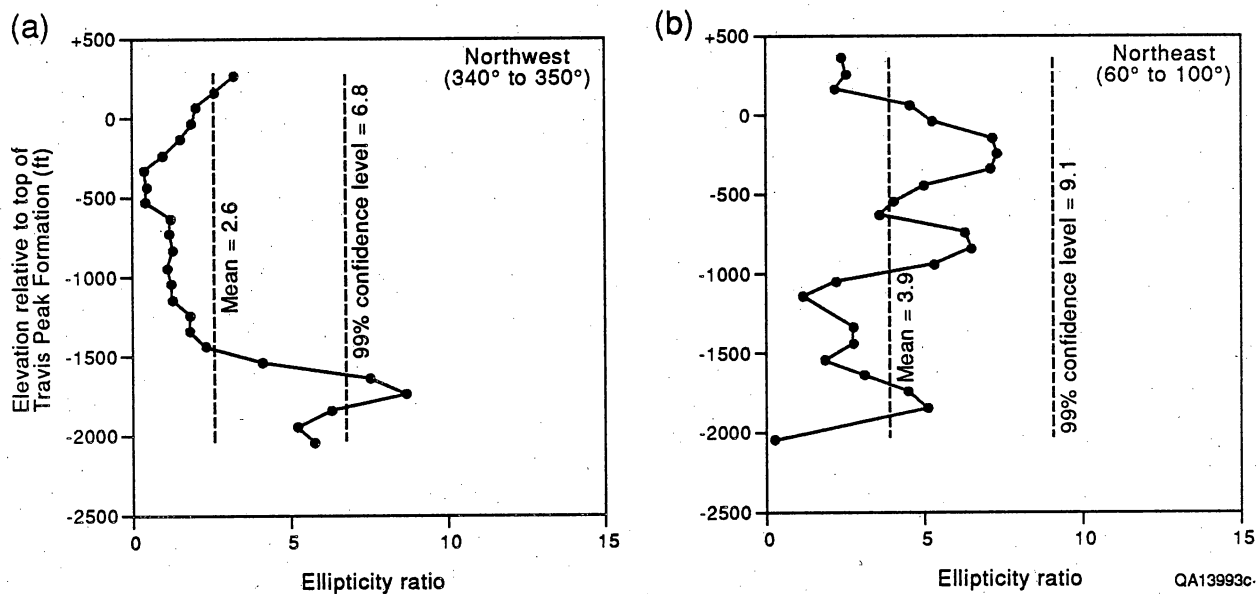


Figure 43. Plots of ellipticity ratio versus stratigraphic depth in the Travis Peak Formation. (a) Northwest-trending ellipticity is found mostly below -1,500 ft (-460 m). (b) Northeast-trending ellipticity is found mostly above -1,000 ft (-300 m).

the bottom of the logged well (3,455 to 4,000 ft [1,055 to 1,220 m] depth) had a mean azimuth of 300 degrees, parallel to the interpreted direction of least horizontal principal stress, and perpendicular to the natural and drilling-induced fractures.

A comparison of borehole breakouts with lithology reveals a different relationship. Between a depth of 8,078 and 10,081 ft (2,462 and 3,073 m) in Holditch SFE No. 2, 28 breakouts were compared with the lithology in which they were found. These are the best-defined axisymmetrical breakouts seen on the BHTV log. Most are less than 2 ft (0.6 m) high, and all are less than 90 degrees wide. Twenty-two of these breakouts (78 percent) are in sandy interbeds or thick sand layers. The remainder are in shaly and calcite-rich zones. Throughout most of this interval, shale constitutes less than 20 percent of the rock. Most breakouts are in sand, the most abundant rock type in this interval. This is the inverse of the relationship between elliptical zones and lithology in the eight boreholes studied.

Combining the results of ellipticity and lithologic analysis from the Holditch SFE No. 2 well with those of the other seven wells previously analyzed showed no change in relationships between lithology and depth or ellipticity and depth (Baumgardner and Meador, 1987). Most elliptical zones are found in shaly intervals (fig. 44). To distinguish between possible effects of depth and lithology on wellbore ellipticity, the orientation of elliptical zones was compared to lithology logs. Elliptical boreholes develop more commonly in shale than in sandstone. Almost half of all elliptical zones are found in shale (fig. 44), although shale constitutes only 19 percent of the logged lengths of the boreholes. Thus, elliptical zones develop in shale more than twice as often as they would if distribution of ellipticity were unrelated to lithology.

Furthermore, as the ellipticity (horizontal elongation) of the elliptical zones increases, so does the percentage of those zones found in shale. Forty-one percent of all elliptical zones that have ellipticity values between 0.11 and 0.20 are in shale, whereas 56 percent of elliptical zones larger than 0.20 are in shale (fig. 44).

The orientation of elliptical zones is unaffected by lithology, even though most shaly zones are in the upper 500 ft (150 m) of the Travis Peak Formation (fig. 44) where northeast-

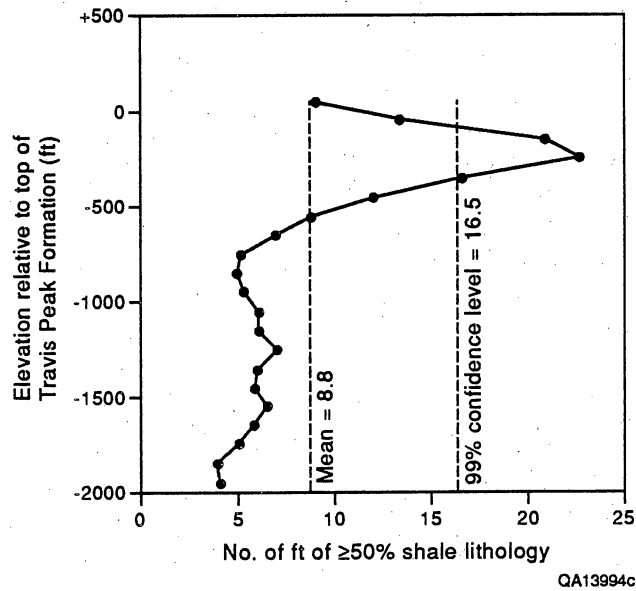


Figure 44. Plot of shale lithology (≥50 percent shale on FRACLOG) versus stratigraphic depth in the Travis Peak Formation. Most shale lies in the upper 500 ft (150 m) of the formation. FRACLOG is produced by ResTech, Inc. Lithology is based on an algebraic model of data from wireline logs such as density, neutron, gamma ray, and resistivity logs.

trending ellipticity prevails (fig. 43b). Most elliptical zones in sandstone and shale are about evenly divided between northeast and northwest orientation. Elliptical zones oriented north-south and east-west are less common, in proportion to their smaller fraction (20 degrees each) of the total range of orientation values (180 degrees).

Comparison of the BHTV and ellipticity logs from Holditch SFE No. 2 well has revealed some important differences between elliptical zones and breakouts. Less than half of the elliptical zones coincide with breakouts. Nearly half of the total length of elliptical zones is in the interval between 8,200 and 8,600 ft (2,500 and 2,620 m) in depth (fig. 45a). Less than 8 percent of the total length of BHTV breakouts is present in the same interval (fig. 45b). Most BHTV breakouts are between 9,600 and 9,900 ft (2,930 and 3,020 m) in depth. Unfortunately, ellipticity logs do not cover all of the deeper interval, so comparison there is impossible. BHTV breakouts are shorter (average height = 2.6 ft [80 cm]) and less common than the elliptical zones (average height = 7.6 ft [2.3 m]), partly because the caliper log has lower resolution than the BHTV log. It does not show features smaller than 2 ft (60 cm) high (the smallest vertical interval on the caliper log), whereas the BHTV can detect breakouts as small as 6 inches (15.2 cm) in height. The total length of BHTV breakouts for the interval between 8,250 and 9,928 ft (2,515 and 3,026 m) is 74 ft (23 m). For the same interval elliptical zones cover 242 ft (74 m), more than 3 times as much. There are 28 separate breakouts on the BHTV log, but 32 breakouts on the ellipticity log. Nevertheless, mean orientations for the two data sets are essentially the same. Mean orientation of elliptical zones is 333 degrees \pm 7 degrees. Mean orientation of all BHTV breakouts between 8,200 ft and 11,000 ft (2,500 and 3,350 m) in depth is 340 degrees \pm 2 degrees (fig. 46). These orientation values overlap 2 degrees at the 95-percent confidence level, and are not significantly different at the 99-percent confidence level. Considering that breakout and ellipticity azimuths are measured only to the nearest 5 degrees, the extent of similarity is probably even greater.

Vertical stripes on the BHTV log may result from either an excentered tool or an elliptical borehole, as discussed earlier. But the caliper log does not always record ellipticity where there

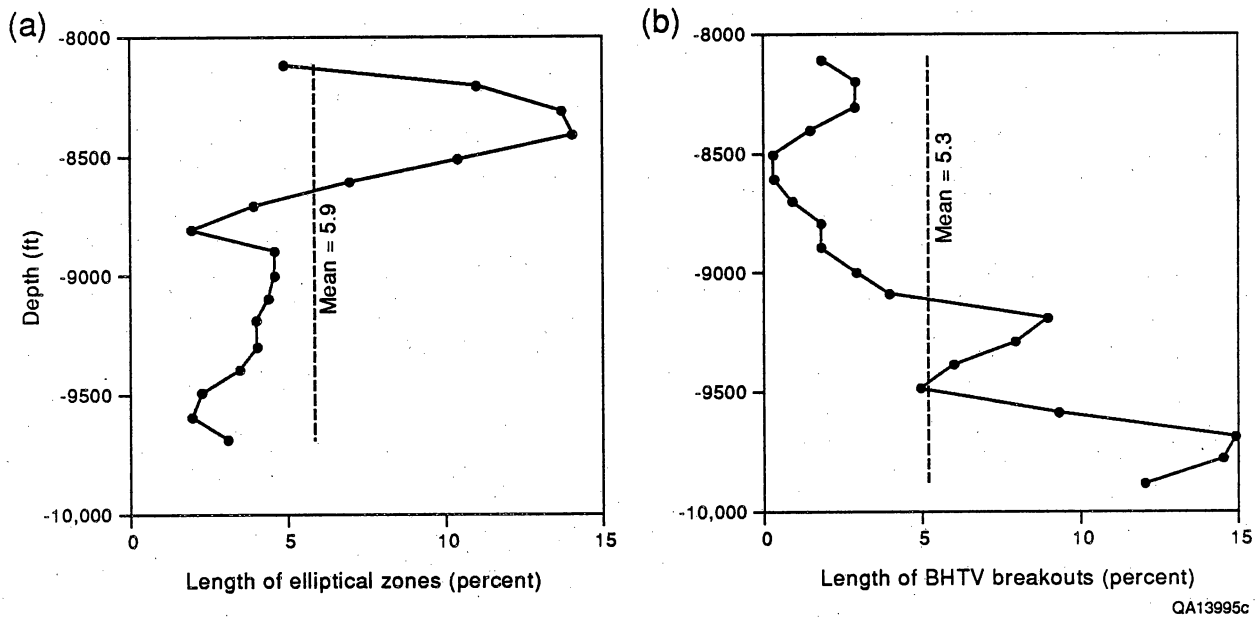


Figure 45. Plots of length of elliptical zones and BHTV breakouts versus depth. (a) Almost half of the total length of elliptical zones is found between -8,200 and -8,600 ft (-2,500 and -2,620 m) depth. (b) Most breakouts occur deeper than -9,500 ft (-2,900 m).

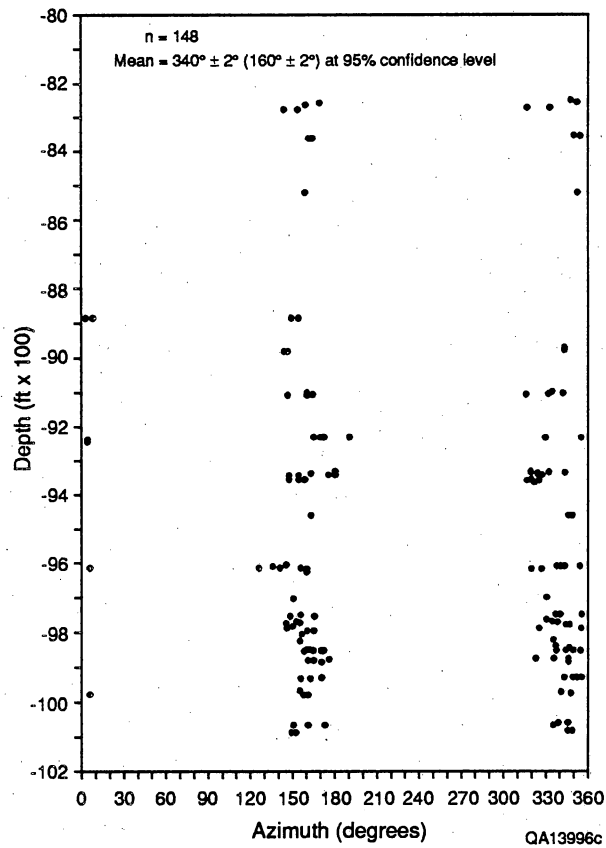


Figure 46. Plot of the azimuth of borehole breakouts versus depth. Mean orientation of breakouts is 340 degrees ± 2 degrees, at the 95-percent confidence level. These features parallel the minimum principal horizontal stress, indicating that they formed as a result of the regional stress regime.

are vertical stripes on the BHTV log, so it is impossible to know whether the borehole is elliptical or the tool is off-center in all cases. Where ellipticity is recorded coincident with vertical stripes on the BHTV log, the orientation of the elliptical zone is usually the same as the bright stripe between one set of dark stripes (as expected), indicating that the BHTV is detecting a strong return signal from the ends of the elongated borehole.

These results show that even though the elliptical zones on the ellipticity logs usually are not the same features as breakouts identified on BHTV logs, they indicate essentially the same north-northwest orientation of least horizontal principal stress in the study area. Of the 32 breakouts identified on ellipticity logs, 16 are associated directly with breakouts identified on BHTV logs or are indirectly affected by breakouts just below them in the borehole wall. Of the 2,000 ft (610 m) of BHTV log examined, nearly 60 percent of all BHTV breakouts are concentrated in the 500 ft (150 m) between 9,600 and 10,100 ft (2,930 and 3,080 m) in depth, the deepest part of the log (fig. 45b), which overlaps with the zone of northwest-trending wellbore ellipticity (fig. 44a).

If rock strength is constant with depth but mean stress is increasing, then one might expect more stress-induced breakouts to occur in the deeper intervals. If rock strength in the upper sections is greater than the effective (amplified) stress near the borehole, then no true breakouts would be expected, and elliptical boreholes would be where fractures or other local weaknesses are present or where drilling operations had altered the borehole shape.

Features Visible on FMS Logs

In the Travis Peak Formation fractures have dark (conductive) traces on FMS logs (figs. 47 to 53). Fractures form dark traces when they are filled with conductive drilling mud or some conductive vein-filling mineral. Figure 48 shows the linear vertical features on Holditch Howell No. 5 and Mobil Cargill No. 15 FMS logs classified into three image types. Differences between the image types are gradational. Type 1 features are curvilinear, narrow, conductive



| Type | Description | Corresponding feature in core |
|--------|---|---|
| Type 1 | Dark, curvilinear conductive anomalies to faint, discontinuous anomalies with sharp, clearly defined boundaries. (1- to 10-ft long) | Drilling-induced fractures, locally natural fractures. |
| Type 2 | Curvilinear to irregular, wide, with diffuse boundaries. Irregular ends. | Natural fractures, drilling-induced fractures, or sedimentary structures. |
| Type 3 | Contacts between mottled or textured log patterns and wide, short conductive areas. | Locally, sedimentary structures. |

QA13846c

Figure 47. Linear vertical features seen on FMS logs, classified into three types. Examples are from the Holditch Howell No. 5 (SFE No. 1) well, Waskom field, Harrison County.

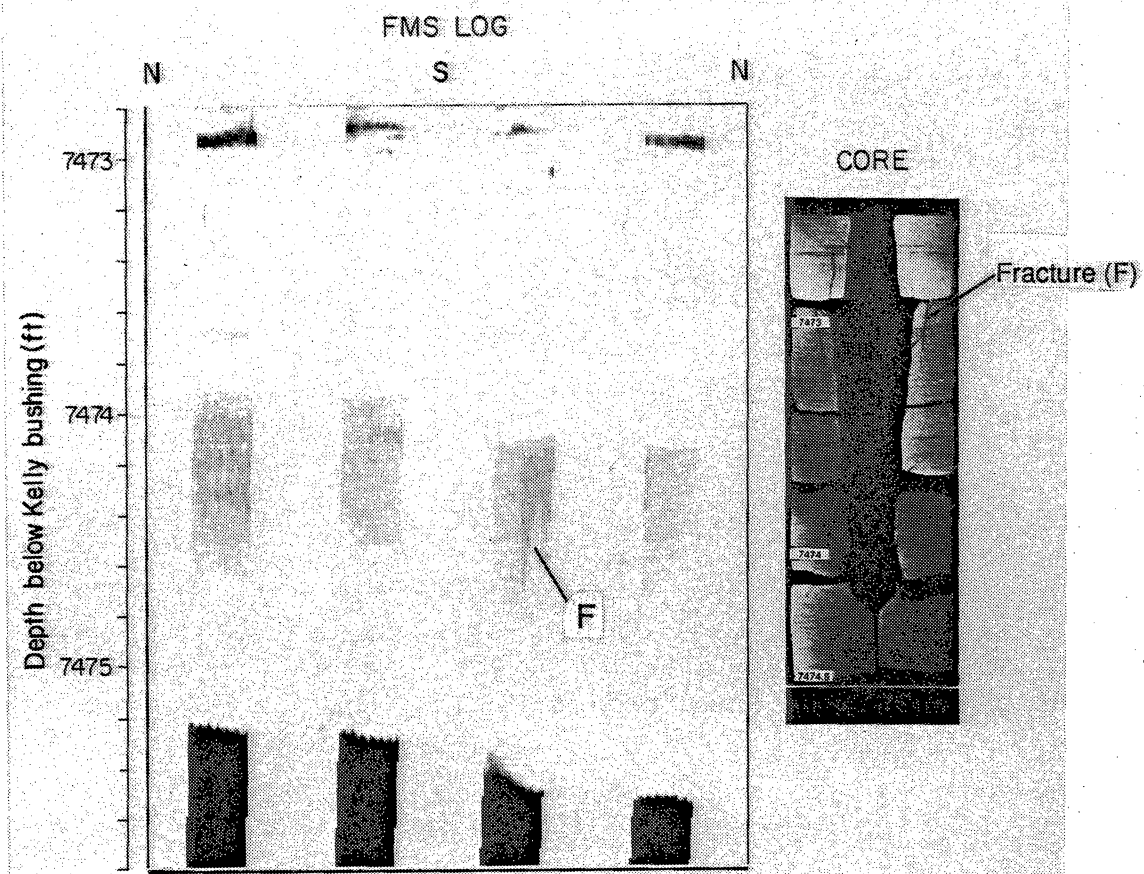


Figure 48. Natural fracture in sandstone core and imaged by FMS, Holditch Howell No. 5 (SFE No. 1) well, Waskom field, Harrison County.

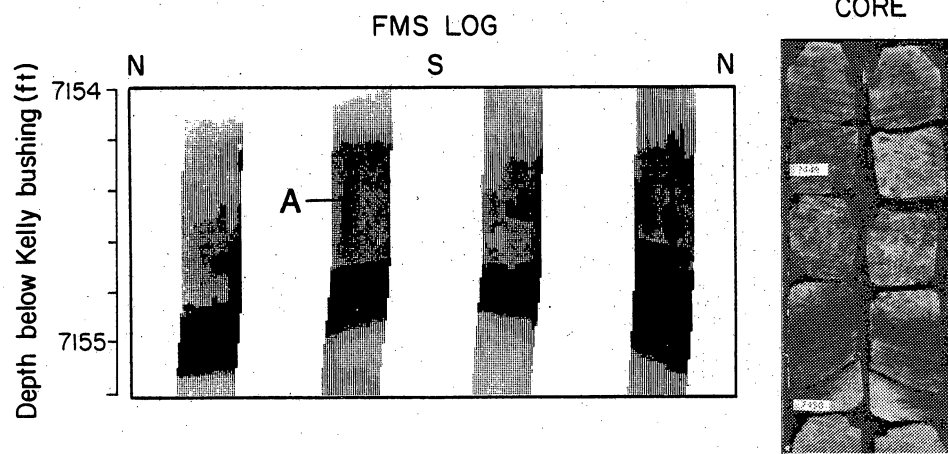


Figure 49. Example of a vertical FMS feature (A) that does not correspond to any structure visible in core, Holditch Howell No. 5 (SFE No. 1) well, Waskom field, Harrison County.

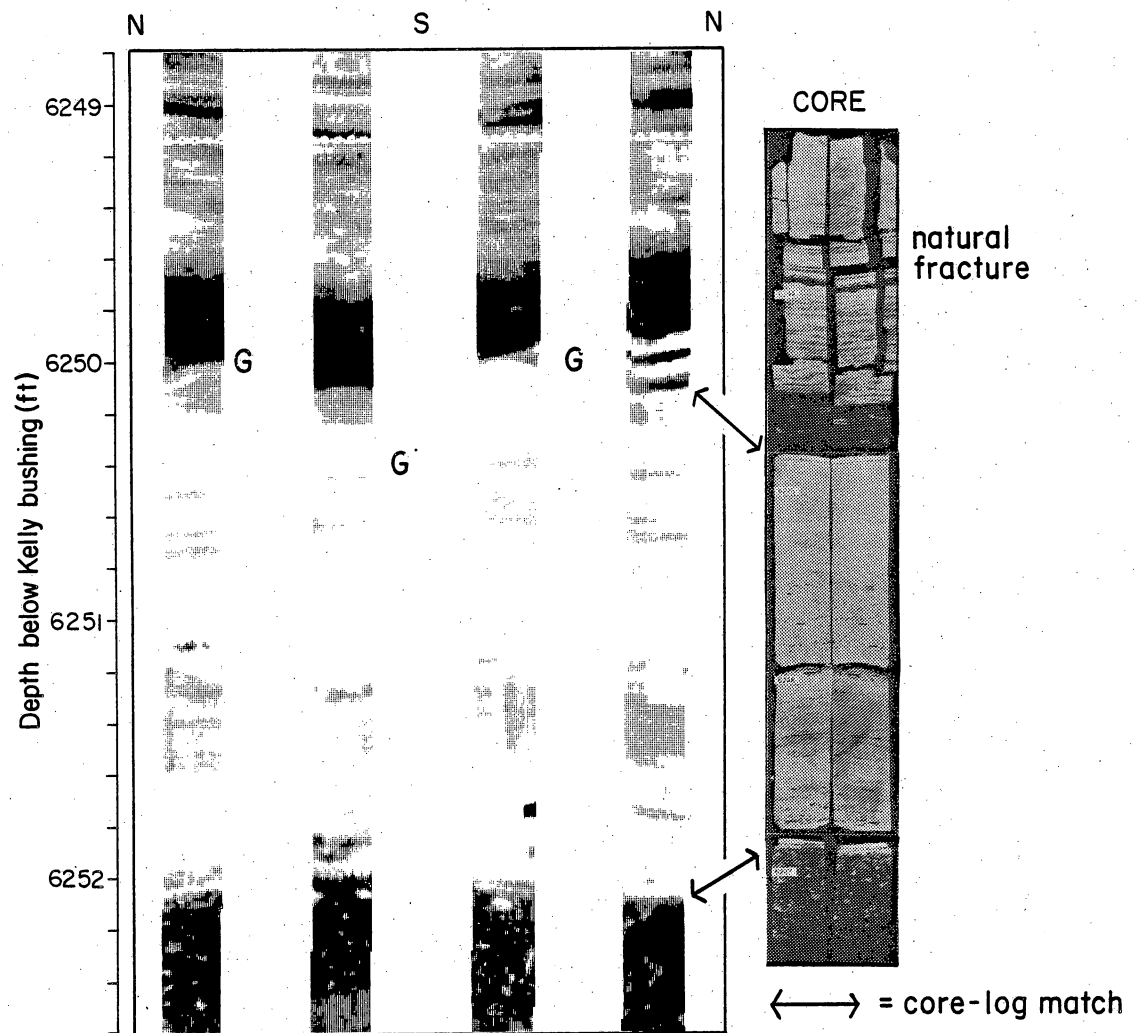


Figure 50. Prominent natural fracture in core that was missed by FMS pads, Holditch Howell No. 5 (SFE No. 1) well, Waskom field, Harrison County. G = gaps in coverage of borehole wall.

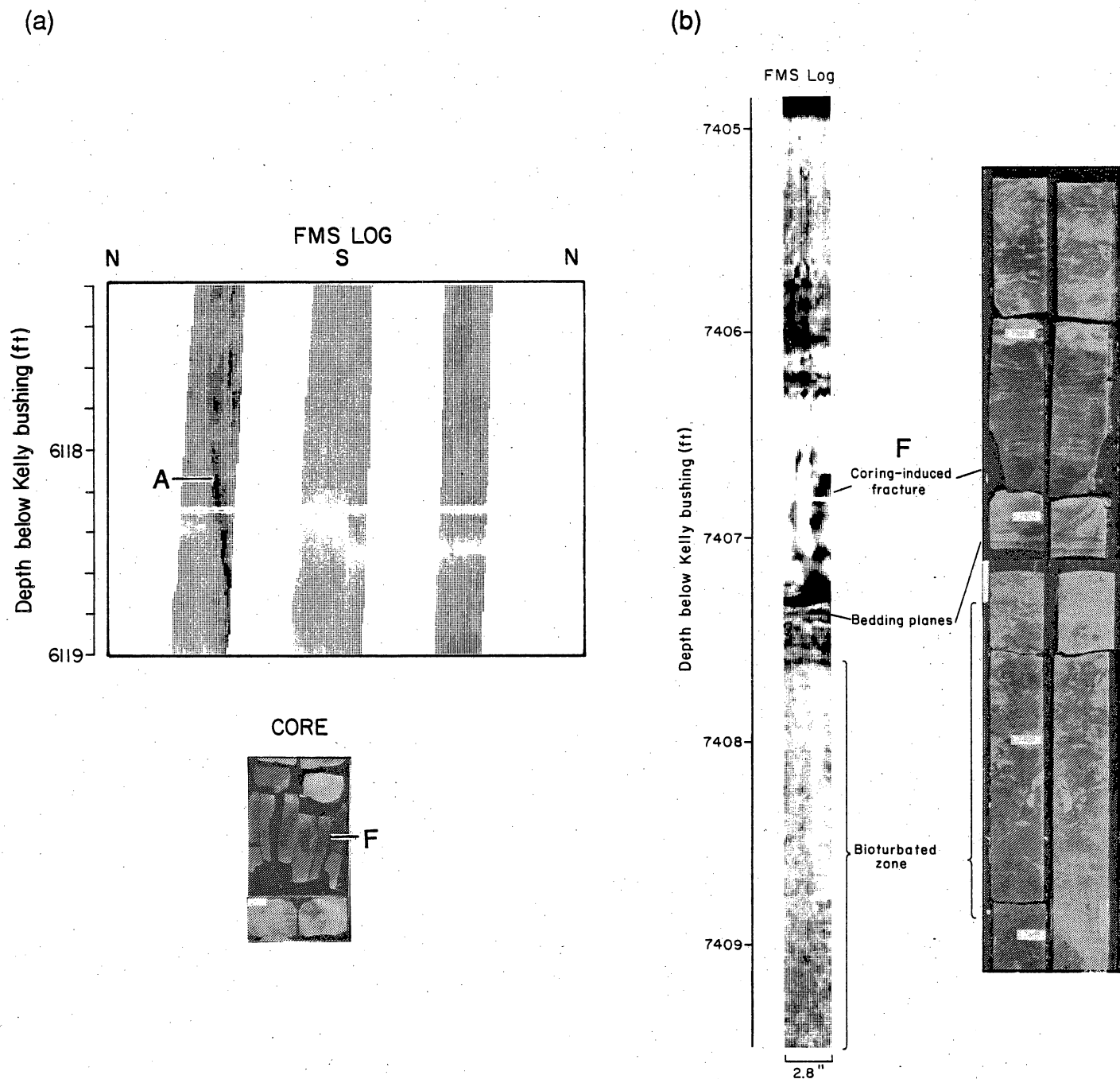
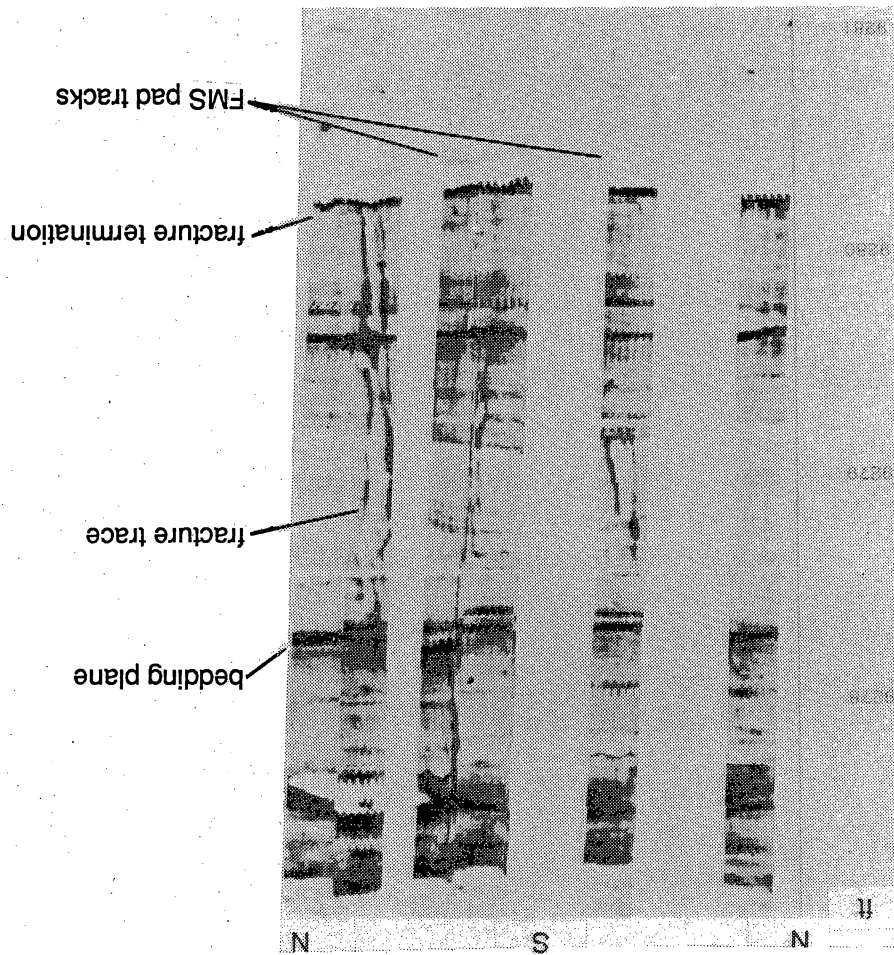


Figure 51. Coring-induced fractures imaged by FMS. (a) FMS log and petal and petal-centerline fractures (F) in the core, Mobil Cargill No. 15 well. Fractures (A) on the log are diffuse type 2 features. (b) Coring-induced fracture (F) in core and on log from Holditch Howell No. 5 well.

Figure 52. FMS image of fractures and bedding illustrating fracture terminations at bedding plane, Mobil Cargill No. 15 well.



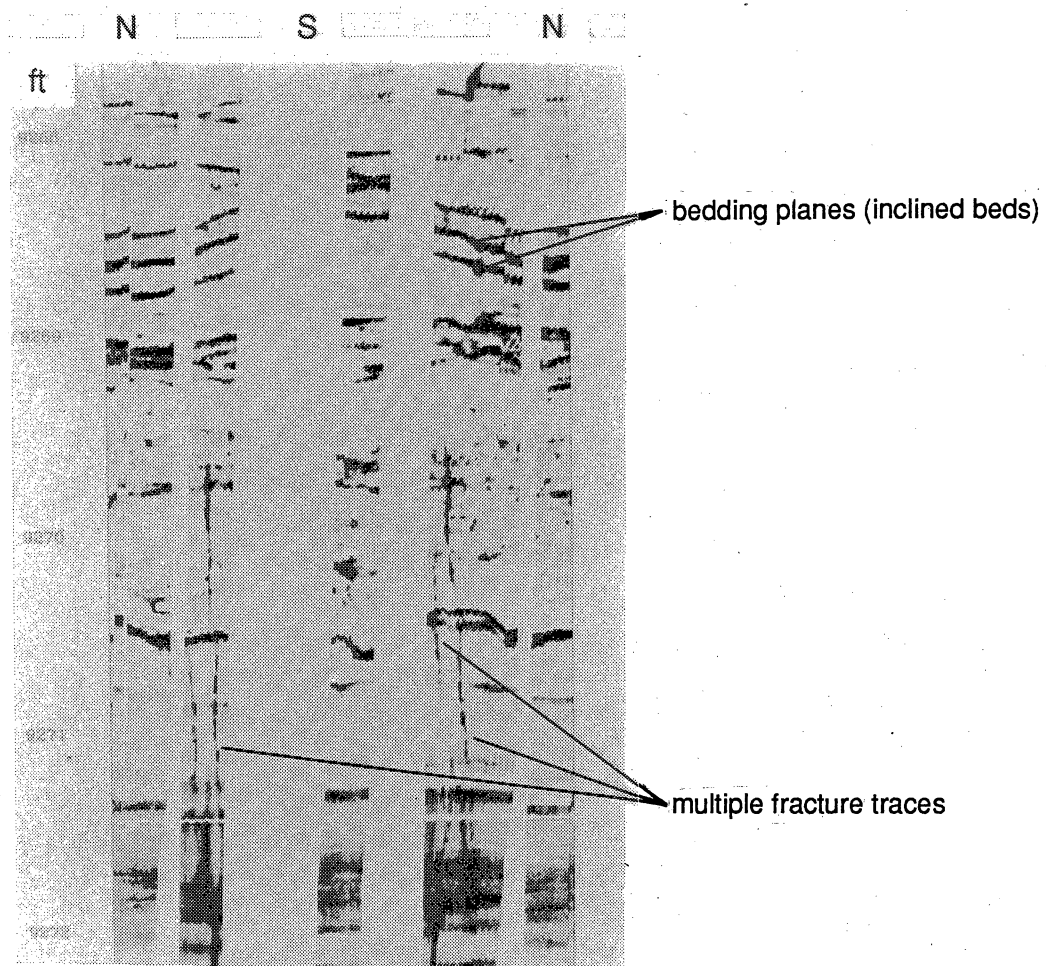


Figure 53. FMS image of fractures and bedding, illustrating multistranded fracture traces, Mobil Cargill No. 15 well.

dark bands that have sharp, clearly defined boundaries in a lighter background. Feature edges are either straight or slightly irregular and wavy (scalloped). These features range from less than 1 ft (30 cm) to as much as 10 ft (3 m) in length, and commonly have tapered ends. Type 1 features occur where the FMS log sharply delineates bedding and other sedimentary structures, indicating good tool contact with the borehole wall and maximum resolution. Type 2 features are linear to irregular in shape and are wider than Type 1 features. They have diffuse, gradational boundaries. Type 2 features occur where bed resolution is good and where it is poor. Caliper logs locally show evidence of irregular or rough borehole surfaces in sections of borehole having poor bed resolution and this type of image, suggesting that locally the image may be unfocused as a result of pad standoff. Type 3 features are contacts between textured log patterns and short wide conductive dark areas. Edges of conductive areas are curved and can be either sharp or diffuse.

Comparison of FMS Images with Cores

Examples of all three FMS feature types correlate with structures in core, but only 32 percent of Type 1 and 2 features on the Holditch Howell No. 5 FMS log matched fractures visible in core. Fractures in core generally correspond to either Type 1 or Type 2 features, where they are visible on the log. In Holditch Howell No. 5 some fractures appear as dark, linear features having sharp edges (Type 1 features) similar to conductive anomalies described by Ekstrom and others (1986) and by Dennis and others (1987). Other fractures are represented by subtle conductivity anomalies that are faint or discontinuous (Type 2) with the processing used in this study. Type 1 features on FMS logs from Holditch Howell No. 5 correspond primarily to drilling-induced fractures in core, possibly because this fracture type is prevalent in this well (fig. 51). However, not all Type 1 features have corresponding fractures in core. Some of these Type 1 features could be image artifacts or grooves in the wellbore produced by drill-pipe wear (Bourke and others, 1989, p. 24), and others are probably fractures that do not intersect the

core. Some Type 1 features correspond to fractures in core that are so narrow (less than 0.025 cm) that they were overlooked during preliminary core description. Type 2 features are natural fractures, drilling-induced fractures, or vertical sedimentary structures (fig. 48); there may even be no corresponding structure visible in the core (fig. 49). Type 3 features (fig. 47) are most likely breakouts and washouts, although some are irregularly shaped sedimentary structures, and some may be spalled fractures or fractures intersecting only the edge of the tool pad. Some examples may correspond to areas of poor pad contact.

Core orientation methods that are independent of the logs generally were not precise enough to determine unambiguously whether fractures in core having no corresponding FMS feature were missed by the tool pad. Some prominent natural fractures in core were probably simply missed on the borehole wall by the FMS because of the limited (approximately 20 percent) borehole coverage of the two-pad tool (fig. 50). Locally, multiple logging passes significantly increased the borehole coverage to 50 to 60 percent, but even in these areas, fractures were missed.

For Type 1 features, the high-resolution FMS image reveals aspects of fracture-pattern shape, height, and relation to bedding (fig. 53). Terminations of Type 1 features at interbeds are common on FMS logs (Part One). These observations are consistent with core results that show both natural and drilling-induced petal-centerline fractures terminating at thin (<1 inch [<2.5 cm]) mudstone or siltstone interbeds. The FMS detects multiple fracture strands that are observed in core in heterogeneous rocks (fig. 54). Detailed resolution of thin beds would permit extension and shear fractures to be identified on the basis of the presence or absence of offset beds or laminae, but shear fractures in the Travis Peak are in beds that have little distinct internal stratification. Width of FMS fracture traces varies, and although the general shape of fractures is accurately portrayed, we found no consistent relation between widths of fracture images and fracture width measured in core. Recent advances in FMS processing suggest that more accurate width determinations using this log, in combination with other logs, may be possible in the future (Bourke and others, 1989).

Where natural fractures on FMS logs from Holditch Howell No. 5 are Type 2 features, details of fracture shape and their relation to bedding are less apparent. Type 2 features commonly have no corresponding features in core. Some Type 2 images could be fractures that are in the borehole wall but that do not intersect the core (fig. 36), but full borehole coverage would be needed to demonstrate this by confirming that symmetric pairs of fracture traces had a small enough angular divergence that they would not intersect the core. Some Type 2 features are vertically elongate sedimentary structures. In the Travis Peak, sedimentary features that resemble fractures on fracture-imaging logs include fluid-escape structures, root casts, and contorted bedding. Sedimentary features detected by the FMS are discussed further in Part One. Some Type 2 images that resemble images of natural fractures have no corresponding features in core or on the BHTV. These Type 2 features are probably image artifacts (spurious features on logs caused by tool malfunction or processing errors). Because we could not systematically separate Type 2 features that represent faint images of real fractures from probable artifacts, this type of image is less useful for estimating fracture abundance than is Type 1.

Drilling-induced fractures on the FMS are commonly Type 1 features. Our observations did not lead us to any consistent criteria for distinguishing natural and drilling-induced fractures in the Travis Peak.

Fracture Orientation from Core Data and Logs

One of the most useful aspects of the analysis of fractures in the subsurface is the determination of fracture orientation, or strike. Fractures in Travis Peak sandstone are typically near vertical and strike east-northeast to east, having a range of strikes from 028 to 130 degrees and a mean strike of 083 degrees (fig. 30) as determined by downhole core orientation techniques (Nelson and others, 1987), core orientation by rock magnetic (paleomagnetic) methods (Van Alstine, 1986), and borehole-imaging logs. In the Travis Peak,

using any of these methods, considerable variation in fracture strike is evident from well to well, within a given well, and within any depth interval in a single well.

Orientation of inclined fractures can be obtained readily either from the BHTV or from the FMS if the top and/or bottom of the curved, sinusoidal fracture trace is visible on logs (Zemanek, 1970; Crary and others, 1986; Ekstrom and others, 1986; Lau and others, 1987). However, most fractures in Travis Peak sandstone are vertical. Orientation of these vertical fractures can be ambiguous, especially where multiple fracture traces are present (figs. 54 and 55). Nevertheless, fracture orientations derived from BHTV and FMS logs are similar to fracture orientations from multishot and paleomagnetic core orientation methods. Average strike of all vertical fractures measured using the BHTV in Holditch Howell No. 5 is 085 degrees, in agreement with the vector mean strike of 084 degrees determined for 15 fractures oriented by paleomagnetic methods. The lower resolution of sedimentary structures and bed boundaries that was accomplished using the BHTV in these wells made exact depth correlations with core problematic, especially where many gaps exist in the core. This method is most useful where bedding is distinct and prominent fractures are present.

A comparison of fracture orientations in core derived from inspection of the BHTV in cored intervals and the same fractures oriented using the paleomagnetic method was made in nine intervals from the Holditch SFE No. 2 and Mobil Cargill No. 15 wells (fig. 56). A determination was made for each interval of the orientation of the master orientation line (MOL), a reference line marked on the core. BHTV determinations were made by identifying a distinctive geologic feature or set of features on the log and in the core (these were generally fractures and bedding planes) and using the orientation of the feature to orient the MOL. In several instances separate geologic features within the same continuous core interval were used to orient the MOL, and the results based on different geologic features agree within 5 degrees. Under optimal conditions, the orientation precision of the BHTV is on the order of 1 degree or better (Nelson and others, 1987; R. A. Plumb, personal communication, 1987). Using the paleomagnetic method, magnetic north is determined from plug samples within the cored

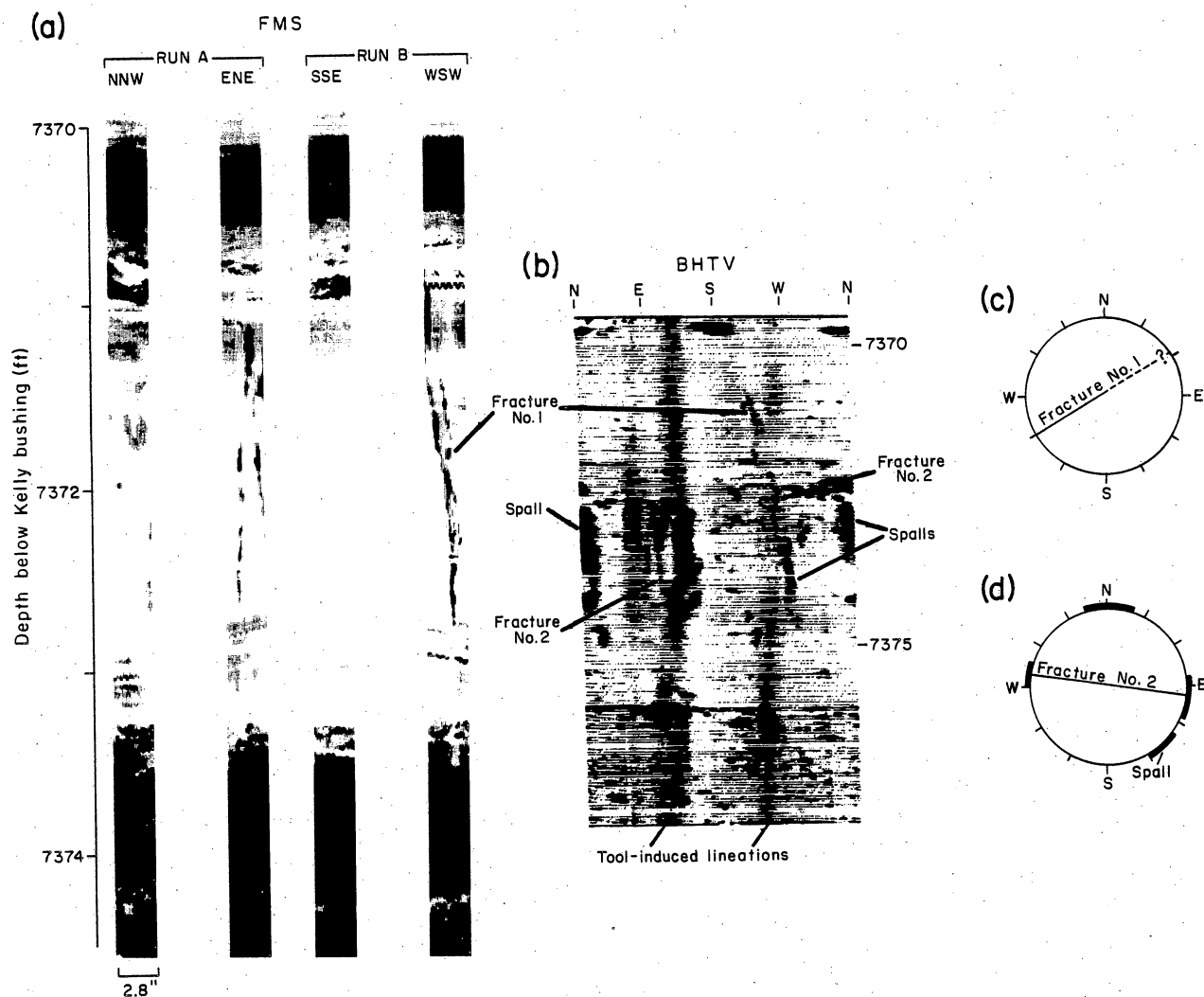
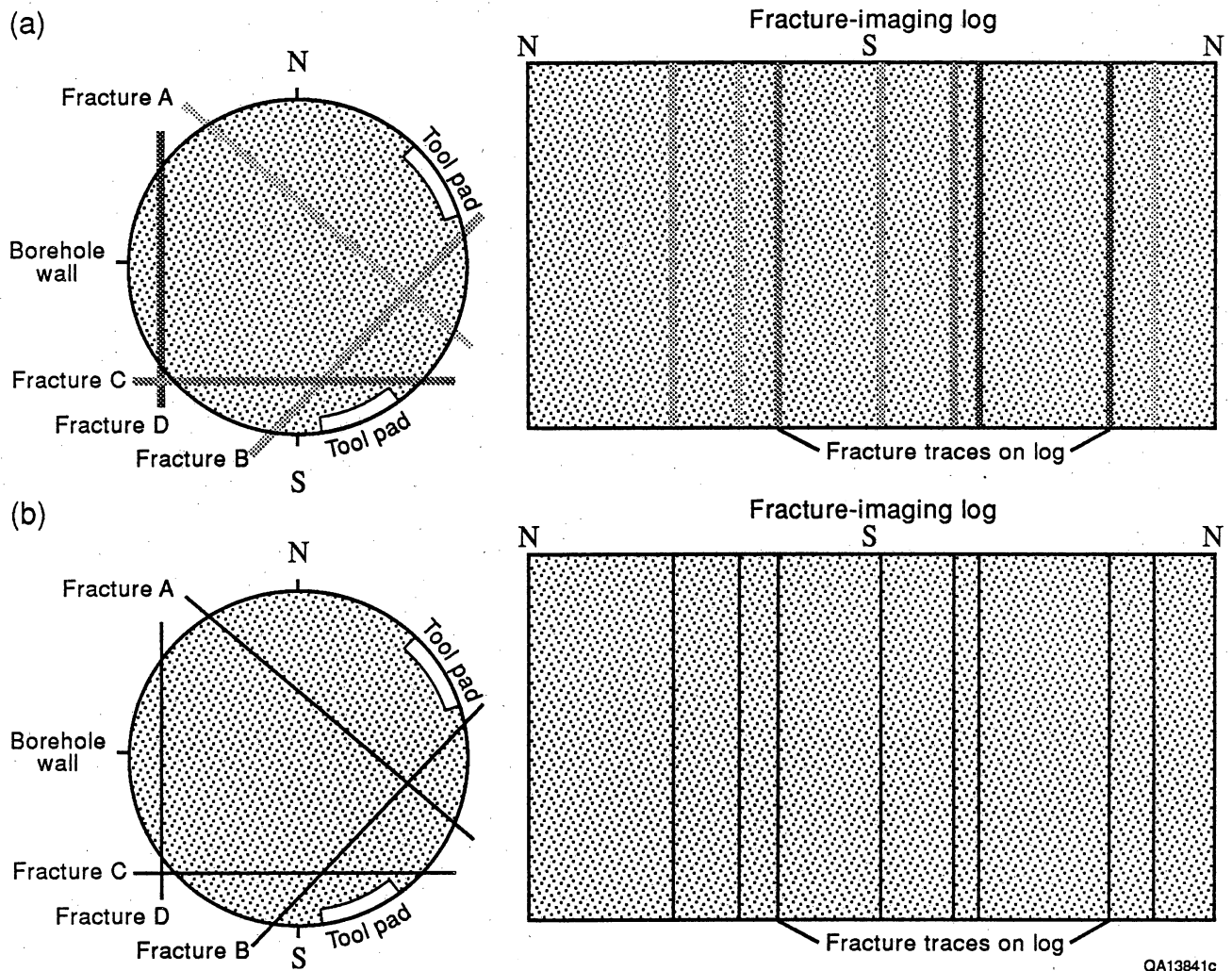


Figure 54. Features on FMS and BHTV logs, Holditch Howell No. 5 well. (a) Two FMS runs through the same interval. Linear vertical features on pads oriented east-northeast and west-southwest are fractures. Dipping beds are visible at 7,372.7 ft (2,247 m). (b) BHTV log over same interval. Fractures are visible at 7,371 ft (2,246.5 m) and 7,372.7 ft (2,247 m). Fracture number 1 at 7,371 ft (2,246.5 m) probably corresponds to fracture on FMS log. Fracture number 2 is not visible on FMS log because neither FMS logging pass sampled the fracture. On the BHTV log, dark, irregular areas in the east and west quadrants are spalls that intersect fracture number 2. Dark areas in the north and southeast quadrants are spalls that do not intersect fractures. Straight, parallel, dark vertical bands extending the length of the log in the east-southeast and west-southwest quadrants are toolmarks. (c) and (d) Directional plots of borehole features illustrate orientation of fractures and spalls on BHTV log.



QA13841c

Figure 55. Diagram illustrating inherent uncertainties in matching vertical fracture traces on borehole-imaging logs. Left-hand part of diagram shows fractures intersecting borehole, as viewed from above (down the borehole). Tool pads represent FMS-imaging pads. Right-hand part shows fracture traces on borehole-imaging log. (a) Vertical fractures having a range of strikes that can be identified and correlated on the log. Such identifications and correlations are seldom unique or certain. (b) Vertical fractures having a range of strikes that cannot be identified and correlated on the log. This situation is common.

| Well | Core No. | MOL ¹ Azimuth | | Difference ⁴ |
|-----------|----------|---------------------------------|-------------------|-------------------------|
| | | Paleomag- netic ² | BHTV ³ | |
| SFE No. 2 | 2 | 246° | 94° | 108° |
| SFE No. 2 | 7 | 132° | 121° | 11° |
| SFE No. 2 | 14 | 68° | 59° | 9° |
| SFE No. 2 | 15 | 133° | 133° | 4° |
| SFE No. 3 | 8 | 19° | 21° | 2° |
| SFE No. 3 | 9(a) | 252° | 272° | 20° |
| SFE No. 3 | 9(b) | 179° | 181° | 2° |
| SFE No. 3 | 10 | 272° | 284° | 12° |
| SFE No. 3 | 12 | 316° | 314° | 2° |

¹ Master orientation line (a reference line marked on the core).

² Paleomagnetic method

³ Borehole televiewer method

⁴ Absolute difference between paleomagnetic and borehole televiewer strikes.

QA13997c

Figure 56. Chart showing the orientation of core by paleomagnetic methods and the BHTV. It shows the azimuths of a reference line on core (the master orientation line, MOL) determined by the paleomagnetic method and by correlation of features on the BHTV along with the difference between the results of the two methods.

interval, and the component of magnetization corresponding to present-day north is used to orient the core (Van Alstine and others, 1983; Van Alstine, 1986). Orientation error of as little as 5 degrees is reported to be possible using this method (Nelson and others, 1987, p. 366). In figure 56, the MOL azimuth determined by the magnetic method and BHTV should agree if there are no errors in either method. Given the accuracy of the two methods and errors in measuring fracture strike, the absolute difference between the two methods should not be greater than 10 degrees. The measured differences range from 2 to 108 degrees with a mean of 18.9 degrees. If the result from Holditch SFE No. 2 core number 2 is disregarded as being from core misorientation during handling, the mean difference is only 7.8 degrees. The two methods agree within expected tolerances in some intervals, but not in others. We were not able to determine how much of the error arose from miscorrelation of features on logs to core and how much derives from errors in the paleomagnetic method.

In the Travis Peak wells, the BHTV log is more reliable for obtaining fracture orientation in elliptical boreholes where borehole coverage by the FMS is inadequate. The position of fracture traces on FMS images is oriented with respect to north, but for vertical fractures that do not have a sinusoidal trace, an imaged trace might correspond to another trace that is in a part of the borehole that is not imaged. In Holditch Howell No. 5, for example, even where both pads detected fractures, fracture orientations obtained using the FMS alone were commonly ambiguous because additional fracture traces may exist in parts of the borehole wall that were missed by FMS pads and not imaged. The FMS image reveals a vertical fracture on the east-northeast and west-southwest borehole wall that crosses inclined beds at 7,372.7 ft (2,247.2 m) and ends at a mudstone interbed (7,374 ft [2,247.5 m]) (fig. 54). The BHTV log over the same interval is at a more compressed scale but clearly shows the same fractures that are visible on the FMS log. Fracture number 1 at 7,371 ft (2,246.5 m) on the BHTV log corresponds to one fracture trace on the FMS log. Fracture number 2 at 7,374 ft (2,247.5 m) on the BHTV is not visible on the FMS log because neither FMS logging pass crossed the fracture. Dark, irregular

areas on the east and west BHTV quadrants are spalls (borehole breakouts) that are not delineated by FMS.

Subvertical drilling-induced fractures and natural extension fractures have similar strikes, but observations of fractures in continuous core intervals show that natural and drilling-induced fractures are not precisely parallel. For example, in one continuous core (where core orientation methods cannot affect relative orientations of fractures) from Prairie Producing Mast No. A-1, the average angle between natural and induced fractures is 22 degrees. Strikes of natural and drilling-induced fractures in the same core locally deviate by as much as 85 degrees, although the difference is commonly 5 degrees or less. Mean angle between natural and drilling-induced fractures is 17 degrees, and the mean angle in individual wells is between 10 and 20 degrees (Laubach and Monson, 1988).

FRACTURE INTERPRETATION USING BOREHOLE-IMAGING LOGS

Using the BHTV transducer, Georgi (1985) detected fractures that had minimum apertures of 0.01 inch (0.025 cm) in physical models. However, Nelson (1987) found that fractures are detected by BHTV only if they are wider than 0.03 inch (0.076 cm) or have been modified by drilling to produce a topographic feature on the borehole wall. Fractures that in core are as narrow as 0.025 inch (0.06 cm) were detected in Holditch SFE No. 2 using the BHTV. Travis Peak fractures that are narrow in core possibly have been widened by erosion in the borehole wall. Such erosion and widening of fractures is observed along the outer surface of the core (fig. 37). Thus, the detection limits of the BHTV cannot be rigorously tested using our observations. Detecting narrow fractures and low-angle fractures depends on vertical sampling rate and scale of image (for example, 1:6 or 1:24) more than on tool physics of the BHTV and FMS.

In the Travis Peak, the FMS detected narrow (>0.01 inch [>0.025 cm]) fractures. The high density of measurements along the axis of the hole enables features only centimeters apart to

be resolved (Pezard and Lovell, 1990). Plumb and others (1985) reported vertical resolution of better than 0.4 inch (1 cm) for sedimentary structures and detection of fractures that have apertures of less than 0.04 inch (0.1 cm) using the FMS. Casarta and others (1989) found a minimum detectable fracture width of 10 to 20 microns. The width of conductive features visible on FMS logs in the Travis Peak does not correspond exactly with widths of geologic features in core. This is partly because the logging tool is imaging features in the borehole wall rather than the core, and thin beds and fractures can vary in width over this distance. Furthermore, apparent widths of geologic features may vary because of inherent limitations in resolution and detection limits arising from the size and configuration of detectors on the FMS pad (Schlumberger, Ltd., 1987). Short fractures (<4 inches [<10 cm]) and the shapes of longer fractures may be poorly defined because of loss of pad contact with the borehole wall, and images may be blurred by improper tool-speed corrections.

The high sensitivity of the FMS to thin conductive features makes it possible to detect small fractures and to distinguish them from sedimentary features. An advantage of the FMS is its ability to create images of subtle sedimentary features and to reveal their spatial relation to fractures, which can be used to help interpret the style of fracturing. This information is useful for determining the causes of fracturing, but care should be taken to distinguish conductive anomalies that are unrelated to fractures or bedding and that may be caused by the action of the bit and drill string. Analysis of fracture origin and relation of fractures to bedding, which is useful for evaluating the relation between matrix and fracture permeability, is augmented by high-resolution FMS images of fracture shape and sedimentary structures. Sedimentary features visible on FMS logs in the Travis Peak and Cotton Valley are described and discussed in Part One.

An advantage of the BHTV for fracture studies is the complete borehole coverage this tool provides. The 360-degree borehole coverage of the BHTV generally enhances fracture identification, orientation, and estimates of fracture abundance, whereas with the FMS these determinations are more ambiguous because part of the borehole is not sampled. By having

complete borehole coverage, borehole breakouts, from which principal stress directions can be deduced, are more easily recognized and distinguished from other types of fractures. Incomplete borehole coverage by FMS results from the limited size of the sampling pads and a tendency for tool orientation to be locked in by even a slightly elliptical borehole. Where this happens, vertical fractures between the FMS pads are missed entirely. In Holditch Howell No. 5, FMS pads tended to follow long axes of the elliptical borehole even in cases where the difference between orthogonal caliper readings was consistently less than 0.5 inch (<1.3 cm). Consequently, multiple tool passes did not significantly increase coverage of the borehole wall in Holditch Howell No. 5. Much more complete borehole coverage was achieved using multiple tool passes in Mobil Cargill No. 15, where locally borehole coverage is as much as 75 percent. In Holditch Howell No. 5 multiple tool passes did not generally provide enough coverage to reliably determine fracture abundance or unambiguous fracture orientation. Other studies, however, report 40 to 80 percent wellbore coverage using multiple runs of the two-pad FMS (Dennis and others, 1987), and more complete borehole coverage is provided by four-pad FMS tools. Using this tool, borehole coverage of 40 percent can be attained without multiple tool passes, and the influence of preferred tool tracking on borehole coverage is diminished.

Image artifacts on the Travis Peak BHTV logs include the vertical striping that is found in cases where holes are elliptical or enlarged or where the tool is off-center. Such artifacts can lead to fewer fractures being detected using the BHTV than actually exist in the borehole wall because the borehole wall is obscured. This type of artifact is almost completely absent on BHTV logs from Holditch SFE No. 2. Artifacts can also limit fracture detection using the FMS, and some artifacts resemble fractures (Bourke and others, 1989).

In Holditch Howell No. 5 and Holditch SFE No. 2 more fractures are visible on the BHTV logs because their coverage of the borehole wall is more complete than that of the FMS, and few image artifacts are present. In contrast, Dennis and others (1987) compared the BHTV and the FMS in a limestone reservoir and found more fractures using the FMS. The difference was attributed to the higher sampling rate of the FMS and a conductivity contrast that was larger

than the acoustic contrast between fractures and matrix. A higher sampling rate for the BHTV might have increased fracture resolution in this instance.

A critical issue in the analysis of subsurface fractures is distinguishing natural fractures that existed in the reservoir before drilling, from fractures that were created by the drilling or coring process. Fractures in the latter category include coring-induced petal and petal-centerline fractures, fractures related to borehole breakout and washout, and those inadvertent hydrofractures created by drilling under overbalanced pressure conditions. This distinction may be straightforward where inclined wellbores intersect vertical natural fracture sets or vertical wellbores cross inclined natural fractures (Casarta and others, 1989), but where natural and induced fractures are parallel to the borehole axis and have closely similar strikes, as in the Cotton Valley and Travis Peak Formation in East Texas, the problem of separating natural and induced fractures is more difficult. Well-developed or mature borehole breakouts and all other fracture types can be readily distinguished using the BHTV, but we found no unambiguous criteria for systematically differentiating between natural and narrow drilling-induced fractures such as petal and petal-centerline fractures on the basis of the appearance of the fracture trace alone. In principle, the FMS can distinguish natural from induced fractures if a sufficient conductivity contrast exists between fracture-filling minerals and host rock, but in the Travis Peak natural and drilling-induced fractures could not be separated because natural fractures are either open or filled primarily with quartz, which does not have a conductivity contrast with the host quartzarenite. Healed fractures are detectable by BHTV if the material filling the fracture has an acoustic impedance that is significantly different from that of the host rock (Rambow, 1984), but it does not in the Travis Peak core we studied.

The presence of induced fractures should be suspected when long (tens of meters) fractures symmetrically divide the borehole on BHTV images (Schlumberger, Ltd., 1987; Bourke and others, 1989). Distinctive drilling-induced fracture shapes might be used to differentiate natural and induced fracture types. For example, the characteristic concave-downward curve

of drilling-induced petal-centerline fractures (Laubach and Monson, 1988) in principle could be used to discriminate between drilling-induced and natural fractures. However, observations of natural and drilling-induced fractures in Travis Peak core show that this method is unreliable here because inclined drilling-induced petal fractures commonly curve or hook into vertical natural fractures, creating composite fractures that have shapes similar to those of drilling-induced petal-centerline fractures. Plumb (1989) recognized distributions of fracture traces on the Holditch SFE No. 2 BHTV log that are associated with the early development of certain breakout types. Recognition of these features can help distinguish natural and drilling-induced fractures on logs, but reliable rules for systematically distinguishing natural and induced fractures based on trace patterns have not yet been developed.

Our log analysis relied primarily on visual examination of standard log output, although parts of the Holditch Howell No. 5 FMS log were studied on Schlumberger's interactive log analysis workstation, and portions of the BHTV log from Holditch SFE No. 2 were studied on a workstation. More sophisticated image processing or analysis, or perhaps the use of BHTV and FMS logs in conjunction with other logs or techniques could provide additional criteria for distinguishing drilling-induced fractures.

SUMMARY

(1) Many details of sedimentary structures are visible on the FMS logs from the Cotton Valley and Travis Peak Formation. Some structures can be interpreted without reference to core, but most require core-to-log calibration for optimal assessment of sedimentary and diagenetic environment.

(2) In low-permeability Travis Peak Formation sandstone, both BHTV and FMS logs detect vertical and near-vertical extension fractures and borehole breakouts, but the FMS provides a higher resolution image of fracture shape. Low-angle natural shear fractures in shale were not detected by either logging tool. Because of limited FMS coverage of the borehole

wall and the tendency for tool orientation to be locked in by even a slightly elliptical borehole, vertical fractures can be missed by FMS pads.

(3) Distinguishing natural from drilling-induced fractures using the FMS or BHTV in the Travis Peak Formation is difficult.

(4) Present commercial techniques do not give an accurate fracture aperture (open width) in the Travis Peak, and methods devised to assess fracture width will need to take into account possible erosion of fractures near the borehole.

(5) Reliable orientation of inclined fractures can be obtained from either the BHTV or FMS if the top and/or bottom of the curved sinusoidal fracture trace is visible on logs. Orientation of vertical fractures can be ambiguous, especially if multiple fracture traces are present. Nevertheless, vertical fracture orientations from BHTV and FMS logs are similar to fracture orientations from core based on multishot and paleomagnetic orientation methods. The BHTV log is more reliable for obtaining fracture orientation where coverage by the FMS is inadequate.

(6) Borehole breakouts and elliptical zones detected on BHTV and caliper logs provide information on variation of horizontal stress that generally agrees with orientations inferred from drilling- and stress-test-induced fractures.

These results show that BHTV and FMS logs are useful and complementary adjuncts to core-based fracture studies for evaluating fractured low-permeability sandstone reservoirs in East Texas.

ACKNOWLEDGMENTS

This study was prepared for and funded by the Gas Research Institute under contract number 5082-211-0708, Shirley P. Dutton, Principal Investigator. The cooperation of AMOCO Production Company (USA), ARCO Oil and Gas Company, Cities Service Company, Dowell-Schlumberger, Mobil Producing Texas and New Mexico, and Prairie Producing

Company are gratefully acknowledged. K. J. Meador assisted with core and log descriptions, and helpful discussions with R. A. Plumb and Ercill Hunt are appreciated. We thank Mark Johnson, W. B. Ayers, Jr., and S. P. Dutton for review of the report. Figures were drafted by Annie K. Kearns, Wade Kolb, Joel L. Lardon, Patrice Porter, Maria E. Saenz, and Tari Weaver under the supervision of Richard L. Dillon, Chief Cartographer. Word processing was by Susan Lloyd and Melissa Snell under the direction of Susann Doenges. Illustrations were prepared by Margaret L. Evans. Lana Dieterich edited the report.

REFERENCES

- Baumgardner, R. W., Jr., and Meador, K. J., 1987, Analysis of fracturing and wellbore elongation based on borehole televiewer, Formation Microscanner, and ellipticity logs, *in* Laubach, S. E., Baumgardner, R. W., Jr., and Meador, K. J., Analysis of natural fractures and borehole ellipticity, Travis Peak Formation, East Texas: The University of Texas at Austin, Bureau of Economic Geology, topical report prepared for the Gas Research Institute under contract no. 5082-211-0708, p. 79-111.
- Bebout, D. G., Budd, D. A., and Schatzinger, R. A., 1981, Depositional and diagenetic history of the Sligo and Hosston Formations (Lower Cretaceous) in South Texas: The University of Texas at Austin, Bureau of Economic Geology Report of Investigations No. 109, 69 p.
- Bell, J. S., and Gough, D. I., 1979, Northeast-southwest compressive stress in Alberta: Evidence from oil wells: *Earth and Planetary Science Letters*, v. 45, p. 475-482.
- Bourke, L. T., Delfiner, P., Trouiller, J-C., Fett, T., Grace, L. M., Luthi, S. M., Serra, O., and Standen, E., 1989, Using Formation Microscanner images: The Technical Review, v. 37, no. 1, p. 16-40.
- Buffler, R. T., Watkins, J. S., Shaub, F. J., and Worzel, J. L., 1980, Structure and early geologic history of the deep central Gulf of Mexico, *in* Proceedings, symposium on the origin of the Gulf of Mexico and early opening of the central North Atlantic Ocean: Baton Rouge, Louisiana State University, School of Geosciences, p. 3-16.
- Casarta, L. J., McNaughton, D. A., Bornemann, E., and Bettis, F. E., 1989, Fracture identification and matrix characterization using a new wellbore imaging device in the Lisburne carbonate, Prudhoe Bay, Alaska: Society of Professional Well Log Analysts, 1989 symposium volume, unpaginated.

- Crary, S., and 23 others, 1986, Fracture detection with logs: The Technical Review, v. 35, no. 1, p. 23-31.
- Dennis, B., Standen, E., Georgi, D. T., and Callow, G. O., 1987, Fracture identification and productivity predictions in a carbonate reef complex: SPE Paper 16808, p. 579-588.
- Dutton, S. P., 1987, Diagenesis and burial history of the Lower Cretaceous Travis Peak Formation, East Texas: The University of Texas at Austin, Bureau of Economic Geology Report of Investigations No. 164, 58 p.
- Dutton, S. P., Laubach, S. E., Tye, R. S., Baumgardner, R. W., Jr., and Herrington, K. L., 1990, Geology of the Lower Cretaceous Travis Peak Formation, East Texas — depositional history, diagenesis, structure, and reservoir engineering implications: The University of Texas at Austin, Bureau of Economic Geology, topical report prepared for the Gas Research Institute under contract no. 5082-211-0708, 166 p.
- Dutton, S. P., Laubach, S. E., Tye, R. S., Herrington, K. L., and Diggs, T. N., in press, Geologic analysis of the Travis Peak Formation and Cotton Valley Sandstone, in Peterson, R. E., ed., Advancements in Travis Peak Formation evaluation and hydraulic fracture technology, Gas Research Institute Staged Field Experiment No. 3, Part I, GRI Report.
- Ekstrom, M. P., Dahan, C. A., Chen, Min-Yi, Lloyd, P. M., and Rossi, D. J., 1986, Formation imaging with microelectrical scanning arrays: Society of Professional Well Log Analysts, 27th Annual Logging Symposium Transactions, p. 1-21.
- Galloway, W. E., Ewing, T. E., Garrett, C. M., Tyler, Noel, and Bebout, D. G., 1983, Atlas of major Texas oil reservoirs: The University of Texas at Austin, Bureau of Economic Geology Special Publication, 139 p.
- Georgi, D. T., 1985, Geometrical aspects of borehole televiewer images: Society of Professional Well Log Analysts, 26th Annual Logging Symposium Transactions, I, Paper O.

- Grace, L. M., and Stephens, W. C., Jr., 1987, Exploration in braided stream environments using dipmeter analysis (abs.): American Association of Petroleum Geologists Bulletin, v. 71, no. 3, p. 238-239.
- Hackbarth, C. J., and Tepper, B. J., 1988, Examination of BHTV, FMS, and SHDT images in very thinly bedded sands and shales: Proceedings, 1988 Society of Petroleum Engineers Annual Technical Conference, SPE Paper No. 18118, p. 119-127.
- Harker, S. D., McGann, G. J., Bourke, L. T., and Adams, J. T., 1990, Methodology of Formation Microscanner image interpretation in Claymore and Scapa fields (North Sea), *in* Hurst, A., Lovell, M. A., and Morton, A. C., eds., Geological application of wireline logs: Geological Society of London Special Publication No. 48, p. 11-25.
- Holditch, S. A., 1989, GRI's Tight Gas Sands program: five years of progress: Gas Research Institute, *In Focus—Tight Gas Sands*, v. 6, no. 1, p. 5-11.
- Holditch, S. A., in press, SFE No. 2 report, *in* Peterson, R. E., ed., Advancements in Travis Peak Formation evaluation and hydraulic fracture technology: Gas Research Institute, Staged Field Experiment No. 2, Part II, GRI Report.
- Holditch, S. A., Robinson, B. M., and Whitehead, W. S., 1987, The analysis of complex Travis Peak reservoirs in East Texas: Society of Petroleum Geologists/Department of Energy Joint Symposium on Low Permeability Reservoirs, SPE Paper 16427, p. 381-399.
- Hunt, Ercill, 1990, Summary of independent analysis of fracture heights compared to the continuous microseismic radiation survey on GRI's SFE#3 (Mobil Cargill Unit #15): Ercill Hunt & Associates, Inc., topical report prepared for the Gas Research Institute under contract no. 5088-211-1682, 9 p.
- Kulander, B. R., Barton, C. C., and Dean, S. L., 1979, The application of fractography to core and outcrop fracture investigations: Morgantown Energy Technology Center, report prepared for U.S. Department of Energy, METC/SP 79/3, 174 p.

- Lau, J. S. O., Auger, L. F., and Bisson, J. G., 1987, Subsurface fracture surveys using borehole television camera and acoustic televiewer: *Canadian Geotechnical Journal*, v. 24, p. 499-508.
- Laubach, S. E., 1988a, Significance of natural and coring-induced fractures in the Travis Peak Formation for reservoir stimulation: *Gulf Coast Association of Geological Societies Transactions*, v. 38, p. 591.
- Laubach, S. E., 1988b, Subsurface fractures and their relationship to stress history in East Texas basin sandstone: *Tectonophysics*, v. 156, p. 37-49.
- Laubach, S. E., 1989, Fracture analysis of the Travis Peak Formation, western flank of the Sabine Arch, East Texas: The University of Texas at Austin, Bureau of Economic Geology Report of Investigations 185, 55 p.
- Laubach, S. E., Baumgardner, R. W., Jr., and Meador, K. J., 1987, Analysis of natural fractures and borehole ellipticity, Travis Peak Formation, East Texas: The University of Texas at Austin, Bureau of Economic Geology, topical report prepared for Gas Research Institute under contract no. 5082-211-0708, 128 p.
- Laubach, S. E., Baumgardner, R. W., Jr., Monson, E. R., Hunt, Ercill, and Meador, K. A., 1988, Fracture detection in low-permeability reservoir sandstone: A comparison of BHTV and FMS logs to core: *Proceedings, 1988 Society of Petroleum Engineers Annual Technical Conference*, SPE Paper No. 18119, p. 129-139.
- Laubach, S. E., and Monson, E. R., 1988, Coring-induced fractures: indicators of hydraulic fracture propagation direction in a naturally fractured reservoir: *Proceedings, 1988 Society of Petroleum Engineers Annual Technical Conference*, SPE Paper No. 18164, p. 587-596.
- Lloyd, P. M., Dahan, C., and Hutin, R., 1986, Formation imaging with micro electrical scanning arrays: a new generation of stratigraphic high resolution dipmeter tool: *Transactions of the Society of Professional Well Log Analysts 10th European Symposium*, Aberdeen, Scotland, April 22-25, paper L.

- Luthi, S. M., 1990, Sedimentary structures of clastic rocks identified from electrical borehole images, in Hurst, A., Lovell, M. A., and Morton, A. C., eds., Geological applications of wireline logs: Geological Society of London Special Publication No. 48, p. 3-10.
- Luthi, S. M., and Banavar, J. R., 1988, Application of borehole images to three-dimensional geometric modeling of eolian sandstone reservoirs, Permian Rotliegende, North Sea: American Association of Petroleum Geologists Bulletin, v. 72, no. 9, p. 1074-1089.
- Medlin, W. L., and Fitch, J. L., 1988, Abnormal treating pressures in massive hydraulic fracturing treatments: Journal of Petroleum Technology, v. 40, no. 5, p. 633-642.
- Moore, C. H., 1983, The Upper Smackover of the Gulf rim: depositional systems, diagenesis, porosity evolution, and hydrocarbon production: Louisiana State University, Applied Carbonate Research Program, Technical Series Contribution 12, 41 p.
- Nelson, R. A., 1987, Fractured reservoirs: turning knowledge into practice: Journal of Petroleum Technology, v. 39, no. 4, p. 407-414.
- Nelson, R. A., Lenox, L. C., and Ward, B. J., 1987, Oriented core: its use, error, and uncertainty: American Association of Petroleum Geologists Bulletin, v. 71, p. 357-368.
- Paillet, F. L., 1981, A comparison of fracture characterization techniques applied to near-vertical fractures in a limestone reservoir: Society of Professional Well Log Analysts, 22nd Annual Logging Symposium, Transactions, II, Paper XX.
- Pezard, P. A., and Lovell, M., 1990, Downhole images: electrical scanning reveals the nature of subsurface oceanic crust: EOS, v. 71, no. 20, p. 709 and 719.
- Pezard, P. A., and Luthi, S. M., 1988, Borehole electrical images in the basement of the Cajon Pass scientific drillhole, California: fracture identification and tectonic implications: Geophysical Research Letters, v. 15, p. 1017-1020.
- Plumb, R. A., 1989, Fracture patterns associated with incipient wellbore breakouts: Schlumberger-Doll Research Note, 28 p.

- Plumb, R. A., Brie, Alain, and Hsu, Kai, 1985, Fracture detection and evaluation using new wireline methods (abs.): Rapid City, South Dakota, 26th U.S. Symposium on Rock Mechanics, p. 227.
- Plumb, R. A., and Hickman, S. H., 1985, Stress-induced borehole elongation: a comparison between the four-arm dipmeter and the borehole televiewer in the Auburn geothermal well: *Journal of Geophysical Research*, v. 90, p. 5513-5521.
- Plumb, R. A., and Luthi, S. M., 1986, Application of borehole images to geologic modeling of an eolian reservoir: Society of Petroleum Engineers Paper 15487, presented at the 61st SPE Annual Technical Conference and Exhibition, New Orleans, October 5-8.
- Rambow, F. M., 1984, The borehole televiewer: some field examples: Society of Professional Well Log Analysts, 25th Annual Logging Symposium, Transactions, Paper C.
- Saucier, A. E., and Finley, R. J., 1984, The Travis Peak/Hosston Formation of East Texas and North Louisiana: a laboratory of tight gas technology development: Gas Research Institute, *In Focus—Tight Gas Sands*, v. 1, p. 15-25.
- Saucier, A. E., Finley, R. J., and Dutton, S. P., 1985, The Travis Peak (Hosston) Formation of East Texas and North Louisiana: Society of Petroleum Engineers/Department of Energy Joint Symposium on Low Permeability Reservoirs, SPE Paper 13850, p. 15-22.
- Schlumberger, Ltd., 1987, Log interpretation principles/applications: Houston, Schlumberger Educational Services, 198 p.
- Stock, J. M., Healy, J. H., and Hickman, S. H., 1984, Report on televiewer log and stress measurements in core hole USW G-2, Nevada Test Site, October-November, 1982: U. S. Geological Survey Open-File Report 84-172, 31 p.
- Taylor, T. J., 1983, Interpretation and application of borehole televiewer survey: Society of Professional Well Log Analysts, 24th Annual Logging Symposium, Transactions, II, Paper QQ.
- Tye, R. S., 1989, Stratigraphy and depositional systems of the Lower Cretaceous Travis Peak Formation, East Texas Basin: The University of Texas at Austin, Bureau of Economic

- Geology, topical report prepared for the Gas Research Institute under contract no. 5082-211-0708, 80 p.
- Tye, R. S., Diggs, T. N., Laubach, S. E., Herrington, K. L., and Dutton, S. P., 1989a, Preliminary Geologic Description, Mobil Cargill No. 15: The University of Texas at Austin, Bureau of Economic Geology, report prepared for the Gas Research Institute under contract no. 5082-211-0708, 25 p.
- Tye, R. S., Dutton, S. P., Laubach, S. E., and Finley, R. J., 1989b, Geologic analysis of the Travis Peak tight gas sandstones: Gas Research Institute, In Focus—Tight Gas Sands, v. 6, no. 1, p. 63-69.
- Tye, R. S., Laubach, S. E., Dutton, S. P., and Herrington, K. L., 1989c, The role of geology in characterizing low-permeability sandstones, North Appleby field, East Texas basin: Society of Petroleum Engineers, Proceedings, 1989 SPE Joint Rocky Mountain Regional/Low-Permeability Reservoirs Symposium and Exhibition, Paper 18964, p. 355-365.
- Van Alstine, D. R., 1986, Paleomagnetic core orientation results from Holditch Howell No. 5 core: report submitted to CER Corporation, 19 p.
- Van Alstine, D. R., Gillet, S. L., and Bleakly, D. C., 1983, Paleomagnetic applications in hydrocarbon exploration and drilling operations (abs.): American Association of Petroleum Geologists Bulletin, v. 67, p. 563.
- Whitehead, W. S., and Robinson, B. M., 1989, Development of in situ stress testing procedures and analysis: Gas Research Institute, In Focus—Tight Gas Sands, v. 6, no. 1, p. 29-33.
- Zemanek, J., Caldwell, R. L., Glenn, E. E., Holcomb, S. V., Norton, L. J., and Strauss, A. J. D., 1969, The borehole televiewer—a new logging concept for fracture location and other types of borehole inspection: Journal of Petroleum Technology, v. 21, p. 762-774.
- Zemanek, J., Glenn, E. E., Norton, L. J., and Caldwell, R. L., 1970, Formation evaluation by inspection with the borehole televiewer: Geophysics, v. 35, p. 254-269.